



UNIVERSIDADE FEDERAL DE OURO PRETO
ESCOLA DE MINAS
DEPARTAMENTO DE GEOLOGIA



DISSERTAÇÃO DE MESTRADO

**WATER-PRESENT ECLOGITE MELTING – THE EFFECTS
OF THE PHENGITE AND WATER IN THE PARTIAL
MELTING OF BASALTIC ROCKS IN EARTH’S EARLY
CRUST DEVELOPMENT**

Leonardo Azevedo Sá Alkmin

TESE n° 364

Ouro Preto, dezembro de 2014

**WATER-PRESENT ECLOGITE MELTING – THE EFFECTS OF
THE PHENGITE AND WATER IN THE PARTIAL MELTING OF
BASALTIC ROCKS IN EARTH’S EARLY CRUST
DEVELOPMENT**



FUNDAÇÃO UNIVERSIDADE FEDERAL DE OURO PRETO

Reitor

Marcone Jamilson Freitas Souza

Vice-Reitor

Célia Maria Fernandes Nunes

Pró-Reitor de Pesquisa e Pós-Graduação

Valdei Lopes de Araújo

ESCOLA DE MINAS

Diretor

Issamu Endo

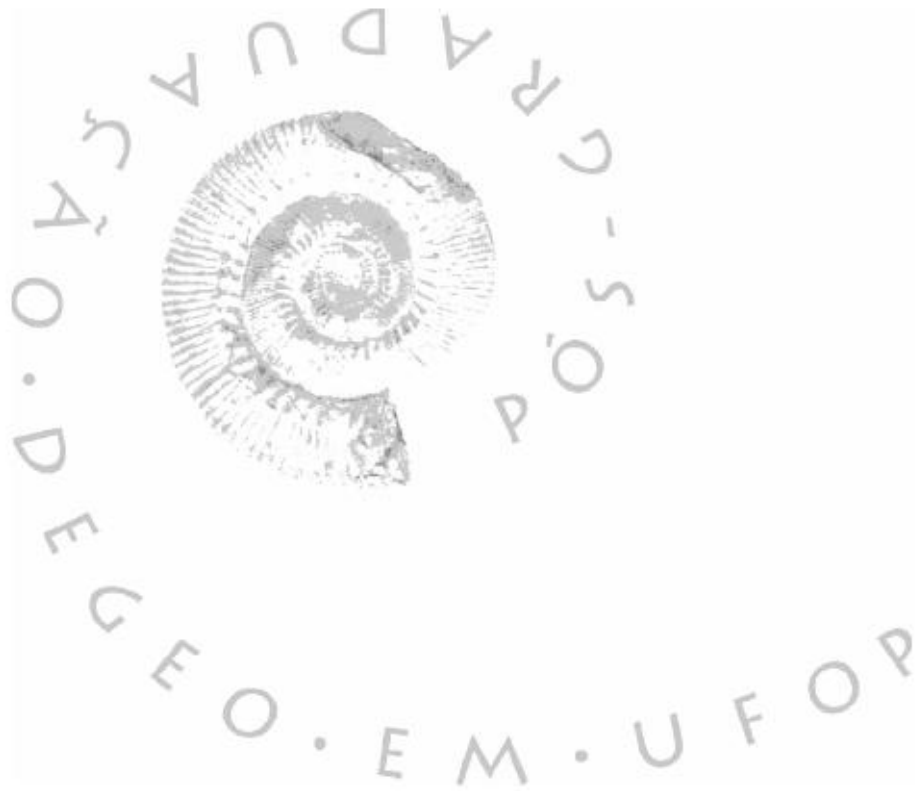
Vice-Diretor

José Geraldo Arantes de Azevedo Brito

DEPARTAMENTO DE GEOLOGIA

Chefe

Fernando Flecha de Alkmim



EVOLUÇÃO CRUSTAL E RECURSOS NATURAIS

CONTRIBUIÇÕES ÀS CIÊNCIAS DA TERRA – VOL.77

DISSERTAÇÃO DE MESTRADO

Nº 364

**WATER-PRESENT ECLOGITE MELTING – THE EFFECTS OF THE
PHENGITE AND WATER IN THE PARTIAL MELTING OF BASALTIC
ROCKS IN EARTH’S EARLY CRUST DEVELOPMENT**

Leonardo Azevedo Sá Alkmin

Orientador

Cristiano de Carvalho Lana

Co-orientador

Gary Stevens

Tese apresentada ao Programa de Pós-Graduação em Evolução Crustal e Recursos Naturais
do Departamento de Geologia da Escola de Minas da Universidade Federal de Ouro Preto
como requisito parcial à obtenção do Título de Doutor Ciência Naturais, Área de Concentração:
Geologia Ambiental e Conservação de Recursos Naturais

**OURO PRETO
2014**

Universidade Federal de Ouro Preto – <http://www.ufop.br>
Escola de Minas - <http://www.em.ufop.br>
Departamento de Geologia - <http://www.degeo.ufop.br/>
Programa de Pós-Graduação em Evolução Crustal e Recursos Naturais
Campus Morro do Cruzeiro s/n - Bauxita
35.400-000 Ouro Preto, Minas Gerais
Tel. (31) 3559-1600, Fax: (31) 3559-1606 e-mail: pgrad@degeo.ufop.br

Os direitos de tradução e reprodução reservados.

Nenhuma parte desta publicação poderá ser gravada, armazenada em sistemas eletrônicos, fotocopiada ou reproduzida por meios mecânicos ou eletrônicos ou utilizada sem a observância das normas de direito autoral.

ISSN 85-230-0108-6
Depósito Legal na Biblioteca Nacional
Edição 1ª

Catálogo elaborado pela Biblioteca Prof. Luciano Jacques de Moraes do
Sistema de Bibliotecas e Informação - SISBIN - Universidade Federal de Ouro Preto

A415w	Alkmin, Leonardo Azevedo. Water-present eclogite melting - the effects of the phengite and water in the partial melting of basaltic rocks in earth's early crust development [manuscrito] / Leonardo Azevedo Alkmin. - 2014. 73f.: il.: color; tabs. (Série M, volume 77, número 364) Orientador: Prof. Dr. Cristiano Lana. Coorientador: Prof. Dr. Gary Stevens. Dissertação (Mestrado) - Universidade Federal de Ouro Preto. Escola de Minas. Departamento de Geologia. Programa de Pós-Graduação em Evolução Crustal e Recursos Naturais. Área de Concentração: Tectônica, Petrogênese e Recursos Minerais - TPRM. 1. Petrologia. 2. Granitóides potássicos. 3. Fusão parcial. I. Lana, Cristiano. II. Stevens, Gary. III. Universidade Federal de Ouro Preto. IV. Título. CDU: 552.123
-------	--

<http://www.sisbin.ufop.br>

FICHA DE APROVAÇÃO



MINISTÉRIO DA EDUCAÇÃO
Universidade Federal De Ouro Preto
Escola de Minas – Departamento de Geologia
Programa de Pós-Graduação em Evolução Crustal e Recursos Naturais

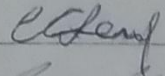



ATA DA REUNIÃO DA BANCA EXAMINADORA DA DISSERTAÇÃO DE Mestrado INTITULADA:

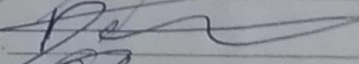
"Water presente eclogite melting – The effects of phengite and water in the partial melting of basaltic rocks in Earth's early crustal development"

APRESENTADA POR : LEONARDO AZEVEDO DE SÁ ALKIMIM

BANCA EXAMINADORA

Prof. Dr. Cristiano Carvalho Lana  _____
Presidente

Prof. Dr. Tiago Amâncio Novo  _____

Prof. Dr. Hermínio Arias Nalini Jr.  _____

Prof. Dr. Gary Stevens  _____

Ouro Preto, 02 de dezembro de 2014

Campus Universitário Morro do Cruzeiro - S/N - CEP: 35400-000 - Ouro Preto - MG - Brasil
Tel.: (0..31) 559.1600 - Fax: (0..31) 559.1606 - e-mail: pgrad@degeo.ufop.br



FORMULÁRIO DE AVALIAÇÃO FINAL

TÍTULO DA DISSERTAÇÃO

"Water presente eclogite melting – The effects of phengite and water in the partial melting of basaltic rocks in Earth's early crustal development"

APRESENTADA POR : LEONARDO AZEVEDO DE SÁ ALKMIM

BANCA EXAMINADORA

Prof. Dr. Cristiano Carvalho Lana
Presidente

Prof. Dr. Tiago Amâncio Novo

Prof. Dr. Hermínio Arias Nalini Jr.

Prof. Dr. Gary Stevens

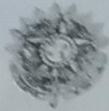
AVALIAÇÃO

APROVADO

REPROVADO

Prof. Dr. Cristiano Carvalho Lana
Presidente

Ouro Preto, 02 de dezembro de 2014



FORMULÁRIO DE AVALIAÇÃO FINAL

TÍTULO DA DISSERTAÇÃO

"Water presente eclogite melting – The effects of phengite and water in the partial melting of basaltic rocks in Earth's early crustal development"

APRESENTADA POR : LEONARDO AZEVEDO DE SÁ ALKMIM

BANCA EXAMINADORA

Prof. Dr. Cristiano Carvalho Lana
Presidente

Prof. Dr. Tiago Amâncio Novo

Prof. Dr. Herminio Anas Nalini Jr.

Prof. Dr. Gary Stevens

AVALIAÇÃO

APROVADO

REPROVADO

Prof. Dr. Tiago Amâncio Novo

Prof. Dr. Cristiano Carvalho Lana
Presidente

Ouro Preto, 02 de dezembro de 2014



FORMULÁRIO DE AVALIAÇÃO FINAL

TÍTULO DA DISSERTAÇÃO

"Water presente eclogite melting – The effects of phengite and water in the partial melting of basaltic rocks in Earth's early crustal development".

APRESENTADA POR : Leonardo Azevedo de Sá Alkmim

BANCA EXAMINADORA

Prof. Dr. Cristiano Carvalho Lana
Presidente

Prof. Dr. Tiago Amâncio Novo

Prof. Dr. Herminio Arias Nalini Jr.

Prof. Dr. Gary Stevens

AVALIAÇÃO

APROVADO

REPROVADO

Prof. Dr. Herminio Arias Nalini Jr.

Prof. Dr. Cristiano Carvalho Lana
Presidente

Ouro Preto, 02 de dezembro de 2014



TÍTULO DA DISSERTAÇÃO

"Water presente eclogite melting – The effects of phengite and water in the partial melting of basaltic rocks in Earth's early crustal development".

APRESENTADA POR : Leonardo Azevedo de Sá Alkimim

BANCA EXAMINADORA

Prof. Dr. Cristiano Carvalho Lana
Presidente

Prof. Dr. Tiago Amâncio Novo

Prof. Dr. Hermínio Arias Nalini Jr.

Prof. Dr. Gary Stevens

AVALIAÇÃO

APROVADO

REPROVADO

Prof. Dr Gary Stevens. _____
(Presidente – University of Stellenbosch – Africa do sul)

Prof. Dr. Cristiano Carvalho Lana _____
Presidente

Ouro Preto, 02 de dezembro de 2014

Dedico esse trabalho a todos que contribuíram para seu desenvolvimento.

I dedicate this work to everyone who contributed to its development.

Acknowledgements

I thank my family, my parents and my sister for the support.

I thank CAPES for the scholarship.

The colleges from post-grad program in UFOP and University of Stellenbosch for the reception, friendship and the academic discussions (and others not so much).

The post-grad program professors in UFOP and University of Stellenbosch for the teaching and guidance.

CAF (Central Analytical Facilities) for the reception and financial support during my period in Stellenbosch, especially prof. Gary Stevens and Mrs. Madelaine Freiburg.

The PhD. Marcos Garcia Arias for aiding with complementary analyses.

I especially thank the prof. Cristiano Lana for his patience and trust during the performance of this work.

I especially thank the prof. Gary Stevens for the dedication, teaching, financial support, academic discussions, patience and general support throughout the whole work.

Summary

ACKNOWLEDGMENTS	ix
FIGURES INDEX	xiii
TABLES INDEX	xv
RESUMO	xvii
ABSTRACT	xix
CHAPTER 1. INTRODUCTION	1
1.1. General Staments	1
1.2. Investigational approach	2
1.3. Objectives	3
1.4. Methods and methodology	3
1.4.1 – Experimental Petrology	3
CHAPTER 2. THE PRODUCTION OF TTG MELTS AND POTASSIC GRANITOIDS IN THE BARBERTON GREENSTON BELT	9
2.1. BARBERTON GREENSTONE BELT	9
2.1.1 – The Onverwacht Group	9
2.1.2 – The Fig Tree Group	10
2.1.3 – The Moodies Group	10
2.1.4 – The Evolution of the BGB	10
2.1.5 – The TTGs of the BGB	11
2.1.6 – Geochemistry and petrogenesis of the TTGs from the BGB	12
2.1.7 – Geochemistry and petrogenesis of the potassic granitoid clasts from the BGB	13
2.2. THE COUCAL FORMATION IN THE EAST PILBARA CRATON	18
CHAPTER 3. PRESENTATION OF THE SCIENTIFIC PAPER	19
3.1. Introduction	20
3.2. Geological settings	21
3.3. Experimental and analytical procedures	22
3.3.1 – Starting material	22
3.3.2 – Experimental settings	25
3.3.3 – Analytical methods	28

3.4. Experimental results	28
3.4.1 – Equilibrium approach	29
3.4.2 – Experimental glass composition	32
3.4.3 – Melting reactions	32
3.4.4 – Further melt modeling	33
3.5 – Discussion	33
3.6 – Conclusion	35
CHAPTER 4. CONCLUSIONS	37
REFERENCES	38
APPENDIX	43
FICHA DE APROVAÇÃO	74

FIGURES INDEX

Figure 1.1 – Experimental set for the simulation of Earth’s thermodynamic conditions	4
Figure 1.2 – Scheme for the experimental set, showing all the components that go inside the pressure vessel	6
Figure 1.3 – Zeiss EVO@MA15 SEM with the cryostage coupled and the computers for the software for analyses.	8
Figure 2.1 – Simplified geological map of the Barberton Greenston Belt (extracted from Sanchez-Garrido et al., 2011).....	10
Figure 2.2 – Ages of the potassic granitoid clasts and felsic volcanism in comparison with the TTG plutons age from the BGB.....	12
Figure 2.3 – Barberton Greenstone Belt map highlighting the TTG plutons and their ages in million years	13
Figure 2.4 – Binary and ternary diagrams showings the geochemistry characteristics of the three TTG groups and the potassic rocks	14
Figure 2.5 – Harker diagrams for major elements displaying the Moodies granites	15
Figure 2.6 – Ternary feldspar diagram from the clasts in the Moodies group and the Hooggenoeg Formation	16
Figure 2.7 – Harker diagrams for some trace elements displaying the Moodies granites (orange squares) and the Theespruit felsic schists	17
Figure 3.1 – Back-scatter electron (BSE) images of the run products.....	30
Figure 3.2 – Major elements diagrams for the experimental glasses and starting material in comparison with the bibliography available data.....	31
Figure 3.3 – Pseudosection of the new bulk rock composition after extracting the potassic melt	34

TABLES INDEX

Table 1.1 - Compositions of Coonterunah F2 basalts and the first Starting Material XRF analyses	5
Table 3.1 - Experimental run conditions and products	23
Table 3.2 - Major element geochemistry of the starting materials ESM-1 and ESM-2 and averaged normalized anhydrous experimental glass major element compositions.....	24
Table 3.3 - Garnet compositions from ESM-1 starting material and experimental run products	26
Table 3.4 - Clinopyroxene compositions from ESM-1 starting material and experimental run products	27
Table 3.5 - Calculated phase proportion by major element squared mass balance for the 2.5 Gpa – 800°C and 2.5 GPa – 850 °C run products	29

RESUMO

As suítes tonalíticas-trondjemíticas-granodioríticas (TTGs) de granitóides eram dominantes durante a formação da crosta oceânica félsica no Éon Arqueano. TTGs são granitóides caracterizados por alto teor de sílica (tipicamente superior a 68 wt.% SiO₂) e sódio, com baixos valores das razões potássio-sódio (Na₂O ~4.65 wt.%; K₂O/ Na₂O ~0.4), baixas razões La/Yb (~48) e baixos valores de concentração de Yb (~0.6 ppm). Laurie e Stevens (2012) demonstraram que magmas TTG com composição similar à média dos trondjemitos arqueanos podem ser produzidos através da fusão parcial de rochas basálticas saturadas em água, sob condições de pressão e temperatura (PT) consistentes com a subducção arqueana em fácies eclogíticas.

O Barberton Granite Greesntone Terrane (BGGT), localizado no oeste da África do Sul e leste de Swazilândia é uma das províncias crustais mais antigas preservadas na Terra e provê um laboratório ideal para os estudos da evolução planetária nos seus estágios mais precoces da formação de crosta continental. Esse terreno é formado por rochas supracrustais associadas a três eventos de magmatismo TTG datados em ca 3.55, 3.42 e 3.23 Ga. Existe ainda um estágio de magmatismo potássico tardio de afinidade granítica-monazítica-sienítica (GMS), originado a partir da fusão parcial dos plutons TTG. Esse estágio potássico não está relacionado, entretanto, com alguns seixos e rochas vulcânicas documentadas em Sanchez-Garrido *et al.* (2011) e Diegaardt (2013). Tratam-se de clastos peraluminosos de granitóides que ocorrem na forma de conglomerados e vulcanismo félsico no *greenstone belt* e possuem idades 3.550±45 Ma, 3.460±34 Ma e 3.270±36 Ma. Eles se diferem de típicos granitóides tipo-S da suíte GMS por seu caráter pouco sódico (0.30 wt.% em média) e concentrações razoáveis de Sr (12 – 330 ppm). Para esses granitos foi proposta uma gênese através da anatexia de rochas sedimentares subductadas junto com a crosta oceânica e isso explicaria a produção contemporânea desses granitóides peraluminosos e dos magmas TTG.

Esse estudo investigou experimentalmente a possibilidade de magmas TTG e granitóides potássicos serem produzidos a partir da mesma fonte como consequência da fusão parcial em elevadas pressões. Os experimentos utilizaram-se de composições propostas por Smithies *et al.* (2009) para a composição média da crosta oceânica arqueana, em conjunto com condições de PT consistentes com as estruturas termais das zonas de subducção arqueanas propostas por Laurie *et al.* (2012). Os experimentos conduzidos demonstraram que em temperaturas relativamente baixas (800°C a 850°C a 2.5 GPa) a fonte máfica produz magmas graníticos peraluminosos com baixo teor de CaO (0.88 wt.% em média).

ABSTRACT

The tonalite-trondhjemite-granodiorite (TTGs) suites of granitoid rocks were dominant during the formation of the felsic continental crust in the Archean. TTGs are granitoids characterized by high contents of silica (typically higher than 68 wt.% SiO₂) and sodium, with low potassium-sodium ratios (Na₂O ~4.65 wt%; K₂O/Na₂O ~0.4), low La/Yb ratios (~48) and low Yb concentration (~0.6 ppm). It was demonstrated by Laurie and Stevens (2012) that TTG melts with compositions similar to the average Archean trondhjemite can be generated through partial melting of water saturated basaltic rocks, under pressure and temperature (PT) conditions consistent with Archean subduction in the eclogite facies.

The Barberton Granite Greenstone Terrane (BGGT), located in west South Africa and east Swaziland is one of the oldest crustal provinces preserved on Earth and it makes an ideal laboratory to study the planetary early evolution. It comprises supracrustal rocks associated to three TTG magmatism events dated at ca 3.55, 3.42 and 3.23 Ga. There is also a later potassic magmatism with granitic-monzonitic-syenitic affinity (GMS) stage, originated from the partial melting of the TTGs. This potassic stage is not related however to the older pebbles and volcanic rocks documented in Sanchez-Garrido *et al.* (2011) and Diegaardt (2013). These peraluminous granites which occur as clasts within conglomerates and felsic volcanism in the greenstone belt have ages of 3.550±45 Ma, 3.460±34 Ma and 3.270±36 Ma. They differ from typical S-type from the GMS suite rocks for they are characterized by very low CaO (0.30 wt% in average) and a reasonable concentration of Sr (12–330 ppm). It has been proposed that these granites formed by anatexis of sedimentary rocks subducted with oceanic crust as an explanation of the coeval production of peraluminous granite and TTG magmas.

This study has experimentally investigated the possibility of TTG and potassic granitic magmas been produced by the same source as a consequence of high pressure melting. The experiments have used compositions proposed by Smithies *et al.* (2009) for average Archean oceanic crust, in conjunction with PT conditions consistent with the Archean subduction zone thermal structure proposed by Laurie *et al.* (2012). Experiments conducted demonstrate that at relatively low temperature (800°C to 850°C at 2.5 GPa) the mafic source produces peraluminous granitic melts with low CaO contents (0.88 wt% in average).

CHAPTER 1

INTRODUCTION

1.1 – GENERAL STATEMENTS

Tonalite-Thronjemitite-Granodiorite (TTG) suites are strongly sodic and represent the archetype of Archean rocks (Jahn *et al.*, 1981; Martin *et al.*, 1983; Schmidt *et al.*, 2004; Moyen and Martin, 2012). They are a product of partial melting of oceanic slabs in an Archean hot subduction environment (Martin, 1986; Laurie and Stevens, 2012). Potassic granitoids, however, are associated with later granitic production (Shoene and Bowring, 2010; Lana *et al.*, 2010; Sanchez-Garrido *et al.*, 2011), coinciding with terrane amalgamation, also in the Archean (Martin *et al.*, 2006). Nevertheless, in the Barberton Greenstonebelt (BGB), South Africa, it has been documented potassic granitoids of older age than the TTGs (Sanchez-Garrido *et al.*, 2011; Diergaardt, 2013).

The models for the production of the TTGs do not take in account the direct association with the k-granitoids and calcium variability of these rocks. Schmidt *et al.* (2004) and Laurie and Stevens (2012) have shown that it is possible to generate significant volumes of TTG melts from partial melting of an eclogite starting material. The experimental work done within these assumptions provided information of the major, trace and rare earth elements (REE) of TTGs run products, which were then compared with the available data of the BGB granitoids and indicated a strong relationship concerning them. Furthermore, Schmidt *et al.* (2004) demonstrated that the partial melting of MORBs with slightly enrichment in potassium is capable of generating k-granitoids and that the phengite plays a major role for the potassium accommodation in high pressure conditions.

The traditional genetic model for potassic granitoids in the Archean is associated with continental crust partial melting, having the TTGs as the primary source. It is also proposed that this magmatism is associated with the stabilization of cratons. Potassic granitoids older than the TTGs though are not broadly documented and hence not given enough insights nor proper genetic models.

1.2 – INVESTIGATIONAL APPROACH

The Barberton Greenstone Belt, located in South Africa and Swaziland, is one of the oldest and well preserved sections of Earth (Lowe and Byerly, 2007). The great extension of outcrops there provides enough resources for the investigation of the early crustal evolution and gives researchers a unique glance into the Archean. BGB is comprised of: a) supracrustal units (3.55 to 3.21 Ga), b) TTG (Tonalite-Thronjemitite-Granodiorite) intrusions and c) the Granite-Monzonite-Syenite (GMS) suite. The supracrustal and TTGs are syngenetic while the GMS postdate the formation of the BGB (Lowe and Byerly, 2007).

The TTGs have a sodic signature, with high ratios of Na/K and Na/Ca and therefore they plot near the Albite vertices in Or-An-Ab diagram (Martin, 1994), far off the calc-alkaline series. The experimental petrology applied in the study of BGB rocks provided information concerning their origin and the results strongly suggest that the partial melting of eclogite subducting slabs is the best fit for it. The GMS group is, then, proposed to be formed by the partial melting of the TTG suite, after the formation of the BGB. The older potassic granitoids registered by Sanchez-Garrido *et al.* (2011) and Diergaardt (2013), on the other hand, could not be formed by the same process.

These k-granitoids were found as clasts in conglomerates of early supracrustal formations in the BGB. They are different from normal k-granitoids for their low content of CaO (< 0.05wt%). In this matter, the normal genetic models are not sufficient to explain this deficiency in CaO. For that reason, one could wonder about the possibility of having both granitoids (older k-granitoid and TTG) derived from the same source and these questions are yet to be answered:

- 1) Can an eclogite starting material, already demonstrate to generate a TTG put under subduction conditions, produce a previous potassic melt?
- 2) If so, does the CaO stay in the rock, generating a CaO depleted melt?
- 3) Is the melt peraluminous, K₂O-Na₂O rich, CaO deficient?
- 4) Would the extraction of this melt and ongoing partial melting generate a TTG melt?

1.3 – OBJECTIVES

This project is focused in providing better understanding for the influence of k-bearing phases in the partial melting of eclogites. The study is based on the partial melting of a synthetic starting material and have the accounted variables controlled in laboratory. The specific goals are:

- Produce a starting material (SM) resembling the oceanic crust/eclogite composition in the early Archean;
- Investigate the run products of the SM in conditions of subduction;
- Analyse and compare the results of the SM with the real rocks found in BGB.

1.4 – METHODS AND METHODOLOGY

The Barberton Greenstone Belt provides insights of Earth's early history and for that was chosen to be used as contrast for the experimental results. Although the TTG and the GMS groups outcrop extensively in South Africa and Swaziland and the k-granitoid clasts somewhat less, the BGB does not present a preserved unaltered Archean oceanic slab or an eclogite for that matter. Looking for a natural starting material candidate to be a TGG protolith would take a large amount of time. In order to achieve the objectives of this research in the proposed period, it was opted to use an analogous synthetic starting material. Before decide the best composition for the experimental work a wide range of bibliography and computer modeling was studied and tested.

1.4.1. – Experimental Petrology

Experimental petrology is a technique to determinate the rock content in a controlled laboratory, in the premise that it is possible to replicate Earth's conditions with the adequate equipment. A piston cylinder is used to simulate different pressures whilst a heater is responsible to control the temperature (Fig. 1.1).

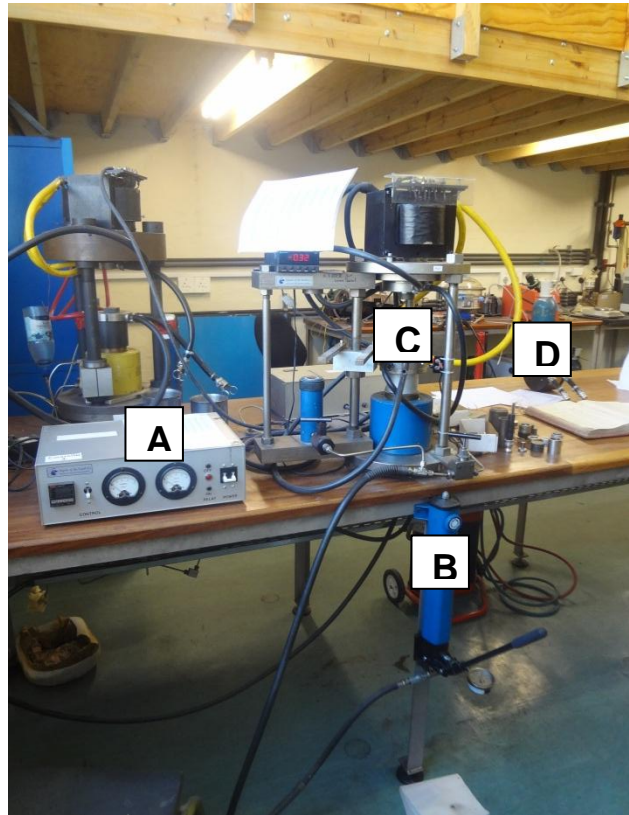


Figure 1.1 – Experimental set for the simulation of Earth’s thermodynamic conditions. The set is composed by **A)** a heater control that provides the assigned temperature; **B)** an oil piston to produce the pressure of desire; **C)** the space for positioning the pressure vessel and **D)** the pressure vessel.

The first thing to do is to determine what composition will be used in the starting material (SM). For this work, we assumed that the SM will have the composition of average Archean basalt, slightly enriched in potassium, documented in Smithies *et al.* (2009) in the east Pilbara Craton, Australia. These basalts are ~3.51 Ga old and part of the Coonterunah F2 series, within the Coucal Formation (Table 1.1).

From this point on, it is necessary to run computer models for the assemblage equilibria and verify the feasibility of the experiment. The program used was the Theriak-Domino (Capitani and Petrakakis, 2010). This program calculates the minimum energy of Gibbs found in a range of pressure vs. temperature and displays the mineral assemblage of each field according to the thermodynamic calculations. All the phases are based in a specific composition provided by the user and the interface of the software allows choosing amongst a database of minerals to contemplate.

Table 1.1 – Compositions of Smithies *et al.* (2009) basalts of Coonterunah F2 and the first Starting Material XRF analyses.

	Smithies <i>et al.</i> (2009)	SM XRF analyses
SiO ₂	46.50	46.12
TiO ₂	2.00	2.09
Al ₂ O ₃	15.00	15.34
FeO	13.80	14.51
MnO	0.20	0.00
MgO	7.20	6.76
CaO	9.20	9.54
Na ₂ O	2.30	2.32
K ₂ O	0.90	0.95
P ₂ O ₅	0.14	-
LOI	2.20	-
Total	99.44	99.40

The crafting of the SM takes 3 days. With an established composition, a “gel” (white powder) is produced in the geochemistry lab. The ingredients used to achieve the composition of SM are TEOS (tetraethylorthosilicate) for the silica, TiO₂ powder for the titanium, Al metal powder for aluminum, Fe²⁺ metal sponge and Fe₂O₃ powder for total iron, Mg powder for magnesium and carbonates of calcium, potassium and sodium for their respective elements. Eventually, fayalite was used as source of iron and kaolinite for the proportional water content. The water was also introduced with a syringe after the gel was ready and sitting in a capsule. The components were processed, dried, grinded, mixed with acid and broken into cations so they would form a sort of gel, with the elements interacting with each other. The mix was then dried and grinded again. This “gel” was stored in a vacuum desiccator, isolated from the atmosphere until the performance of the experiment. 2 grams of the SM were analysed by XRF for the major elements (Table 1.1).

Once the composition of SM was adequate, it was transferred to a golden capsule and sealed with a welder. Before welding, the water, if kaolinite hadn't been used in the gel making, was added via a syringe and corresponded to 10 wt% of the sample, so water saturated condition would be achieved. The water had to be cautiously introduced and the welding had to be done with the capsule in contact with a

barrel of water, so the wet gel wouldn't dry out. Once sealed, the capsule was tested for holes and when approved, inserted into a piston with boron nitride powder. We added 1000 psi of pressure for a minute so the result was a boron nitride rod with the golden capsule inside, ready to be placed inside the experimental set.

The experimental set is composed of a steel plug positioned in the base, a graphite furnace with a salt sleeve around it, a ceramic rod that goes on top of the steel plug and into the furnace, leading to half of its length, a thermocouple insulator (mullite) that goes through the ceramic rod, with two different wires, a ceramic rounded shape lid, the boron nitride rod with the golden capsule, a ceramic bar and a graphite lid, all covered with grease (Fig. 1.2). When all had been put together, we added the set into the pressure vessel and then positioned it to the pressure/temperature machine.

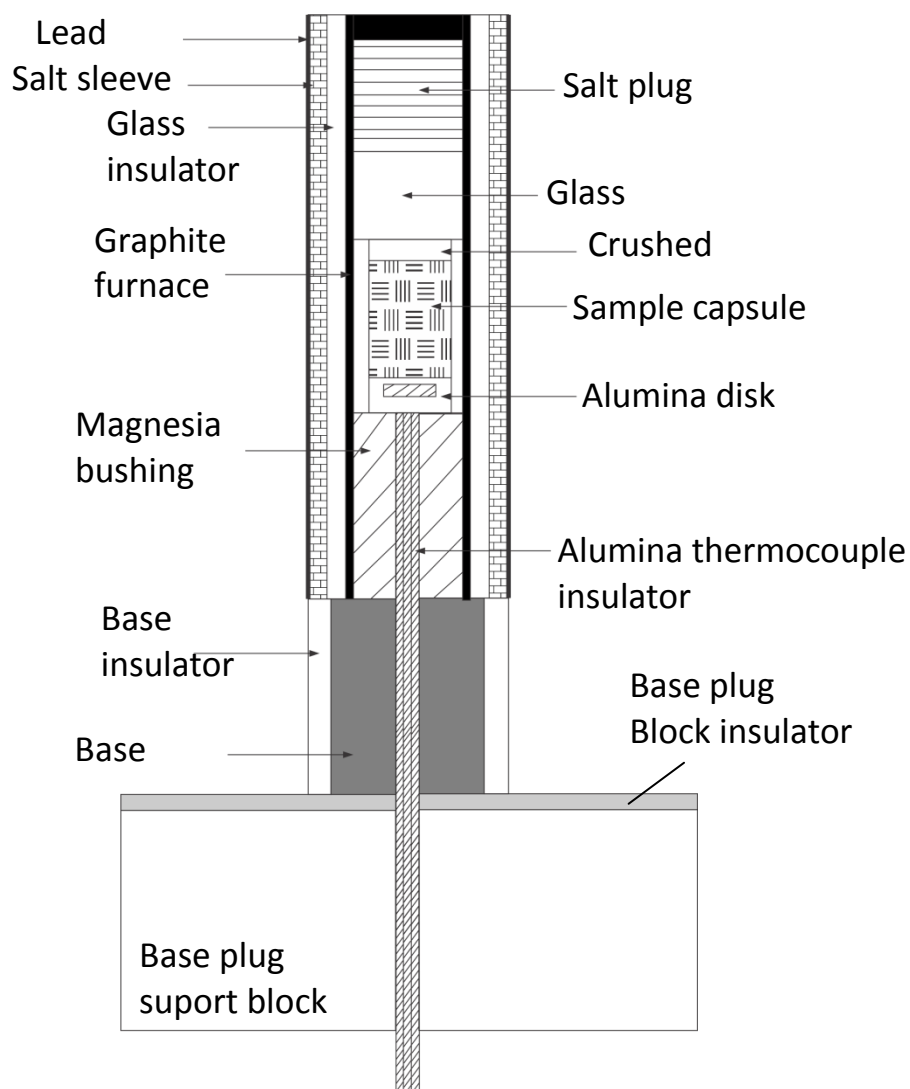


Figure 1.2 – Scheme for the experimental set, showing all the components that go inside the pressure vessel.

The whole idea is to make an experimental set with less space as possible in it, position the thermocouple as close as possible to the boron nitride rod with the golden capsule and avoid shear stress in the structure while applying the pressure.

The pressure is added first and then the temperature, in an isobaric condition. The experiment is left for 6 days in a lower temperature (~600°C) to stabilize and equilibrate the system and start producing minerals. Once that time has passed, the temperature is increased until the experimental conditions set for that capsule and left for 14 days. When the experiment is completed, the capsule is removed, mounted on a thin section, polished until the run products show and analysed in a Scanning Electron Microscope (SEM).

The samples were coated with carbon and analysed with a Zeiss EVO@MA15 Scanning Electron Microscope. Beam conditions during quantitative analyses were set to -20 kV. The working distance was set to 8.5 mm and beam current in approximately -20nA. The counting time was 15 seconds live-time. A cobalt standard was used to calibrate the equipment during initialization and periodically used to correct the detector drift. Secondary electron images and compositions were quantified by an Electron Dispersion Spectrometry (EDS), using Oxford Instruments® X-MAS 20m2 detector and Oxford INCA software (Fig. 1.3). The analyses of the molten glass were also done in the SEM but with a cryo stage. The temperature was drop to -180°C adding liquid nitrogen in the stage to diminish the mobility of the elements in this phase, especially Na.

International standards for minerals and metals were used during analyses to quantify the results. They were introduced in the SEM with the samples at the same time, although the software had already recorded the standards information and made it easy to work with. A faraday cup was used to constantly measure the beam and set the spot size to adjust the current.



Figure 1.3 – Zeiss EVO@MA15 SEM with the cryostage coupled and the computers for the software for analyses. The samples were coated with carbon and loaded in the SEM with mineral standards for quantification. Backscatter images were also taking during analyses.

CHAPTER 2

THE PRODUCTION OF TTG MELTS AND POTASSIC GRANITOIDS IN THE BARBERTON GREENSTONE BELT

2.1 – BARBERTON GREENSTONE BELT

The Barberton Greenstone Belt (BGB) consists mostly of supracrustal rocks. It also displays a trondhjemite-tonalite-granodiorite (TTG) group dating from 3.55 to 3.21 Ga. These granitoids are also distinct by their Na-rich and K-poor character. The rocks of the BGB and the TTG plutons are syngenetic. Postdating both units there is a granite-monzonite-syenite (GMS) group, with ages between 3.14 and 3.10 Ga (Lowe and Byerly, 2007).

The rocks of the BGB form part of the Swaziland Supergroup and can be subdivided into three lithostratigraphic units: 1) the Onverwacht Group (> 3.547-3.260 Ma) at the base; 2) the Fig Tree Group (3.260-3.225 Ma) overlying the Onverwacht Group and 3) the Moodies Groups (3.260-3.225 Ma) at the top (Viljoen and Viljoen, 1969, Kröner *et al.*, 1991; Byerly *et al.*, 1996; Lowe and Byerly, 1999 – Fig. 2.1).

2.1.1 – *The Onverwacht Group*

It consists predominantly of komatiites, komatiitic basalts, basalts and cherts with minor contribute of dacites, rhyolites and clastic sedimentary rocks. It can be divided into Sandspruit Formation (Fm), Theespuit Fm., Komati Fm., Hooggenoeg Fm., Kromberg Fm. and Mendon Fm. (Viljoen and Viljoen, 1969, Kröner *et al.*, 1991; Byerly *et al.*, 1996; Lowe and Byerly, 1999). The Hooggenoeg Formation hosts a set of potassic lavas contemplated in Diergaardt (2013), which is part of the fuel for this work. The Hooggenoeg Fm. is formed by a thick succession of tholeiitic basalts, komatiitic basalts and thin chert layers (Viljoen and Viljoen, 1969). On the top, there are felsic volcanic and volcanoclastic rocks, conglomerates and sandstones, besides some felsic intrusive rocks, dated at 3.451 Ma and 3.445 Ma (Diergaardt, 2013). The Onverwacht Group is interpreted to be deposit in a shallow marine environment between 3.55-3.25 Ga (Lowe and Byerly, 2007).

2.1.2 – The Fig Tree Group

It overlays the Onverwacht Group and consists of interstratified clastic units and dacitic to rhyolitic volcanic and volcanoclastic rocks (Lowe and Byerly, 2007). It is interpreted to be deposit in deep to shallow marine environment.

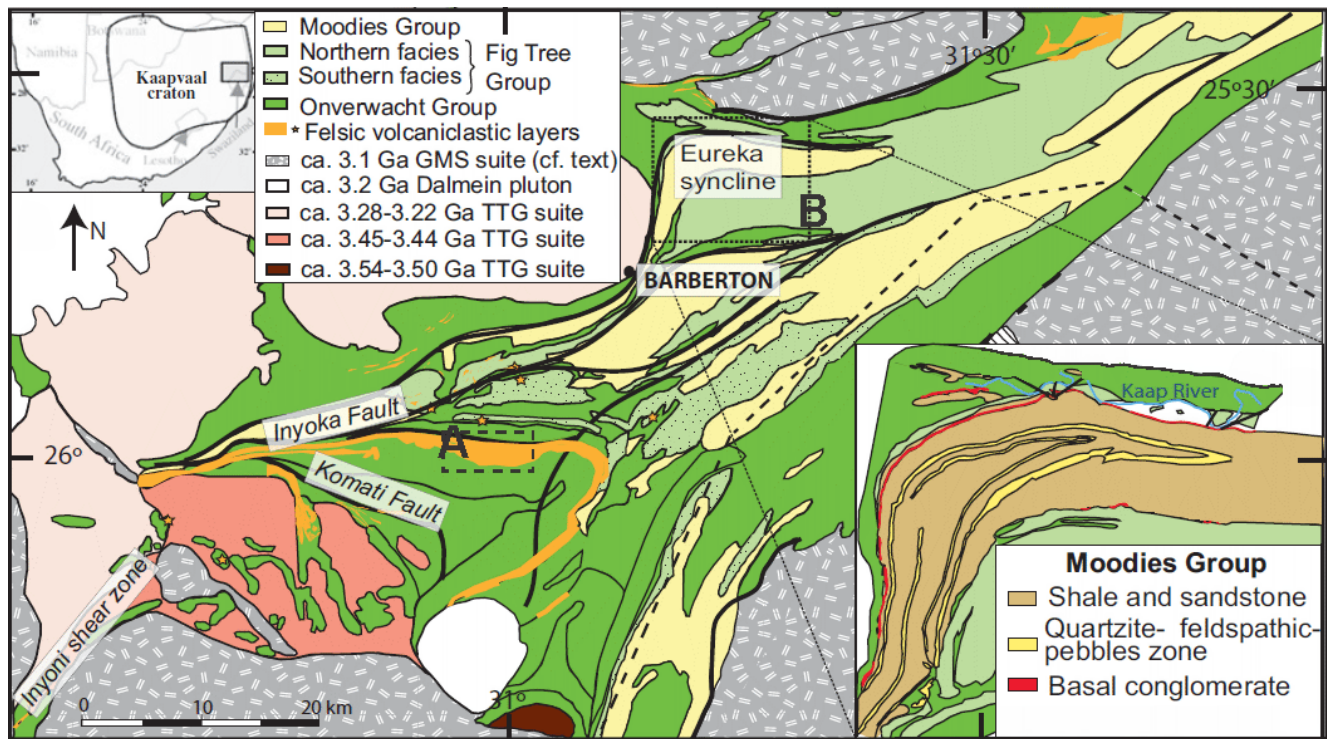


Figure 2.1 – Simplified geological map of the Barberton Greenstone Belt, highlighting the **A**) area of sampling for felsic volcanic rocks in the Hooggenoeg Formation (Diergaardt, 2013) and **B**) a zoom in the Eureka syncline, where some potassic granitic clasts were found within the basal conglomerate in the Moodies Group (extracted from Sanchez-Garrido *et al.*, 2011).

2.1.3 – The Moodies Group

It consists of coarse clastic sedimentary rocks such as sandstones, conglomerates and siltstones of lithic, feldspathic and quartzose composition. The Moodies Group was dated at 3.225-2.215 Ma. It is interpreted to be deposited during discrete contractional and extensional basins, reflecting an orogenic uplift (Lowe, 1999).

2.1.4 – The Evolution of the BGB

Moyen *et al.* (2007) described four evolutionary stages for the BGB. Within the Onverwacht Group, two events can be recognized by and associated with two TTGs intrusions. The first stage is

marked by the production of mafic and subsequent felsic volcanism, forming the Theespruit Formation, which was then intruded by felsic volcanic layers at 3.55-3.50 Ga (Kröner *et al.*, 1996). The geological settings are still unclear (Lowe and Byerly, 2007; Moyen *et al.*, 2007). The second stage is represented by mafic, ultramafic and minor amounts of felsic magmatism that originated the Komati, Hooggenoeg and Kromberg Formations. The felsic layer is located in the Hooggenoeg Formation and was dated at 3.451 Ma (de Vries *et al.*, 2006). Some clastic sediments and conglomerates can also be observed, what illustrate that topography existed in this time of Earth's history (Moyen *et al.*, 2007). Furthermore, it was proposed that these rocks association represents an environment of oceanic arc (Lowe, 1999; Lowe and Byerly, 2007; de Vries *et al.*, 2006).

The third evolutionary event was the amalgamation and suturing of tectono-stratigraphic suites to form a proto-continent, registered in the metamorphism and deformation of 3.230 Ma (Lowe and Byerly, 1999). The metamorphism reached high grade in the south and low-grade greenschist in the north of the BGB (Diener *et al.*, 2005; Kisters *et al.*, 2003; Moyen *et al.*, 2006). The event is also represented by the 3.23-3.21 Ga TTG plutons (Kröner *et al.*, 1991; de Ronde and Kamo, 2000) and sediments deposition of the Fig Tree (transition from deep to shallow marine – Lowe and Byerly, 2007) and Moodies Groups (terrigenous sandstones and conglomerates from the orogenic uplift – Lowe, 1999).

The last evolutionary stage of the BGB is characterized by intraplate thickening and compression, resulting in the crustal melting to form the GMS group at 3.216-3.100 Ma (Lowe, 1999).

The TTG plutons are very well preserved and contain valuable information concerning the development of the BGB, in particular constraints of the magma source conditions and its geodynamic setting. Some of these rocks formed at the same time as the felsic volcanic rocks (Fig. 2.2).

2.1.5 – The TTGs of the BGB

TTG plutons are the main component of the Archaean continental crust today (Martin, 1994). They are sodic leucocratic igneous rocks dominantly formed by plagioclase (~60%) and quartz (15-20%). Biotite is subordinated and k-feldspar is absent or constituent of minor components. Mafic layers are represented by biotite (5-15%) with hornblend rarely showing. The accessory minerals are characterized by epidote, allanite, apatite, secondary chlorite and zircon (Moyen *et al.*, 2007).

The genesis of the TTGs from the BGB can be associated to 1) the 3.55-3.50 Ga, characterized by the tonalitic Steyndorp Pluton (Kröner *et al.*, 1996); 2) the 3.45 Ga TTG production, represented by the Stolzburg and Theespruit plutons and 3) the 3.23-3.21 Ga generation represented by the Kaap Valley and Nelshoogte plutons as well as the Badplaas gneissic unit (Fig. 2.3). There is a fourth plutonic event at 3.14-3.10 Ga which marks the transition to the granite-monzonite-syenite (GMS) magmatism.

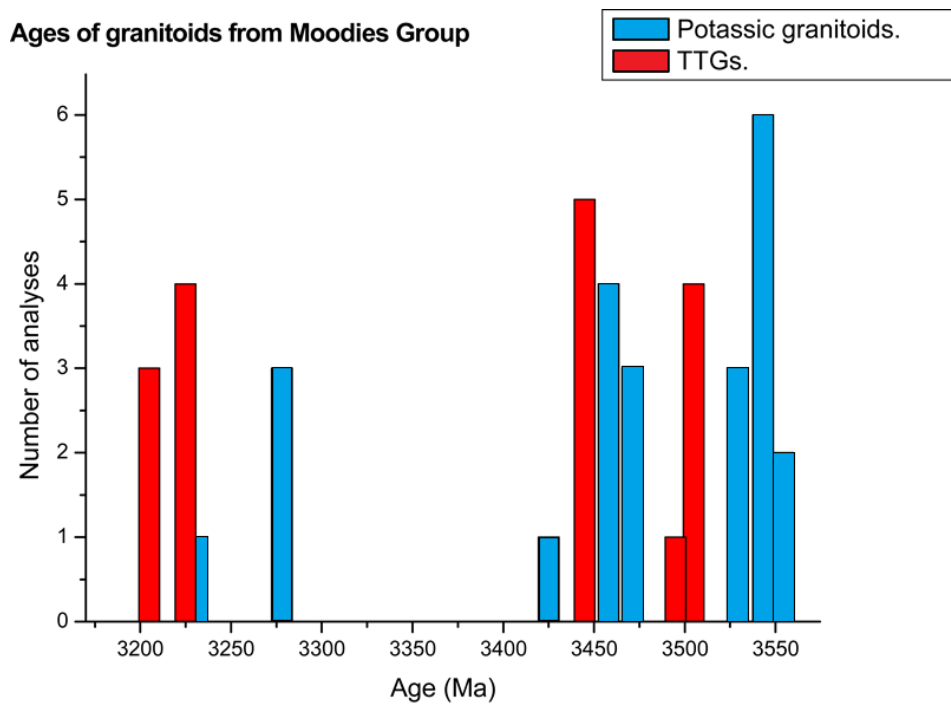


Figure 2.2 – Ages of the potassic granitoid clasts and felsic volcanism in comparison with the TTG plutons age from the BGB.

2.1.6 – Geochemistry and petrogenesis of the TTGs from the BGB

The TTG formation is associated with a high pressure partial melting of hydrous mafic rocks such as amphibolites (Foley *et al.*, 2002) or eclogites (Rapp *et al.*, 2003; Laurie and Stevens, 2012). Experimental and geochemical research has strongly supported this theory (Moyen and Stevens, 2006).

The three generations of TTGs in the BGB have been subdivided into three geochemical types by Moyen *et al.* (2007) based on the K_2O , Na_2O , Al_2O_3 , Sr and Eu content. The three groups are: 1) K_2O -poor with “low” or “high” amounts of Sr; 2) K_2O -rich sub-series and 3) extremely low K_2O , with a positive Eu/Eu* ratio, lower Na_2O and higher Al_2O_3 than those rocks in group 1, “melt depleted” sub-series (Moyen *et al.*, 2007).

It is possible to constrain the pressure conditions of TTG genesis considering which minerals are likely to retain Al_2O_3 , Na_2O , Sr, Y and Yb in the residuum during partial melting. Therefore the conditions for high SiO_2 , Al_2O_3 , Sr, Na_2O and depleted HREE TTG melts can be theoretically recreated by geochemical modelling (Diegaard, 2013). For that, three groups can also be identified: Low Pressure (LP); Medium Pressure (MP) and High Pressure (HP) TTGs (Moyen, 2011 – Fig. 2.4).

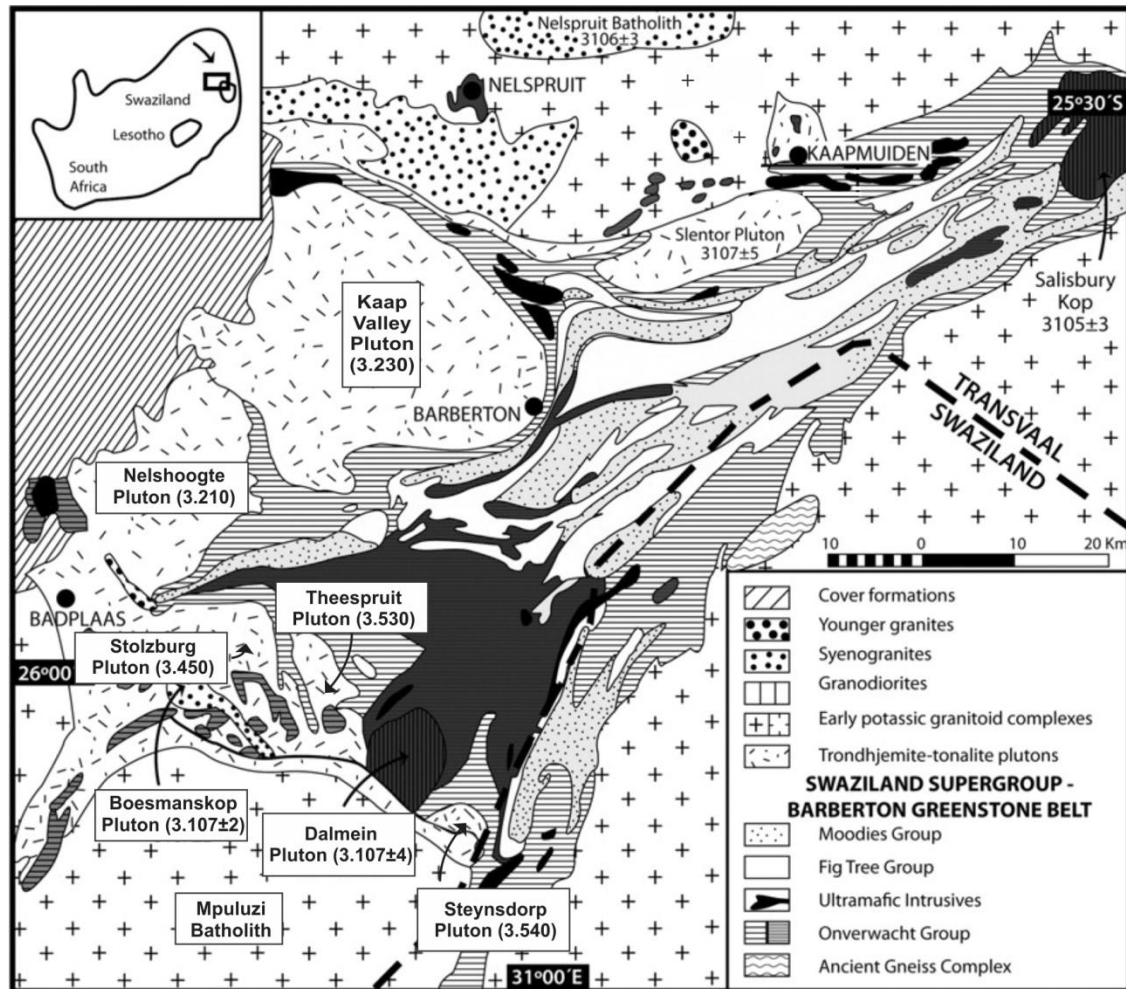


Figure 2.3 – Barbeton Greenstone Belt map highlighting the TTG plutons and their ages in million years Ma (modified from Toulkeridis *et al.*, 2010, based on the ages from Moyén *et al.*, 2011 and Moyén and Martin, 2012).

2.1.7 – Geochemistry of the potassic granitoid clasts from the BGB

In the Barberton Greenstone Belt there is a granite-monzonite-syenite (GMS) suite which corresponds to late felsic batholiths, emplaced after the BGB deformational events, at 3.210 Ma (Schoene *et al.*, 2008; de Ronde and de Wit, 1994). It is interpreted to be synchronous to the terrane amalgamation. Nevertheless, it has been documented a potassic granitoid older than most of the TTGs, but chronocorrelated to them (Sanchez-Garrido *et al.*, 2011,; Sanchez-Garrido *et al.*, 2012; Diegaard, 2013 – Fig. 2.2).

These potassic granitoids have low contents of CaO (0.05 wt% in average) despite displaying reasonable values of Sr (12–330 ppm). They fit into the S-type granites (Fig. 2.5). Schmidt *et al.* (2004) demonstrated that a felsic magma rises from the partial melting of a MORB slightly enriched in

potassium, although in their experimental results the CaO content is quite high (>2 wt%). The amount of experimental work done taking in account the phengite component of the eclogite is still little.

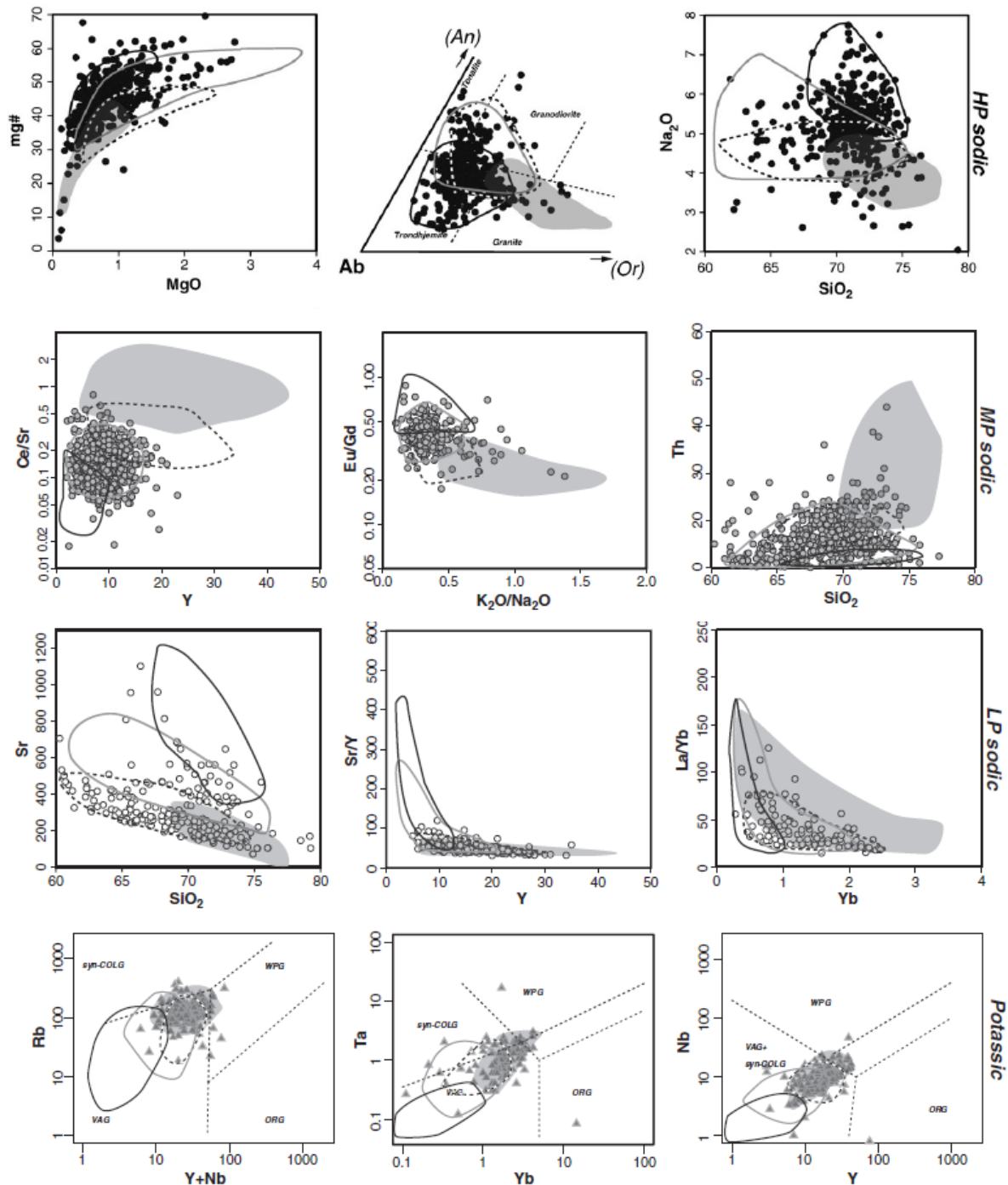


Figure 2.4 – Binary and ternary diagrams showing the geochemistry characteristics of the three TTG groups and the potassic rocks studied by Moyen (2011). In all diagrams, the **LP** (low pressure) group corresponds to white symbols (and the distribution of the data points is outlined by a dashed field); **MP** (medium pressure) group grey symbols and a grey outline; and **HP** (high pressure) group correspond to black symbols with black outline. The **potassic** samples are triangles with a shaded outline (extracted from Moyen, 2011).

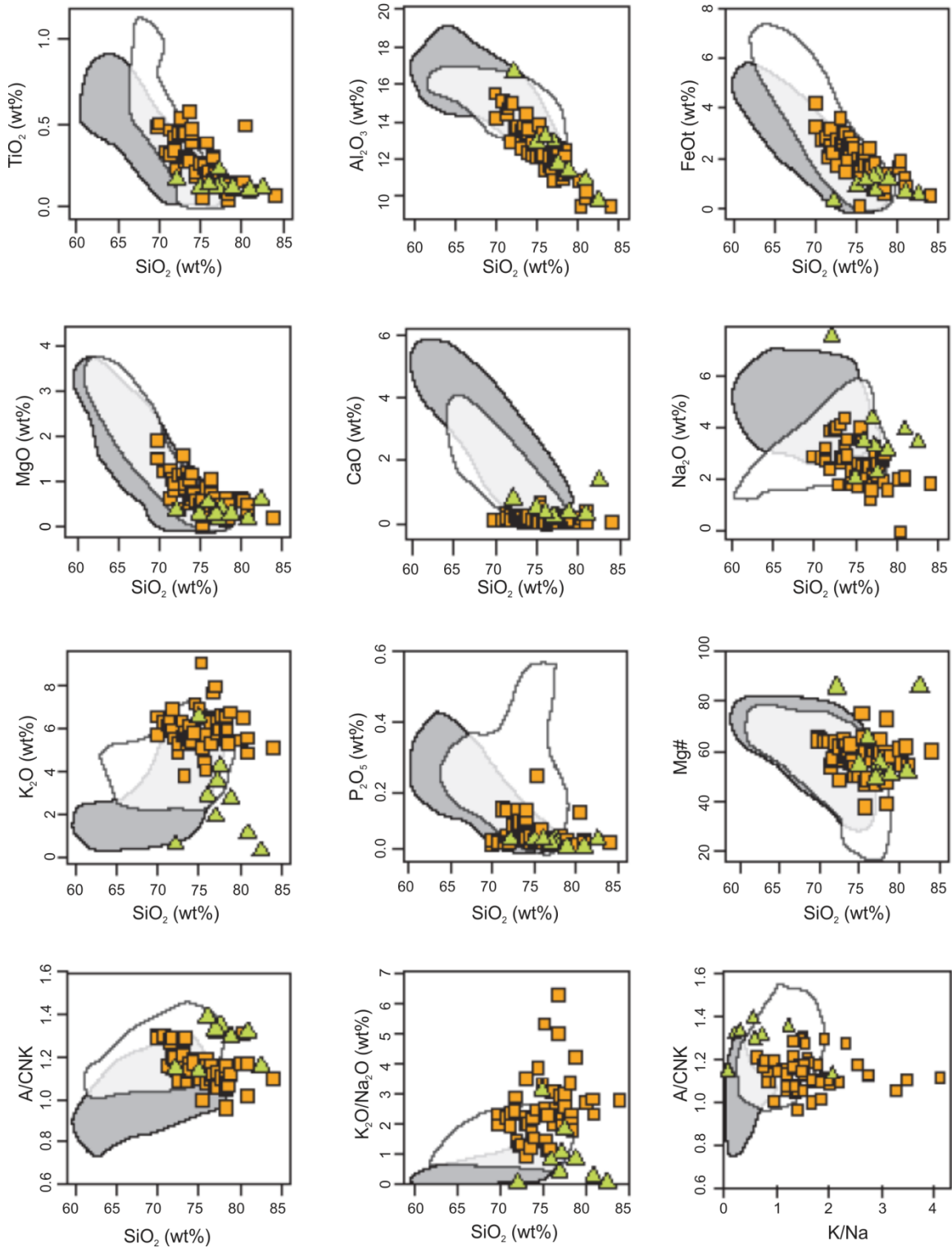


Figure 2.5 – Harker diagrams for major elements displaying the Moodies granites (orange squares) and the Theespruit felsic schists (green triangles). The grey field corresponds to the TTGs of the BGB and the white field to S-type granites (extracted from Sanchez-Garrido, 2011).

The potassic granitoid pebbles were dated at three different ages: 1) 3.55 Ga; 2) 3.43 Ga and 3) 3.23 Ga (Sanchez-Garrido *et al.*, 2011). They are all, in general, older than the TTG plutons. They are however time correlated.

The granitic pebbles from the basal conglomerate of Moodies Group, documented by Sanchez-Garrido (2011), are dominated by K-feldspar and albite. The most Ca-rich plagioclase displays An₁₂. The feldspars show occasionally zoning from the core towards the rim. It also has exsolutions of k-feldspar in albitic plagioclase. It is stated that two feldspars were probably present during crystallization. The whole rock analyses for these clasts have shown that they are silica rich (69.86-84.02 wt.%) and potassium rich (3.78-9.02 wt.%) (Fig. 2.5). They all plot in the granitic field within the An-Ab-Or ternary diagram (Sanchez-Garrido *et al.*, 2011 – Fig. 2.6).

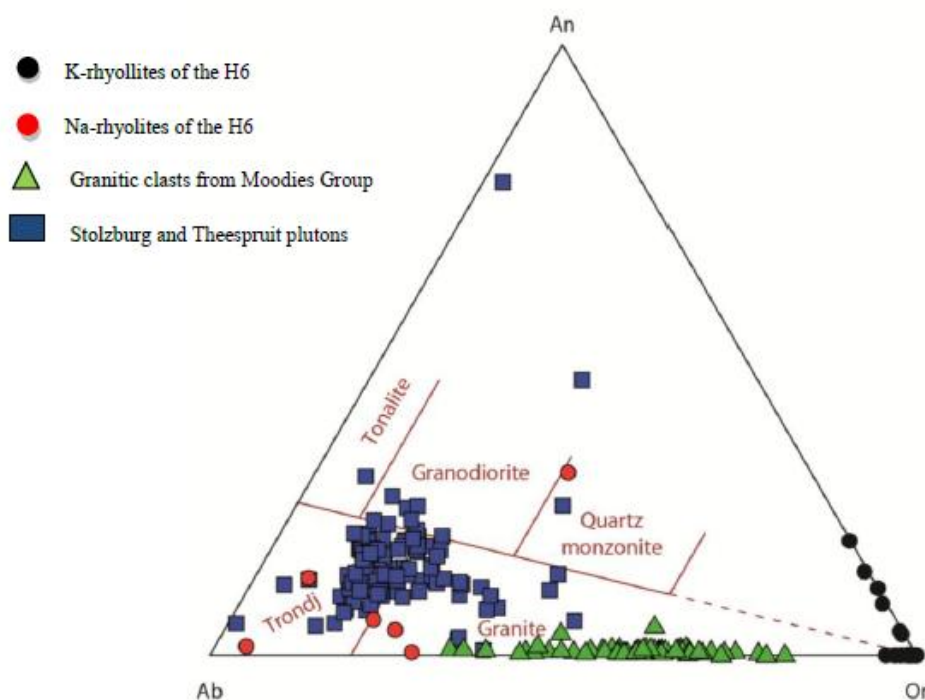


Figure 2.6 – Ternary feldspar diagram from the clasts in the Moodies group (green triangles) and the Hooggenoeg Formation (black and red circles). The blue squares correspond to the TTGs of the Stolzburg and Theespruit plutons (extracted from Diegaard, 2013).

The big difference of these k-rich granitoids from normal ones is their relatively broad range of SiO₂, the anomalous low values of CaO and P₂O₅ and the negative trend of the A/CNK (Al₂O₃/CaO+Na₂O+K₂O) vs. SiO₂. They have low Rb and high Sr content for a S-type granite and thus plot closer to the TTG field, showing some affinity to those rocks. The Ba and Y values, however, are significantly higher and indicate a strong S-type granite correlation (Fig. 2.7). According to this data, the

granitic clasts from Sanchez-Garrido *et al.* (2011) can be classified as S-type granites, but their chemical particularities would support a different origin for them. One possibility is the partial melting of k-rich sediments subducted with the ocean slab.

The rhyolites from Hoogenoeg Formation documented by Diegaardt (2013) are very similar. They are dominated by k-feldspar (up to 61%) and quartz and subordinately, albite (Fig. 2.6). The whole rock analyses provided high contents of SiO₂ (66.09-76.49 wt.%) and K₂O (0.45-9.69 wt.%) whereas the CaO has values often below 1 wt.%. It shows high contents of Light Rare Earth Elements (LREE) and low Heavy Rare Earth Elements (HREE).

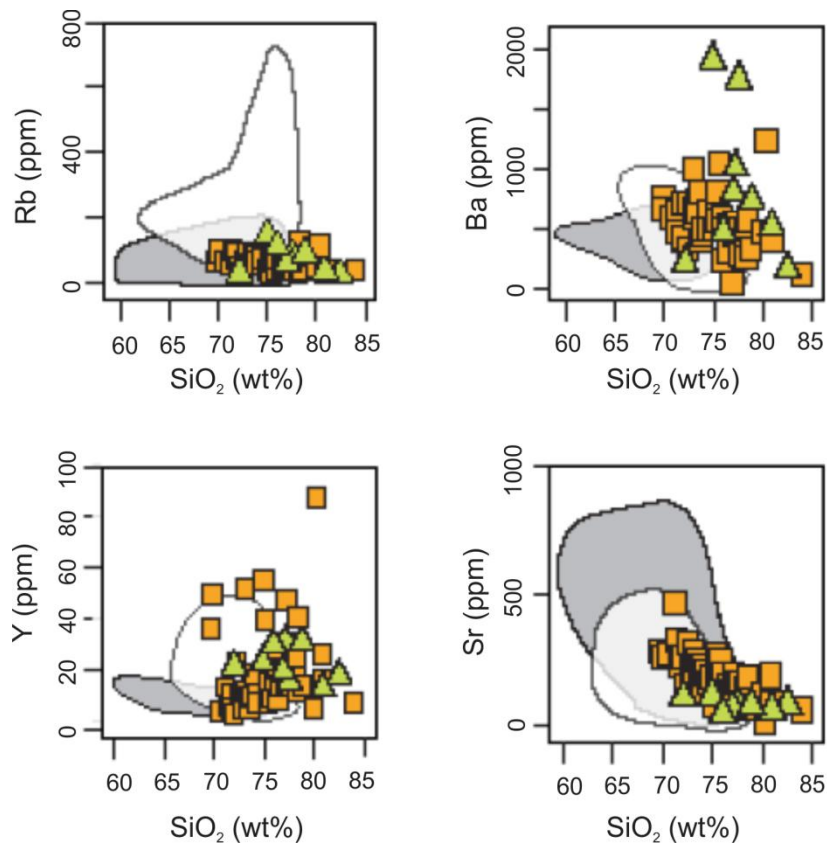


Figure 2.7 – Harker diagrams for some trace elements displaying the Moodies granites (orange squares) and the Theespruit felsic schists (green triangles). The grey field corresponds to the TTGs of the BGB and the white field to the S-type granites (extracted from Sanchez-Garrido, 2012).

2.2 – THE COUCAL FORMATION IN THE EAST PILBARA CRATON

The East Pilbara Terrane is dominated by Paleo to Mesoarchean granite-greenstones. The lowest stratigraphic unit is Warrawoona Group which is a 3.53-3.42 Ga volcanosedimentary succession dominated by pillowed tholeiitic and komatiitic basalt (Van Kranendonk *et al.*, 2007). Felsic volcanic and volcanoclastic rocks regionally comprise less than 15% of the succession, but locally form andesite to rhyolite-dominated sequences. They were dated at 3.47 Ga (Duffer Formation) and 3.43 Ga (Panorama Formation – Jahn *et al.*, 1981; Hickman, 1983). The oldest is the Coucal Formation, comprised of basalts and andesites to dacitic volcanic and volcanoclastic rocks. This formation is 3.53-3.50 Ga (Buick *et al.*, 1995; Smithies *et al.*, 2007). Two groups can be individualized representing a series of mafic to felsic volcanic rocks: the Coonterunah F1 and F2. The Coonterunah F2 ranges from basalt to andesite, with a silica varying from 48 to 58 wt.%. Both groups have low to medium values of potassium, with a K₂O/Na₂O range between 0.05 and 0.45 which shows no evolutionary trend to higher K₂O.

Coonterunah F2 rocks form part of a fractionated tholeiitic series. Basaltic members of Warrawoona Group in general fall within the wide compositional range of typical Archean basalts and show very weakly fractionated MORB-like trace-element patterns that vary from 4 to 10 times primitive mantle values (Smithies *et al.*, 2009).

CHAPTER 3

SCIENTIFIC PAPER PRESENTATION

WATER-PRESENT ECLOGITE MELTING –THE EFFECTS OF PHENGITE AND WATER IN THE PARTIAL MELTING OF BASALTIC ROCKS IN EARTH’S EARLY CRUSTAL DEVELOPMENT

Leonardo Azevedo Sa Alkmin^{1,2}, Gary Stevens², Cristiano de Carvalho Lana¹

Abstract: The tonalite-thondjemite-granodiorite (TTGs) suites of granitoid rocks were dominant during the formation of the felsic continental crust in the Archean. TTGs are granitoids characterized by high contents of silica (typically higher than 68 wt.% SiO₂) and sodium, with low potassium-sodium ratios (Na₂O ~4.65 wt%; K₂O/Na₂O ~0.4), low La/Yb ratios (~48) and low Yb concentration (~0.6 ppm) (Smithies *et al.*, 2009). It was demonstrated by Laurie and Stevens (2012) that TTG melts with compositions very similar to the average Archean trondhjemite can be generated through partial melting of water saturated eclogitic rocks, under pressure and temperature (PT) conditions consistent with Archean subduction. Within the Barberton greenstone belt, TTG magmatism occurred at ca 3.55, 3.42 and 3.23 Ga. Sanchez-Garrido *et al.* (2011) and Diegaard (2013) documented potassic and peraluminous granites which occur as clasts within conglomerates and felsic volcanism in the greenstone belt to have ages of 3.550±45 Ma, 3.460±34 Ma and 3.270±36 Ma. These granites differ from typical S-type granites in that they are characterized by very low CaO (0.30 wt% in average), despite having reasonable Sr (12–330 ppm). Sanchez-Garrido *et al.* (2011) proposed that these granites formed by anatexis of sedimentary rocks subducted with oceanic crust as an explanation of the coeval production of peraluminous granite and TTG magmas. This study has experimentally investigated the possibility that the TTG and S-type granite magmas were produced by the same source as a consequence of high pressure melting. The experiments have used the composition proposed by Smithies *et al.* (2009) for Archean oceanic crust, in conjunction with PT conditions consistent with the Archean subduction zone thermal structure proposed by Laurie *et al.* (2012). Experiments conducted demonstrate that at relatively low temperature (800°C to 850°C at 2.5 GPa) the mafic source produces peraluminous granitic melts with low CaO contents (0.88 wt% in average).

Key-words: Phengite, water-present partial melting, early crustal development, Archean, experimental petrology, TTG, potassic granitoids, Barberton Greenstone Belt.

3.1 – Introduction

The TTG suite (trondhjemite-tonalite-granodiorite) is the main archetype of Archean rocks and lies in the very core of what we understand today as Earth's early crustal development. They have a sodic leucocratic character, showing high ratios of Na:K and Na:Ca (Martin, 1994; Martin and Moyen, 2002). It has been consensual that the origin of these rocks is associated with the partial melting of oceanic slabs under eclogite facies conditions (Moyen and Stevens, 2006; Laurie and Stevens, 2012). Moyen (2011) has defined three different settings for the rising of TTG magmas: low pressure (LP) (<1.5 GPa), medium pressure (MP) (1.5 – 2.0 GPa) and high pressure (HP) (>2.0 GPa). The HP-TTGs are dominantly trondhjemitic with high Sr content (>300 ppm) and low Nb-Ta ratios (<7 ppm Nb; <0.5 ppm Ta). This is interpreted to indicate the absence of plagioclase in the residuum as well as the presence of rutile (Foley *et al.*, 2002; Martin and Moyen, 2002; Schmidt *et al.*, 2004). HP-type Archean TTGs also display high Mg#s compared to other leucocratic magmas (Martin and Moyen, 2002). Production of magma at reasonable temperatures needs water in the source (Tuttle and Bowen, 1958; Wyllie and Tuttle, 1961; Clemens, 1984). Considering the high pressure of partial melting required so the plagioclase would be absent in the residuum, it possibly indicates that HP-type TTG magmas form by anatexis of the upper portions of oceanic slabs within Archean subduction zones (Condie, 1981; Martin, 1999; Smithies and Champion, 2000; Foley *et al.*, 2002; Rapp *et al.*, 2003; Smithies *et al.*, 2003, Laurie and Stevens, 2012). TTG magmas generated by this process have been considered to be a product of fluid-absent melting of amphibole (Moyen and Stevens, 2006). However, water drives the Phanerozoic arc magmatism (e.g. Schmidt and Poli, 1998; Connolly and Pettrini, 2002) and it could have played a major role in the Archean subduction environment. Laurie *et al.* (2012) has demonstrated how water can make oceanic slabs fertile and therefore attain partial melting on their upper part.

The TTGs are usually associated with postdated potassium granitoids (e.g. Lowe and Byerly, 2007; Lana *et al.*, 2013). These granitoids are interpreted to be a byproduct of the partial melting of continental crust during the terrane amalgamation and cratonization stage and are, in general, younger than the TTGs. However, an exception was documented in the Barberton Greenstone Belt (BGB) by Sanchez-Garrido *et al.* (2011, 2012) and Diegaardt (2013). Potassic granitoid pebbles and felsic volcanic rocks were found in basal conglomerates and felsic layers. These rocks are not the typical felsic magmatism with granite-monzogranite-syenite (GMS) series. Firstly, they are older than the TTGs that outcrop along with them and secondly, they have a distinctive geochemistry signature. The whole rock analyses show that they are K-rich (3.5 to 9.0 wt%) and Ca-poor (averages <1 wt% - Sanchez-Garrido *et al.*, 2011; Diegaardt, 2013). They also exhibit relatively high amounts of Sr and Cr and low amounts of Rb, despite fitting the S-type granite series (Sanchez-Garrido *et al.*, 2011).

The genesis of these potassium-rich rocks have been attributed to sedimentary rocks coupled to the subducting slab which would undergo partial melting in high pressure conditions, above the plagioclase stability field. The potassium would then be concentrated in a phengite component. This proposition is nonetheless yet to be tested and thorough investigation needs to be performed in the process that drives the partial melting in high pressure conditions of Archean rocks. Schmidt *et al.* (2004) have successfully produced a felsic run product from partial melting a MORB starting material. The result, however, has a significant concentration of CaO that does not match the older felsic rocks. This study aims to investigate the possibility to produce a felsic magma from partial melting a slightly enriched oceanic slab in the eclogite facies condition, previously to the process which would rise the TTG magmas.

3.2 – Geological settings

The Barberton Greenstone Belt, located in east South Africa and west Swaziland preserve some of the oldest rocks on Earth and is therefore an ideal laboratory to study the early process of continental crustal development. The rocks there are TTG- or GMS-like granitoids and supracrustals from the Swaziland Supergroup. This supregroup can be divided into three units: 1) the Onverwacht Group; 2) the Fig Tree Group and 3) the Moodies Group. The Onverwacht Group is constituted of mafic to ultramafic rocks, interpreted to be deposited in a shallow marine environment between 3.55 to 3.25 Ga (Viljoen and Viljoen, 1969, Kröner *et al.*, 1991; Byerly *et al.*, 1996; Lowe and Byerly, 1999, 2007) and is subdivided into 6 formations. The Hooggenoeg Formation is one of them and comprises a succession of tholeiitic basalts and volcanoclastic rocks, conglomerates, sandstones and some felsic intrusive rocks dated at 3.451 Ma and 3.445 Ma (Diegaardt, 2013). These rocks are remarkable for their different geochemistry character in comparison of normal felsic granitoids. The Fig Tree Group consists of interstratified clastic units and dacitic to rhyolitic volcanic and volcanoclastic rocks deposited in deep to shallow marine environment (Lowe and Byerly, 2007). The Moodies Group comprises coarse clastic sedimentary rocks such as sandstones, conglomerates and siltstones of lithic, feldspatic and quartzose composition. It is interpreted as a discrete contractional and extensional basin deposited during an orogenic uplift at 3.225 Ma to 2.215 Ma (Lowe, 1999). In a basal conglomerate of the Moodies Group in the Eureka syncline, Sanchez-Garrido *et al.* (2011) documented granitoids pebbles with a particular geochemistry composition. They are potassium-rich and calcium-poor, although they fit into the S-type granites geochemistry (Sanchez-Garrido *et al.*, 2011). They were found mainly as clasts, spatially oriented according to a shear zone and to the regional trend, included in the foliation of the hosting conglomerate.

The TTGs are distributed in different plutons around the BGB. They are leucocratic and sodic, with high concentrations of Na and high Na:Ca and Na:K ratios (Moyen *et al.*, 2007). They built part of the Archean continental crust in three episodes: 1) 3.538 to 3.509 Ma; 2) 3.470 to 3.443 Ma and 3) 3.290

to 3.216 Ma (Kamo and Davis, 1994; Schoene *et al.*, 2008; de Ronde and de Wit, 1994; Kisters *et al.*, 2010). Potassic granitoid plutonism in the BGB occurred between 3.236 Ma and 3.100 Ma. It is represented by the Usutu suite (Schoene and Bowring, 2010), the Dalmein pluton (Lana *et al.*, 2010), and the granodiorite-monzogranite- syenogranite (GMS) batholiths (Schoene *et al.*, 2008; de Ronde and de Wit, 1994). This magmatism coincides with the 3.210 Ma terrane amalgamation (Moyen *et al.*, 2006). The exceptions are the pebbles found in the Moodies Group basal conglomerate (Sanchez-Garrido *et al.*, 2011) and the felsic volcanism from the Hooggenoeg Formation (Diegaardt, 2013).

The BGB had four evolutionary stages (Moyen *et al.*, 2007). Within the Onverwacht Group, two events can be recognized associated with two TTG intrusions. The first stage is marked by the production of mafic and subsequent felsic volcanism, which was then intruded by felsic volcanic layers at 3.55-3.50 Ga (Kröner *et al.*, 1996). The geological settings are still unclear (Lowe and Byerly, 2007; Moyen *et al.*, 2007). The second stage is represented by mafic, ultramafic and minor amounts of felsic magmatism. Some clastic sediments and conglomerates were also documented, evidencing an ancient topography (Moyen *et al.*, 2007). Furthermore, it was proposed that these rocks association represents an environment of oceanic arc (Lowe, 1999; Lowe and Byerly, 2007; de Vries *et al.*, 2006). The third evolutionary event was the amalgamation and suturing of tectono-stratigraphic suites to form a proto-continent, registered in the metamorphism and deformation of 3.230 Ma (Lowe and Byerly, 1999). The last evolutionary stage is characterized by intraplate thickening and compression, resulting in crustal melting to form the GMS group at 3.216-3.100 Ma (Lowe, 1999).

3.3 – Experimental and analytical procedures

Water-present partial melting experiments were first equilibrated at 2.5 Ga and 600°C for 6 days and then conducted at 2.5 Ga and between 790 and 850°C for extra 14 days. The experimental conditions are summarized in Table 3.1.

3.3.1 – Starting Material

This experiment tests the hypothesis of felsic melt production from an oceanic crust starting material, analogous to an Archean oceanic slab. For the lack of time in order to find candidates for oceanic crust in situ, well preserved, undeformed, unmetamorphosed and test them previously, it was opted for the use of a synthetic gel. This choice allows the compositional control of the starting material and some adjustments if necessary. It has the disadvantage that in order to achieve equilibrium, the experiment will have to grow a large garnet fraction (~ 35%) and it can affect melt major and trace element compositions. This is especially true for HREE, due to a different diffusion rate in the garnet, which could lead to a zoning in terms of HREE (e.g Chakraborty *et al.*, 1995; Skora *et al.*, 2006). The garnet proportion in the

starting material (~30 wt.%) is according to the conventional metamorphic modelling that suggests that garnet proportions of more than 30% are common in MORB compositions within the high pressure range (Deer *et al.*, 1997).

Table 3.1 - Experimental run conditions and products.

Exp. run	Starting Material	P (Gpa)	Dev.	T (°C)	Dev.	Duration (days)	H ₂ O (wt.%) ^a	Mineral Assemblage ^b
<u>ESM-1</u>								
1		2.5	0.1	600	1	10	10	Cpx, Gt, Wm, Qz, Rt, (Ilm)
2		2.5	0.1	800	1	21	10	Cpx, Gt, Bt, Rt, (Ilm), glass, vapour
3		2.5	0.1	850	2	21	10	Cpx, Gt, Bt, Rt, (Ilm) glass, vapour
<u>ESM-2</u>								
4		2.5	0.1	790	1	21	1.1	Cpx, Gt, Wm, Bt, (Fa), glass
5		2.5	0.2	820	1	16	1.1	Cpx, Gt, Wm, Bt, Rt, (Fa), glass

^a H₂O represents the weight percentage of distilled water added to the experimental capsule before it was sealed. The values are maximum concentrations.

^b Phases in brackets occur as relict phases; Grt—garnet; Cpx—clinopyroxene; Rt—rutile; Ilm—ilmenite; Qtz—quartz; Wm—white mica; Bt—biotite; Fa—fayalite.

The suitable starting material can only be found in collisional zones with exhumation of oceanic crust, so the composition would be low in K₂O and Mg# (Moyen and Stevens, 2006). The bulk compositions of average N-MORB and basaltic rock from Pilbara Craton in Australia (Smithies *et al.*, 2009) have been interpreted as a possible source for the TTGs granitoids. These rocks are found in the Coucal Formation (C-F2b) and its composition was used to craft two different gels, one water saturated and the other subsaturated (Table 3.2).

The starting material ESM-1 was crafted using TEOS (tetraethylorthosilicate) for the silica, TiO₂ powder for the titanium, Al metal powder for aluminum, Fe²⁺ metal sponge and Fe₂O₃ powder for total iron, Mg powder for magnesium and carbonates of calcium, potassium and sodium for their respective elements. The carbonates, Mg and Al powder were added to a beaker with nitric acid (HNO₃ 1:1 distilled water) and heated in a hot plate until all the elements were dissolved. The solution was then left to evaporation until near dryness. The solid nitrates were diluted with deionized water. Then, a mixture of TEOS and ethanol was added (vol. TEOS = vol. ethanol = vol. deionized water). Ammonium hydroxide (NH₄OH) was slowly added until a stiff gel was acquired and then the whole beaker was left to dry in an oven at 110°C for a whole day. In the end, the mixture was heated in a Bunsen beak until all the NO₂ fumes were dismissed and put in a furnace at 1000°C so the remaining nitrates would turn into oxydes.

Table 3.2 - Major element geochemistry of the starting materials ESM-1 and ESM-2 and averaged normalized anhydrous experimental glass major element compositions. The average compositions for high pressure-type Archaean TTG (Moyen, 2011) and the average composition for felsic volcanic rocks (Diegandt, 2013) from the Barberton Granitoid Greenstone Terrain (BGGT), South Africa (Clemens *et al.*, 2006), are provided for comparison. The composition of C-F2b (Smithies *et al.*, 2009) was used as model to the starting material production, while the average global MORB (Winter, 2001) is provided for comparison. Bulk rock analysis for ESM was done via SEM-EDS and glass analyses were done using SEM-EDS with a cryostage.

	Ave. glass compositions					Ave. felsic pebbles (Sanchez-Garrido <i>et al.</i> , 2011)		Ave. felsic volcanic rocks (Diegandt, 2013)	
	ESM-1	ESM-2	C-F2b	Ave. MORB		2.5	2.5	2.5	2.5
P (GPa)					2.5	2.5	2.5	2.5	2.5
T (°C)					800	850	790	820	820
Initial H ₂ O (wt%)					10	10	1.1	1.1	1.1
N					2	3	4	5	
wt.%									
SiO ₂	46.1	47.4	46.5	50.5	73.8	0.2	77.2	0.2	53.6
TiO ₂	2.1	2.4	2.0	1.6	0.0	0.0	0.0	1.0	1.0
Al ₂ O ₃	15.3	15.4	15.0	15.3	16.5	0.1	13.6	0.1	22.4
FeO ^a	14.7	13.8	14.0	10.5	0.8	0.1	0.9	0.1	3.9
MgO	7.2	7.3	7.4	7.5	0.0	0.1	0.2	0.1	5.7
MnO	0.0	0.0	0.2	0.0	0.0	0.0	0.0	0.0	0.0
CaO	9.5	10.0	9.2	11.5	0.9	0.1	0.8	0.1	5.8
Na ₂ O	2.3	2.4	2.3	2.6	3.9	0.2	4.5	0.3	1.7
K ₂ O	1.0	0.8	0.9	0.2	4.2	0.1	2.8	0.1	6.2
P ₂ O ₅	0.0	0.0	0.1	0.1	0.0	0.0	0.0	0.0	0.0
Total	98.2	99.5	97.6	99.8	100	100	100	100	100
H ₂ O ^b					18.3		16.4		8.4
Na ₂ O/CaO					4.3		5.6		0.3
K ₂ O/Na ₂ O					1.1		0.6		3.6
Ferro ^c					0.8		1.1		10.6
Mg# ^d	46.6	48.5	48.5	56.0	-		28.4		78.9
AN/K					1.5		1.3		2.3
AC/NK					1.3		1.1		1.1

^a All Fe is expressed in FeO.

^b The water content was estimated from the total in the analyses.

^c Ferro = TiO₂ + FeO + MgO + MnO

^d Mg# = 100 * Mg / (Mg + Fe²⁺ + Fe³⁺)

The Ti and Fe were added in the end and the starting material “gel” was stored within a vacuum desiccator. Water was added later. For the ESM-2, the same procedures were used, but for the iron and water sources, fayalite and kaolinite respectively were added in the end of the gel making.

The starting materials ESM-1 and ESM-2 are both characterized by their eclogitic composition. They were heat up at 600°C and 2.5 GPa so the gel would attain equilibria. The mineral assemblage at this setting is Omp (~50%) + Gt (~30%) + Phg (~17%) + Qz (~2%) + Rt (~1%) (mineral abbreviations according to Kretz, 1983). Representative garnet and clinopyroxene compositions are provided in Table 3.3 and Table 3.4. The garnet in ESM is almandine-rich (61-68% alm, 18-27% grs, 11-20% prp – Table 3.3). The clinopyroxene is omphacitic but less sodic than the peak metamorphic omphacite (2.0 – 4.0 wt.% Na₂O – Table 3.4).

3.3.2 – *Experimental settings*

The experiments were performed in a non-end-loaded Holloway design with a 10 mm diameter pressure vessel for all the experiments. Temperature was controlled using a Depths of the Earth controller and a type-K (chromel–alumel) thermocouple. Pressure was measured with a Heisse gauge. In this configuration, the apparatus is considered to have an accuracy of approximately ± 5 °C and ± 0.01 GPa (Laurie and Stevens, 2012). The starting material powders were grinded until very fine grain size in an agate mortar under acetone. Small cylindrical-shape golden capsules (4 mm width and 10 mm length) were prepared out of gold foil with a welder. In experiments with ESM-1, water was added before closing the capsule, equivalent to 10 wt.% of the gel, ensuring a water saturation condition in the experiment. The gel was added to the capsule and then sealed with an arc welder, with its bottom in contact with cool water in a barrel to prevent evaporation of the water inside. The capsule was tested for holes in a recipient with water attached to a vacuum machine. If succeeded, the capsule was folded and pressed into a plug with boron nitride at 1000 psi and the resulting cylinder was grinded to fit into the graphite furnace. Inside the furnace, the samples were separated from the thermocouple only by an alumina disc 0.5 mm thick and by the golden walls of the capsules. The experiments used a salt sleeve around the furnace as they were all performed under 850°C. The pressure was added first and then the experimental set was heated isobarically until 600°C and left for 6 days. After this time, used for equilibrate the system before reaching the solidus, the final temperature increment was added and the system was left for 14 days. Once the experiments ended, the capsule was taken out, pierced, weighted and left in the furnace at 110°C for a whole day and then weighted again.

Table 3.3 - Garnet compositions from ESM-1 starting material and experimental run products. Garnet formulas calculated to 12 oxygen.

	Starting material		Experimental run products																	
	1		2				3				4				5					
P (GPa)	2.5		2.5				2.5				2.5				2.5					
T (°C)	600		800				850				790				820					
N	1		2				3				4				5					
wt.%	Ave.	σ	Ave.	Rep.	σ	Ave.	σ	Ave.	σ	Ave.	σ	Ave.	σ	Ave.	σ	Ave.	σ			
	core		core	rim		core	rim	core	rim	core	rim	core	rim	core	rim	core	rim			
SiO ₂	37.5	0.5	37.2	2.2	39.3	1.6	39.1	0.3	39.1	0.6	38.3	0.2	37.3	0.3	38.1	0.4	36.3	0.8	38.7	1.5
TiO ₂	3.0	1.8	1.8	0.5	1.2	0.5	1.1	0.4	1.3	0.8	0.8	0.4	1.0	0.2	0.9	0.2	1.1	0.6	0.6	0.1
Al ₂ O ₃	16.8	2.5	14.5	3.2	21.5	1.0	21.6	0.3	21.8	0.4	20.7	0.3	20.7	0.0	21.2	0.2	20.5	0.3	21.5	0.7
Cr ₂ O ₃	0.0	0.0	0.0	0.0	0.0	0.0	0.0	0.0	0.0	0.0	0.0	0.0	0.0	0.0	0.0	0.0	0.0	0.0	0.0	0.0
Fe ₂ O ₃	0.0	0.0	0.0	0.0	0.0	0.0	0.0	0.0	0.0	0.0	0.0	0.0	0.0	0.0	0.0	0.0	0.0	0.0	0.0	0.0
FeO	31.6	1.5	30.7	4.0	21.7	1.3	22.0	1.1	21.3	1.2	29.4	3.0	27.3	1.0	23.7	0.3	29.9	1.3	24.2	1.0
MnO	0.0	0.0	0.0	0.0	0.0	0.0	0.0	0.0	0.0	0.0	0.0	0.0	0.0	0.0	0.0	0.0	0.0	0.0	0.0	0.0
MgO	3.2	1.1	4.3	1.1	6.6	1.2	5.5	1.2	5.9	0.7	3.6	0.7	4.4	0.2	7.5	0.1	2.4	0.7	7.2	0.2
CaO	7.0	0.3	7.4	1.6	10.4	0.9	10.7	0.8	11.0	0.6	6.3	2.3	9.2	0.0	8.3	0.1	9.0	0.4	8.3	0.3
Na ₂ O	0.0	0.0	0.0	0.0	0.0	0.0	0.0	0.0	0.0	0.1	0.0	0.1	0.0	0.0	0.0	0.0	0.0	0.0	0.0	0.0
K ₂ O	0.0	0.0	0.0	0.0	0.0	0.0	0.0	0.0	0.0	0.0	0.0	0.0	0.0	0.0	0.0	0.0	0.0	0.0	0.0	0.0
Totals	98.3		99.8		100.7		99.9		100.4		99.1		99.9		99.6		99.2		100.5	
Si	3.1	0.0	3.0	0.2	3.0	0.0	3.0	0.0	3.0	0.1	3.0	0.0	2.9	0.0	3.0	0.0	2.9	0.0	3.0	0.0
Ti	0.2	0.1	0.1	0.0	0.1	0.0	0.1	0.0	0.0	0.0	0.1	0.0	0.1	0.0	0.0	0.0	0.1	0.0	0.0	0.0
Al	1.6	0.2	1.4	0.3	1.9	0.1	2.0	0.0	1.9	0.0	2.0	0.0	1.9	0.0	1.9	0.0	1.9	0.1	1.9	0.0
Cr	0.0	0.0	0.0	0.0	0.0	0.0	0.0	0.0	0.0	0.0	0.0	0.0	0.0	0.0	0.0	0.0	0.0	0.0	0.0	0.0
Fe ³⁺ ^a	0.0	0.0	0.0	0.0	0.0	0.0	0.0	0.0	0.0	0.0	0.0	0.0	0.0	0.0	0.0	0.0	0.0	0.0	0.0	0.0
Fe ²⁺	2.2	0.1	2.1	0.3	1.4	0.1	1.4	0.1	2.0	0.2	1.4	0.1	1.8	0.0	1.5	0.0	2.0	0.0	1.6	0.0
Mn	0.0	0.0	0.0	0.0	0.0	0.0	0.0	0.0	0.0	0.0	0.0	0.0	0.0	0.0	0.0	0.0	0.0	0.0	0.0	0.0
Mg	0.4	0.1	0.5	0.1	0.8	0.1	0.6	0.1	0.4	0.1	0.7	0.1	0.8	0.1	0.7	0.1	0.8	0.1	0.7	0.1
Ca	0.6	0.0	0.7	0.1	0.8	0.1	0.9	0.1	0.6	0.2	0.9	0.0	0.0	0.0	0.0	0.0	0.0	0.0	0.0	0.0
Na	0.0	0.0	0.0	0.0	0.0	0.0	0.0	0.0	0.0	0.0	0.0	0.0	0.0	0.0	0.0	0.0	0.0	0.0	0.0	0.0
K	0.0	0.0	0.0	0.0	0.0	0.0	0.0	0.0	0.0	0.0	0.0	0.0	0.0	0.0	0.0	0.0	0.0	0.0	0.0	0.0
Sum	8.0		8.0		8.0		8.0		8.0		7.9		8.0		8.0		8.0		8.0	
Mg# ^b	15.3		17.4		35.3		30.7		17.2		33.4		22.3		35.9		12.5		34.6	
Gr ^c	18.9		18.2		28.6		29.8		21.3		30.7		25.1		22.3		25.3		22.3	
Alm ^d	68.3		62.0		47.7		48.6		65.2		46.2		58.2		49.7		65.4		50.8	
Prp ^e	12.3		14.3		26.0		21.5		13.6		23.1		16.7		27.9		9.4		26.9	

^a Fe³⁺ calculated using method from Droop (1987).
^b Mg# = 100 * Mg / (Mg + Fe²⁺ + Fe³⁺).
^c Gr = Ca / (Ca + Fe + Mg + Mn).
^d Alm = Fe / (Ca + Fe + Mg + Mn).
^e Prp = Mg / (Ca + Fe + Mg + Mn).

Table 3.4 - Clinopyroxene compositions from ESM-1 starting material and experimental run products. Pyroxene formulas calculated to 6 oxygen.

	Starting Material		Run Products		Ave.	σ	wt.%	σ
	2.5	800	2.5	850				
P (GPa)	2.5	800	2.5	850	2.5	790	2.5	820
T (°C)	600	800	790	850	790	850	790	820
N	1	2	3	4	4	5	Ave.	Ave.
	Ave.	Ave.	Ave.	Ave.	Ave.	Ave.	σ	σ
wt.%	σ	σ	σ	σ	σ	σ	σ	σ
SiO ₂	46.7	53.2	1.9	54.1	54.6	54.8	0.9	0.6
TiO ₂	2.7	0.8	0.4	0.4	0.4	0.2	0.1	0.2
Al ₂ O ₃	15.9	11.1	1.2	9.0	10.9	10.8	0.3	0.5
Cr ₂ O ₃	0.0	0.0	0.0	0.0	0.0	0.0	0.0	0.0
Fe ₂ O ₃	0.0	0.0	0.0	0.0	0.0	0.0	0.0	0.0
FeO	11.8	6.0	1.1	5.6	5.3	4.8	0.4	0.2
MnO	0.0	0.0	0.0	0.0	0.0	0.0	0.0	0.0
MgO	8.1	8.5	1.0	10.3	9.5	9.9	0.3	0.5
CaO	10.5	13.8	1.3	15.6	15.1	15.0	0.4	0.8
Na ₂ O	2.8	4.2	0.5	4.7	4.4	5.0	0.1	0.3
K ₂ O	0.9	0.4	0.6	0.0	0.0	0.0	0.0	0.0
Totals	99.5	98.1	0.0	99.6	100.1	100.4	0.0	0.0
Si	1.7	1.9	0.0	2.0	1.9	2.0	0.1	0.0
Ti	0.1	0.0	0.0	0.0	0.0	0.0	0.0	0.0
Al	0.7	0.5	0.0	0.4	0.5	0.5	0.0	0.1
Cr	0.0	0.0	0.0	0.0	0.0	0.0	0.0	0.0
Fe ³⁺ ^a	0.0	0.0	0.0	0.0	0.2	0.1	0.0	0.0
Fe ²⁺	0.4	0.2	0.0	0.2	0.0	0.0	0.0	0.0
Mn	0.0	0.0	0.0	0.0	0.5	0.5	0.0	0.0
Mg	0.5	0.5	0.1	0.6	0.6	0.6	0.1	0.1
Ca	0.4	0.5	0.1	0.6	0.3	0.3	0.1	0.1
Na	0.2	0.3	0.0	0.3	0.0	0.0	0.0	0.0
K	0.0	0.0	0.0	0.0	0.0	0.0	0.0	0.0
Sum	4.0	3.9	0.0	4.0	4.0	4.0	0.0	0.0
Mg# ^b	56.3	72.7	76.6	76.6	76.2	78.6	4.0	4.0
Class ^c	Omp	Omp	Omp	Omp	Omp	Omp	Omp	Omp

^a Fe³⁺ calculated using method from Droop (1987).

^b Mg# = 100*Mg/(Mg + Fe²⁺ + Fe³⁺).

^c Clas = Omp – Omphacite.

3.3.3 – Analytical methods

The minerals and glasses from the run products and the starting materials were analysed under a Zeiss Evo MA 15 Electron Microscope (SEM), by a quantitative EDS (Energy Dispersive X-ray Spectrometry) and WDS (Wavelength Dispersive X-ray Spectrometry). Major elements were determined using EDS, through Oxford Instruments® X-MAS 20 m2 detector and Oxford INCA software. The glasses were quantified with WDS. The beam conditions during analyses were 20 kV, working distance of 8.5 mm and current around -20 nA. The live time counting was 15 s. Natural mineral and metals standards were used for standardization during analyses. The error range from ± 0.6 to 0.1 wt.% for major elements on EDS and ± 0.01 to 0.03 wt.% on major and trace elements on WDS. High resolution images were taken at the same time. When the glasses were analysed a cryo stage technique was used (e.g. Diener *et al.*, 2005; Moyer and Stevens, 2006) and the sample was cooled to -180°C . This way, the mobility of elements in a hydrous aluminous silicate glass became less likely. For Na_2O this is especially true (e.g. Vielzeuf and Clemens, 1992).

3.4 – Experimental results

Garnet and clinopyroxene coexisted with the melt in all the experiments performed and their composition is shown in Tables 3.3 and 3.4. In the water saturated experiments, quartz and phengite were consumed to produce the melt whilst they were still present in underwater saturated experiment (Fig. 3.1). The clinopyroxene in the run products are more sodic (Na_2O 4.2 – 4.7 wt.%), calcic (CaO 13 – 15 wt.%) and slightly more magnesian (MgO 8.5 – 10.2 wt.%). The garnet crystals have grown rapidly in the early stages of the experiments and kept a core slightly different than the rims. Most of these relicts are iron particles (ilmenite) trapped and kept unreactant to the melt components. The newly formed garnet are more calcic (CaO ~ 8.0 wt.%), magnesian (MgO 5.4 – 7.4 wt.%) and aluminium-rich (Al_2O_3 20.0 – 21.7 wt.%). They have less titanium (TiO_2 0.6 – 1.4 wt.%) and less iron (FeO 22.0 – 25.0 wt.%). One exception is the garnet found in the high temperature condition (850°C) which resemble the composition of the starting material. Garnet textures are consistent with garnet breakdown. Rutile was stable throughout the experiments and some fraction of ilmenite persisted in garnet core. Phase proportions of the run products were determined by least squared mixing calculations using the phase and starting material major element composition (Table 3.5). The results are concordant to the visual estimative from the BSE images acquired in the SEM. The experimental glass was found in large domains or interstitial to the minerals in a much smaller scale (Fig. 3.1). In the water saturated experiments, large pools of glass were formed adjacent to the capsule walls and also within some garnet agglomerates. The segregation degree of the melt in these capsules is a result of the water-saturation experiment itself. The capsule shape also promoted melt

segregation because in its crimped ends there is a large void of starting material powder where the melt can migrate into. In the low temperature and sub-saturated water experiments, the glass is almost exclusively interstitial, rarely forming small ponds. EDS analyses of interstitial, pooled and garnet-surrounded glass indicate that there is no segregation of the elements and no systematic compositional variation.

Table 3.5 - Calculated phase proportion by major element squared mass balance for the 2.5 Gpa – 800°C and 2.5 GPa – 850 °C run products.

<u>P (Gpa)</u>	<u>2.5</u>	<u>2.5</u>
<u>T (°C)</u>	<u>800</u>	<u>850</u>
Melt	0.11	0.12
Gt	0.44	0.44
Omp	0.33	0.32
Bt	0.10	0.09
Rt	0.01	0.02
Ilm	0.01	0.01
Sum	1.00	1.00
SSR	0.50	0.40

SSR – Sum of Square Residuals; Gt – Garnet; Omp – Omphacite; Bt – Biotite; Rt – Rutile; Ilm – Ilmenite

3.4.1 – Equilibrium approach

The investigations of run products display features that appear to have reached a reasonable equilibrium. Core and rim compositions of garnets and clinopyroxene do not show significant systematic variances, nor does the glass accumulated in different areas of the capsules. The new phases formed corresponded to the increase in temperature as expected. The presence of ilmenite in the garnet cores shows that the equilibrium was not completely attained. These features, however, are not rare in almost all near-solidus partial melting experiments (Tepley *et al.*, 2000). It may be attributed to a persistent large iron grain, unable to react to the other elements that rather registered the deformation of the process under some shear stress.

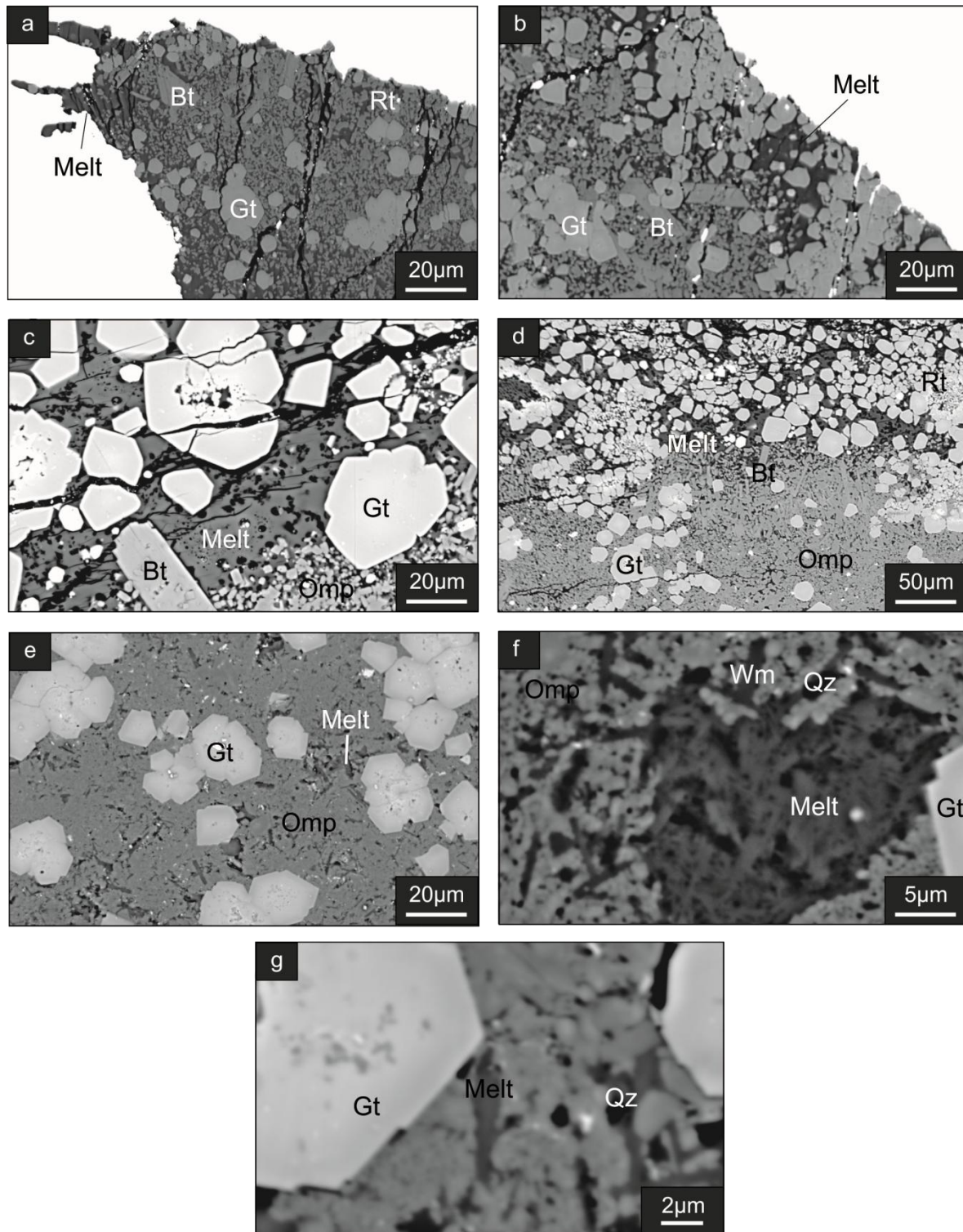


Figure 3.1 – Back-scatter electron (BSE) images of the run products. Melt segregation resulted in different domains (a - d) of melt rich adjacent to the golden capsule mainly in contact with garnet, but also with omphacite. Some garnets have iron rich core. The other domain is a sea of omphacite. with less garnet. (a) and (b) were performed at 800°C and (c) and (d) at 850°C. These four experiments correspond to the water saturated conditions. In the images (e-g) there is no melt domain. Instead, the glass is interstitial with the crystals and results in smaller and surrounds the faceted minerals. The experiments (e) and (f) were performed at 790°C and (g) at 820°C. All the run products were obtained from a fixed pressure at 2.5 GPa. Gt – garnet; Omp – omphacite; - Bt – biotite; Qz – quartz; Rt – rutile; Wm – phengite.

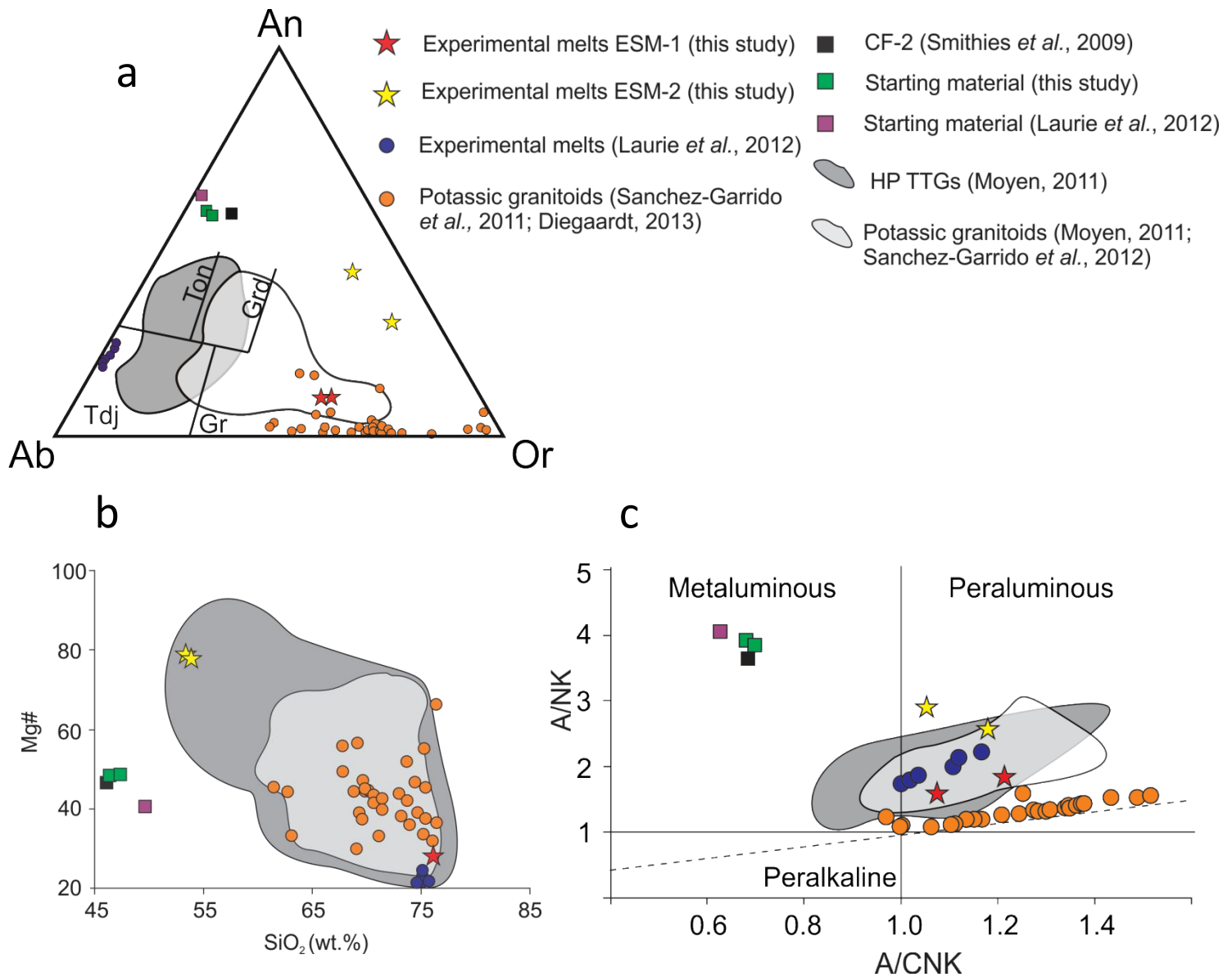


Figure 3.2 – Major elements diagrams. The red stars represent the experimental glasses from the ESM-1 starting material (water-saturated condition). The yellow stars represent the experimental glasses from the ESM-2 starting material (under water-saturated conditions). Orange circles are equivalent to the potassic granitoids documented by Sanchez-Garrido *et al.* (2012) and Diegaard *et al.* (2013). The blue circles represent the experimental TTG glasses from Laurie *et al.* (2012). The green squares are equivalent to the starting materials of this study despite water-saturation. The black squares represent the archean basalts of the Coucal Formation (Smithies *et al.*, 2009). The purple square represents the starting material from Laurie *et al.* (2012). The dark grey area represent the HP TTG (Moyen, 2011) and the lighter grey represent the potassic granitoids (Moyen, 2011; Sanchez-Garrido, 2011, 2012). (a) Ternary diagram of normative feldspar; (b) Mg# vs. SiO₂; (c) A/NK vs. A/CNK.

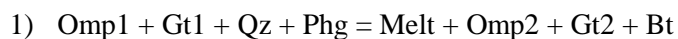
3.4.2 – Experimental glass composition

Two different glasses were attained in function of the water saturated and the phengite component. The first glasses obtained from ESM-1 water saturated experiment have composition of a peraluminous granite (4.3 – 5.6 Na₂O/CaO)(1.3 – 1.5 A/NK; 1.1 – 1.3 A/CNK) (Fig. 3.2) (Table 3.2). They are silica rich (73.8 – 77.2 wt.% SiO₂; >1.2 wt.% MgO + MnO + FeO + TiO₂). They have moderate K₂O:Na₂O ratios (0.6 – 1.1) and low Mg# (~28.4 – when magnesium was found in the glass). The high K₂O reflects the slightly enriched starting material (1.0 wt.% K₂O) and the breakdown of the phengite component. The results shown in Table 3.2 are anhydrous equivalents of normalized analyses. The water content was estimated from the raw data, assuming that the deviation analyses of the glass from the 100% total is due to the non-measurement of the water by the SEM. The water content for the ESM-1 glasses is quite high (16.4 – 18.3 wt.% H₂O) as expected for high pressure melts. The second glasses obtained from ESM-2 were under water saturated conditions (1.1 wt% H₂O) and have the composition of a peraluminous trachyandesitic rock (7.9 – 9.1 Na₂O + K₂O wt.%)(53.6 – 54.2 wt.% SiO₂). They are rich in ferros (~10.6 wt.% TiO₂ + FeO + MgO + MnO), K₂O (6.2 – 7.8 wt.% K₂O) and MgO contents (5.7 – 5.8 wt.% MgO). Consequently, they have relatively high K₂O:Na₂O ratios (2.1 – 3.6) and Mg# (78.1 – 78.9) (Table 3.2).

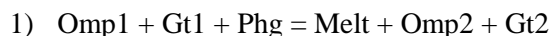
3.4.3 – Melting Reactions

The evidences in this study suggest that clinopyroxene, quartz and phengite are the principal reactants in the wet melting. The clinopyroxene was consumed along with quartz, the phengitic white mica and some minor garnet to produce a potassic granitic melt. A relatively sodium-rich pyroxene was formed as the main solid product of the reaction. Some new garnet and biotite were also formed. The quartz and phengite were completely consumed and incorporated into the melt.

The reactions at 2.5 GPa and 800°C and 850°C respectively are both characterized by:



In the sub-water saturated conditions (ESM-2), the evidence shows that the reaction was anhydrous. The main reagents were the clinopyroxene and garnet. Phengite was incorporated to the melt with increasing temperature. The clinopyroxene and garnet were the solid products of the reaction. The clinopyroxene is, again, sodium-rich and similar to the ones found in ESM-1 experiment. The garnet in the other hand is magnesium-rich and depleted in iron in comparison with the starting material. The reaction at 790 °C and 820°C 2.5 GPa is characterized by:



At 790°C the phengitic component is not completely incorporated into the melt and is present as relict mineral, whilst at 820°C it is completely consumed. Quartz is present throughout the whole process but does not take part in the melting thus the glass show low values of SiO₂ wt.%.

3.4.4 – Further melt modeling

The experimental work has produced potassic glasses by incorporating the phengite in the partial melting reaction. The granitic run product glass is derived from a fertile source in function of the water. The absence of water for the reaction produces an anhydrous silica-deficient melt with trachyandesitic affinity, far off the compositions of TTGs from the Archean. The extraction of the potassic melt and further modeling of the behavior of the rock in the eclogite facies condition (Fig. 3) provides insights about the new process of partial melting that takes place in the ongoing subduction. They suggest that for the high pressure conditions (~2.5 GPa) the new residuum formed after extraction of the potassic melt still holds enough amounts of water (Laurie and Stevens, 2012) and hence kept the source fertile for further melting. They also show that the residual phases are similar to the normal eclogite assemblage at high pressure (Gt + Omp) and resembles the residuum found in Laurie and Stevens (2012). If the conditions are sustained, the new bulk rock is likely to produce a TTG melt.

3.5 – Discussion

TTG granitoid's composition have been interpreted to have petrogenetic significance (Moyen and Stevens, 2006; Moyen *et al.* 2007; Laurie and Stevens 2012). The HP-type TTG, Na-rich, reflect the partial melting of a metabasaltic source. Laurie and Stevens (2012) demonstrated quite convincingly that TTG melts can arise from the partial melting of basaltic-like rocks in eclogite facies conditions.

However, when the basaltic source is slightly enriched in potassium, the phengite component plays an important role in the wet partial melting. The potassium in high pressures is mostly retained in a phengitic white mica. When water is present, the phengite, although little in comparison to the other phases in the starting material, is completely absorbed into the reaction along with quartz and partitioned into the melt and biotite. Thus, the first melt produced was a peraluminous granite with a potassic character. The melt obtained within these conditions has a very similar composition to the granitic pebbles and rhyolitic volcanic rocks documented in Sanchez-Garrido *et al.* (2011, 2012) and Diegaardt (2013) respectively (Table 3.2). They are also older than the TTGs and are in accordance with the early production of a potassic melt predating the TTG generation.

The absence of water in the same bulk rock composition and the same conditions for a basaltic starting material has provided a very different melt. The glass obtained is a K₂O-rich trachyandesite. Phengite in this case is gradually consumed by the reaction up to <820°C. At this point, all the phengite is

incorporated to the melt and produce a high potassic silica-depleted glass. Although this process deviate from the TTG and potassic granitoid genesis, it shows that to achieve rocks with high silica contents from a basaltic starting material in high pressure conditions, the presence of water is of essence.

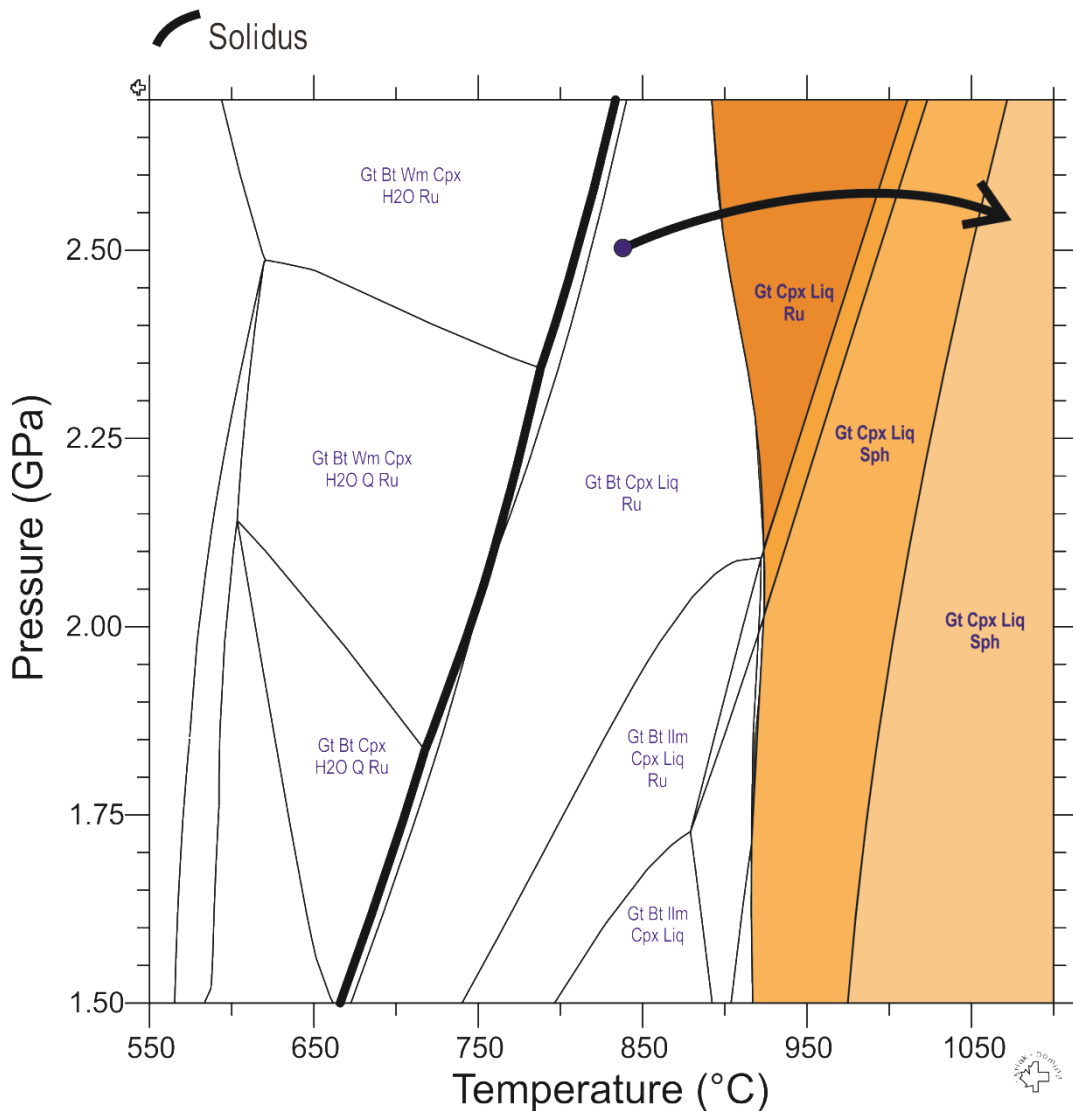


Figure 3.3 – Pseudosection of the new bulk rock composition after extracting the potassic melt. The modeling suggests that the residuum is similar to the one found in Laurie *et al.* (2012). The melt composition also resembles a TTG melt in water-saturated condition ($A/NK = 1.7$; $A/CNK = 1.1$; $Na_2O/CaO = 2.0$; $K_2O/NaO = 0.4$). The arrow indicates the way the progressive metamorphism would lead the new bulk rock. The orange fields correspond to those that would produce similar residuals and melts according to the TTG formation process.

3.6 – Conclusion

This study has produced potassic glass via high pressure (2.5 GPa) water-present partial melting in the eclogite-facies conditions from a starting material (ESM-1) with basaltic composition, similar to Archean mafic rocks from the Coucal Formation in the Pilbara Craton (Smithies *et al.*, 2009). The produced melt is a peraluminous granite, similar to the pebbles found by Sanchez-Garrido *et al.* (2011, 2012) in a basal conglomerate from the Moodies Group and to the rhyolitic felsic volcanic rocks reported by Diegardt (2013). The modelling has suggested that further melting extraction would lead to the production of a HP-type Archean TTG melt in accordance with Laurie and Stevens (2012) experimental work. The ages of the rocks also suggest that the k-granitoids were generated before but associated with the three TTG production events. The proposed model can explain both k-granitoid and TTG genesis as products from the same source and this reiterates the similarities of some of their trace elements. The production of a trachyandesitic glass also verifies for the necessity of water saturation to produce silica-rich melts from basaltic rocks. The phengite presence in the starting material and the availability of water also influenced the first melt produced, which had a potassic character. We proposed that the granitic rocks founded in the Barberton Greenstone Granite Terrane (BGGT) from 3.55 Ga, 3.45 Ga and 3.25 Ga (Sanchez-Garrido *et al.*, 2011; Diegardt, 2013) could be generate in analogous conditions to this experiment in a subduction environment in the Archean, partial melting k-enriched basalts. The ongoing process would then generate the TTGs from 3.5 Ga, 3.45 Ga and 3.21 Ga. (e.g. Lowe and Byerly, 2007; Moyen *et al.*, 2007) from a potassium depleted source or could reflect heterogeneous concentrations of potassium in the protolith.

CHAPTER 4

CONCLUSIONS

The experimental work done with the basaltic rocks provided insights about the partial melting in high pressure conditions simulating the Archean subduction thermal structure. The phengite-presence in the potassium-enriched protolith has shown that melting takes a different path throughout the subduction process. The water also determines the SiO₂ concentration in the liquid phase.

The experiments ran with ESM-1 at 2.5 GPa, 800 and 850°C in water saturated conditions produced a peraluminous granite similar to the potassic pebbles documented in Sanchez-Garrido *et al.* (2011) from the basal conglomerate in the Moodies Groups and also to the felsic volcanic-volcanoclastic rocks from the Hooggenoeg Formation (Diegaard, 2013). This work has taken into account the potassium-restriction to the phengite phase from the protolith. In the run products, the phengite and quartz are consumed along with pyroxene and garnet in the presence of water to produce a felsic potassic melt. The residuum is characterized by garnet, omphacite and biotite, also similar to the Archean basaltic potassium-depleted rocks. The modelling suggests that the ongoing process could produce a TTG melt from the new potassium-depleted bulk rock. The restricted outcropping of the k-granitoids however support a local concentration of potassium as the main reason for the peraluminous potassic-melt production. Areas without this enrichment should produce TTG melts instead. Thus, the k-granitoids rocks might have formed earlier than TTGs for the phengite is incorporated in the melted first and then, in a similar environment, the increasing temperature should give rise to the most common TTG melt.

The experiments ran with ESM-2 at 2.5 GPa, 790 and 820°C in water subsaturated conditions have produced a trachyandesitic melt. This outcome has shown the importance of water to the production of potassic granitoids as well for the TTG melts. The anhydrous to water subsaturated environment does not provide the conditions for the typical Archean rocks generation.

The water determines the amount of SiO₂ in the melt, as the phengite presence and concentration determine the path of partial melting evolution, either for a fractional partial melting with a potassic stage previously to the TTG or for a partial melting resulting in the Archean TTGs. As for the Barberton Granite Greenstone Terrane (BGGT), the low-CaO high-K₂O granitoids could have been produced previously than the TTGs through analogous conditions to this experiment. The k-granitoids could also been formed as a result of local accumulations of potassium in the source, but from the same basaltic protolith.

References

- Buick, R., Thorne, J.R., McNaughton, N.J., Smith, J.B., Barley, M.E., Savage, M., 1995. Record of emergent continental crust ~3.5 billion years ago in the Pilbara cráton of Australia. *Nature* 375, 574-577.
- Byerly, G.R., Kröner, A., Lowe, D.R., Todt, W., Walsh, M.M., 1996. Prolonged magmatism and time constraints for sediments deposition in the Early Archean Barberton greenstone belt: evidence from the upper Onverwacht and Fig Tree groups. *Precambrian Research* 78, 125-138.
- Capitani C. and Petrakakis K. 2010. The computation of equilibrium assemblage diagrams with Theriak/Domino software. *American Mineralogist* 95, 1006-1016.
- Chakraborty, S., Dingwell, D.B., Rubie, D.C., 1995. Multicomponent diffusion in ternary silicate melts in the system K₂O-Al₂O₃-SiO₂: I. Experimental measurements. *Geochimica et Cosmochimica Acta* 59 (2), 255-264.
- Clemens, J.D., 1984. Water contents of silicic to intermediate magmas. *Lithos* 17, 273-287.
- Clemens, J.D., Yearron, L.M., Stevens, G., 2006. Barberton (South Africa) TTG magmas: geochemical and experimental constraints on source-rock petrology, pressure of formation and tectonic setting. *Precambrian Research* 151, 53-78.
- Condie, K.C., 1981. *Archaean Greenstone Belts*. Elsevier, Amsterdam, p. 434.
- Connolly, J.A.D., Pettrini, K., 2002. An automated strategy for calculation of phase diagram sections and retrieval of rock properties as a function of physical conditions. *Journal of Metamorphic Geology* 20, 697-708.
- Deer, W.A., Howie, R.A., Zussman, J., 1997. *Rock Forming Minerals*. The Geological Society, London, p. 570.
- Diegaard, B. N., 2013. Rhyolitic volcanism in the Onverwacht Group, Barberton Greenstone Belt. M.S.c. University of Stellenbosch, South Africa.
- Diener, J.F.A., Stevens, G., Kisters, A.F.M., Poujol, M., 2005. Metamorphism and exhumation of the basal parts of the Barberton greenstone belt, South Africa: constraining the rates of Mesoarchean tectonism, *Precambrian Research*, 143,87-112.
- Foley, S., Tiepolo, M., and Vannucci, R., 2002. Growth of early continental crust controlled by melting of amphibolite in subduction zones, *Nature*, 417, 837-840.
- Hickman, A.H., 1983. Geology of the Pilbara block and its environs. *Western Australia Geological Survey Bulletin* 127, 268.
- Jahn, B.M., Glikson, A.Y., Peucat, J.J. and Hickman, A.H., 1981. REE geochemistry and isotopic data of Archaean silicic volcanics and granitoids from the Pilbara Block, western Australia: implications for the early crustal evolution. *Geochim. Cosmochim. Acta*, 45, 1633-1652.
- Kamo, S.L., Davis, D.W., 1994. Reassessment of Archaean crustal development in the Barberton Mountain Land, South Africa, based on U-Pb dating. *Tectonics* 13, 167-192.
- Kisters, A.F.M., Stevens, G., Dziggel, A., Armstrong, R.A. (2003). Extensional detachment faulting and core-complex formation at the base of the Barberton greenstone belt: evidence for a 3.2 Ga orogenic collapse. *Precambrian Research* 127, 355-378.
- Kisters, A.F.M., Belcher, R., Poujol, M., Dziggel, A., 2010. Continental growth and convergence-related arc plutonism in the Mesoarchean: evidence from the Barberton granitoid-greenstone terrain, South Africa. *Precambrian Research* 178, 15-26.
- van Kranendonk, M.J., Smithies, R.H., Hickman, A.H., Champion, D.C., 2007. Secular tectonic evolution of Archean continental crust: Interplay between horizontal and vertical processes in the formation of the Pilbara cráton, Australia. *Terra Nova* 19, 1-38.
- Kretz, 1983. Symbols for rock-forming minerals. *American Mineralogist* 68, 277-279.

- Kröner, A., Byerly, G.R., Lowe, D.T., 1991. Chronology of early Archaean granite-greenstone evolution in the Barberton Mountain Land, South Africa, based on precise dating by single zircon evaporation. *Earth and Planetary Sciences Letters* 103, 41-54.
- Kroner, A., Hegner, E., Wendt, J. I., Byerly, G. R., 1996. The oldest part of the Barberton granitoid-greenstone terrain, South Africa: evidence for crust formation between 3.5 and 3.7 Ga. *Precambrian Research* 78, 105-124.
- Lana C., Alkmin F., Richard Armstrong R., Scholz R., Romano R., Nalini Jr. H.A., 2013. The ancestry and magmatic evolution of Archaean TTG rocks of the Quadrilátero Ferrífero province, southeast Brazil. *Precambrian Research*, 231:157-173.
- Lana, C., Tohver, E., and Cawood, P., 2010. Quantifying rates of dome-and-keel formation in the Barberton granitoid-greenstone belt, South Africa: *Precambrian Research*, v. 177, p. 199–211.
- Laurie, A., Stevens, G., 2012. Water-present eclogite melting to produce Earth's early felsic crust. *Chemical Geology* 2012, p. 83-95.
- Laurie, A., Stevens, G., van Hunen, J., 2012. The end of continental growth by TTG magmatism. *Terra Nova* 2012, p. 1-7.
- Lowe, D.R., 1999. Geological evolution of the Barberton greenstone belt and vicinity. In: Lowe, D.R., G.R. Byerly. (Eds), *Geologic Evolution of the Barberton Greenstone Belt, South Africa*, Geological Society of America, Special Paper 329, 287-312.
- Lowe, D.R., Byerly, G.R., 1999. Stratigraphy of the west-central part of the Barberton Greenstone Belt, South Africa. In: Lowe, D.R., Byerly, G.R. (Eds), *Geologic Evolution of the Barberton Greenstone Belt, South Africa*. Geological Society of America Special Paper, 329, 1-36.
- Lowe, D.R., Byerly, G.B., 2007. An overview of the geology of the Barberton Greenstone Belt and vicinity: implications for early crustal development. In: Van Kranendonk, M.J., Smithies, R.H., Bennett, V. (Eds.), *Earth's Oldest rocks. : Developments in Precambrian Geology*. Elsevier, pp. 481-526.
- Martin, H., Chauvel, C. and Jahn, B.M., 1983. Major and trace element geochemistry and crustal evolution of Archaean granodioritic rocks from eastern Finland. *Precambrian Res.*, 21, 159–180.
- Martin, H., 1986, Effect of steeper Archean geothermal gradient on geochemistry of subduction-zone magmas: *Geology*, v. 14, p. 753–756.
- Martin, H., 1994. In: Condie, K.C. (Ed.), *The Archean Grey Gneisses and the Genesis of the Continental Crust in Archean Crustal Evolution*. Elsevier, Amsterdam, pp. 205–259.
- Martin, H., 1999. The adakitic magmas: modern analogues of Archean granitoids. *Lithos* 46 (3), 411–429.
- Martin, H., Moyen, J.-F., 2002. Secular changes in TTG composition as markers of the progressive cooling of the Earth. *Geology* 30 (4), 319–322.
- Moyen, J.-F., Stevens, G., 2006. Experimental constraints on TTG petrogenesis: implications for Archean geodynamics. In: Benn, K., *et al.* (Ed.), *Archean Geodynamics and Environments*, 164. American Geophysical Union Geophysical Monograph, pp. 149–175.
- Moyen, J.-F., Stevens, G., Kisters, A., 2006. Record of mid-Archaean subduction from metamorphism in the Barberton terrain, South Africa. *Nature* 442, 559–562.
- Moyen, J.-F., Stevens, G., Kisters, A.F.M., Belcher, R.W., 2007. TTG plutons of the Barberton granitoid-greenstone terrain, South Africa. In: Van Kranendonk, M.J., Smithies, R.H., Bennett, V. (Eds.), *Earth's Oldest rocks. : Developments in Precambrian geology*. Elsevier, pp. 606–668.
- Moyen, J.-F., 2011. The composite Archaean grey gneisses: petrological significance, and evidence for a non-unique tectonic setting for Archaean crustal growth. *Lithos* 123, 21–36.
- Moyen, J.-F., Martin, H., 2012. Forty years of TTG. *Lithos* 148, 312-336.
- Rapp, R.P., Shimizu, N., Norman, M.D., 2003. Growth of early continental crust by partial melting of eclogite. *Nature* 425, 605–609.

- de Ronde, C.E.J., and de Wit, M.J., 1994. Tectonic history of the Barberton greenstone belt, South Africa: 490 million years of Archean crustal evolution: *Tectonics*, v. 13, p. 983–1005.
- Sanchez-Garrido, C.J.M.G., Stevens, G., Moyen, J-F., Martin, H., Doucelance, R., 2011. Diversity in Earth's early felsic crust: Paleoproterozoic peraluminous granites of the Barberton Greenstone Belt. *Geology* 39, 963-966.
- Sanchez-Garrido, C.J.M.G., Doucelance, R., Martin, H., Moyen, J-F., Stevens, G., Farina, F., Frei, D., Gerdes, A., Bosq, C., 2012. Successive tapping of an old reservoir to form Paleo- and Meso-Archean felsic granitic crust: A Sm/Nd and Lu/Hf isotopic study of granitic clasts within the basal conglomerate of the Moodies group, Barberton Mountain Land, South Africa. *Chemical Geology* 261, 115-139.
- Schmidt, M.W., Poli, S., 1998. Experimentally based water budgets for dehydrating slabs and consequences for arc magma generation. *Earth and Planetary Science Letters* 163, 361–379.
- Schmidt, M.W., Dardon, A., Chazot, G., Vannucci, R., 2004. The dependence of Nb and Ta rutile-melt partitioning on melt composition and Nb/Ta fractionation during subduction processes. *Earth and Planetary Science Letters* 226, 415–432.
- Schoene, B., De Wit, M. J. and Bowring, S. A., 2008. Mesoarchean assembly and stabilization of the eastern Kaapvaal craton: A structural-thermochronological perspective. *University of Stellenbosch. Tectonics* 27, TC5010.
- Schoene, B., and Bowring, S.A., 2010. Rates and mechanisms of Mesoarchean magmatic arc construction, eastern Kaapvaal craton, Swaziland: *Geological Society of America Bulletin*, v. 122, p. 408–429.
- Skora, S., Baumgartner, L.P., Mahlen, N.J., Johnson, C.M., Pilet, S., Hellebrand, E., 2006. Diffusion-limited REE uptake by eclogite garnets and its consequences for Lu–Hf and Sm–Nd geochronology. *Contributions to Mineralogy and Petrology* 152 (6), 703–720.
- Smithies R.H., Champion D.C., Van Kranendonk M.J., 2009. Formation of Paleoproterozoic continental crust through infracrustal melting of enriched basalt. *Earth and Planetary Science Letters* 2009, v. 281, p. 298-306.
- Smithies, R.H., Champion, D.C., 2000. The Archean high-Mg diorite suite: links to tonalite–trondhjemite–granodiorite magmatism and implications for early Archean crustal growth. *Journal of Petrology* 41, 1653–1671.
- Smithies, R.H., Champion, D.C., Cassidy, K.F., 2003. Formation of Earth's early Archean continental crust. *Precambrian Research* 127 (1–3), 89–101.
- Smithies, R.H., Champion, D.C., Van Kranendonk, M., 2009. Formation of Paleoproterozoic continental crust through infracrustal melting of enriched basalt. *Earth and Planetary Science Letters* 281 (3–4), 298–306.
- Tepley III, F.J., Davidson, J.P., Tilling, R.I., Arth, J.G., 2000. Magma mixing, recharge and eruption histories recorded in plagioclase phenocrysts from El Chichón Volcano, Mexico. *Journal of Petrology* 41 (9), 1397–1411.
- Toulkeridis, T., Peucker-Ehrenbrink, B., Clauer, N., Kröner, A., Schidlowski, M., Todt, W., 2010. Pb Pb age, stable isotope and chemical composition of Archean magnesite, Barberton Greenstone Belt, South Africa. *Journal of the Geological Society* 2010; v. 167; p. 943-952.
- Tuttle, O.F., Bowen, N.L., 1958. Origin of granite in the light of experimental studies in the system NaAlSi₃O₈–KAlSi₃O₈–SiO₂–H₂O. *Geological Society of American Memoirs* 74.
- Vielzeuf, D., Clemens, J.D., 1992. Fluid-absent melting of phlogopite+quartz: experiments and models. *American Mineralogist* 77, 1206–1222.
- Viljoen, M. J., Viljoen, R. P., 1969. The geology and geochemistry of the lower ultramafic unit of the Onverwacht Group and a proposed new class of igneous rocks. *Geological Society of South Africa, Special Publication* 2, 55-86.
- de Vries, S.T., Nijman, W., Armstrong, R.A. 2006. Growth-fault structure and stratigraphic architecture of the Buck Ridge volcano-sedimentary complex, upper Hooggenoeg Formation, Barberton Greenstone Belt, South Africa. *Precambrian Research* 149, 77-98.
- Wyllie, P.J., Tuttle, O.F., 1961. Experimental Investigation of silicate systems containing two volatile components, Part II. The effects of NH₃ and HF, in addition to H₂O, on the melting temperatures of albite and granite. *American Journal of Science* 259, 128–143.

Appendix

APPENDIX A – Accuracy and precision of the EDS and WDS analyses.

Accuracy and precision of EDS and WDS analyses from the University of Stellenbosch SEM configuration.

Cert. Std	Obsidian ^a			Almandine			Plagioclase An65					
	Actual	Measured ave.	σ	r	Actual	Measured ave.	σ	r	Actual	Measured ave.	σ	r
N=10												
SiO ₂	73.9	74.5	0.1	0.4	39.2	39.1	0.3	0.0	54.2	53.3	0.8	0.8
TiO ₂	0.1	0.1	0.0	0.0								
Ti ^b	0.06	0.05	0.0	0.0								
Al ₂ O ₃	13.1	12.9	0.1	0.0	22.1	22.3	0.4	0.1	28.5	29.0	0.7	0.2
FeO	1.7	1.8	0.1	0.0	23.3	22.9	0.1	0.1	0.4	0.5	0.0	0.0
MnO					0.6	0.4	0.0	0.1				
MgO	0.1	0.1	0.0	0.0	10.7	11.2	0.1	0.3				
Mg ^b	0.04	0.03	0.0	0.0								
CaO	0.8	0.8	0.0	0.0	4.2	4.2	0.0	0.0	11.8	12.0	0.1	0.0
Na ₂ O	4.1	4.1	0.1	0.0					4.4	4.6	0.7	0.0
K ₂ O	5.0	5.4	0.0	0.0					0.4	0.4	0.0	0.0
Sr ^b									0.08	0.11	0.0	0.0
H ₂ O ^c	0.8	0.8	0.3	0.0								
Cl	0.4	0.5	0.0	0.0								
Total	99.9	100.0			100.0	100.1			100.0	99.8		

σ – standard deviation; r – residual difference between the actual certified composition of the certified standard (Cert. Std) (International Astimex Scientific Mineral) and the measured average composition.

^a Cryostage was used during analysis.

^b Elements which were measured using WDS.

^c Deduced from the difference between the measured total and 100 wt. %.

APPENDIX B – Ages of the potassic granitoids

Isotopic data of Lu-Hf from the granitic clastis of Moodies Groups, extracted from Sanchez-Garrido et al. (2011) Diegaardt (2013).

Sample	Ages^a (Ma)	Ages^b (Ma)	Method
A5 46	3756 ± 29	3552 ± 29	LA ICP-MS
B1 004	3606 ± 10	3436 ± 10	LA ICP-MS
B1 010	3546 ± 11	3454 ± 11	LA ICP-MS
B1 012	3573 ± 26	3432 ± 26	LA ICP-MS
B1 013	3588 ± 12	3418 ± 12	LA ICP-MS
B1 014	3535 ± 10	3443 ± 10	LA ICP-MS
B1 015	3598 ± 10	3455 ± 10	LA ICP-MS
B1 020	3572 ± 18	3454 ± 18	LA ICP-MS
B1 022	3553 ± 17	3459 ± 17	LA ICP-MS
C4 078	3687 ± 7	3454 ± 7	LA ICP-MS
C4 080	3635 ± 7	3454 ± 7	LA ICP-MS
C4 081	3590 ± 7	3454 ± 7	LA ICP-MS
C4 085	3688 ± 7	3454 ± 7	LA ICP-MS
C4 088	3670 ± 7	3454 ± 7	LA ICP-MS
C4 088	3699 ± 7	3454 ± 7	LA ICP-MS
C4 090	3607 ± 7	3454 ± 7	LA ICP-MS
C4 091	3559 ± 7	3454 ± 7	LA ICP-MS
C4 094	3568 ± 7	3454 ± 7	LA ICP-MS
C4 099	3559 ± 11	3454 ± 11	LA ICP-MS
C4 100	3645 ± 7	3454 ± 7	LA ICP-MS
C4 103	3580 ± 7	3454 ± 7	LA ICP-MS
C4 104	3610 ± 7	3454 ± 7	LA ICP-MS
C19 27	3996 ± 18	3503 ± 18	LA ICP-MS
C19 28	3617 ± 10	3536 ± 10	LA ICP-MS
C19 29	3745 ± 10	3531 ± 10	LA ICP-MS
C19 34	3706 ± 10	3531 ± 10	LA ICP-MS
C19 38	3750 ± 10	3523 ± 10	LA ICP-MS
C19 39	3736 ± 10	3531 ± 10	LA ICP-MS

a Model age for two stages from the average of Lu and Hf isotopes.

b Pb-Pb age concordantly determined by LA ICP-MS.

Isotopic data of Sm-Nd from the TTGs within the Moodies Group, extracted of Sanchez-Garrido et al.(2011).

Sample	Ages (Ma)	Method	Age CHUR ^a (Ma)	Age T _{DM} ^b	One Stage Model	Age T _{DM} ^c	Two stage Model	Age T _{DM} ^d	Regression Model
STEY 2.2/08	3510	TIMS	3291 ± 26	3450	3450	3410	3410	3360	3360
STEY 1.4/08	3510	TIMS	3652 ± 35	3760	3760	3730	3730	3680	3680
STEY 1.5/08	3510	TIMS	3667 ± 29	3760	3760	3730	3730	3690	3690
STEY 1.7/08	3510	TIMS	3691 ± 48	3820	3820	3780	3780	3730	3730
VLK 2/08	3500	TIMS	3395 ± 29	3540	3540	3500	3500	3450	3450
ST-J7	3450	TIMS	3518 ± 27	3640	3640	3600	3600	3560	3560
ST-J19	3450	TIMS	3505 ± 29	3630	3630	3590	3590	3550	3550
ST-J23	3450	TIMS	3541 ± 29	3660	3660	3630	3630	3580	3580
ST-J33	3450	TIMS	3549 ± 39	3690	3690	3650	3650	3600	3600
ST-J6	3450	TIMS	3557 ± 29	3680	3680	3640	3640	3590	3590
KV 3.1/08	3230	TIMS	3222 ± 36	3430	3430	3380	3380	3320	3320
KV 4.1/08	3230	TIMS	3236 ± 41	3460	3460	3410	3410	3340	3340
KV 1.1/08	3230	TIMS	3241 ± 32	3430	3430	3380	3380	3320	3320
KV 2.1/08	3230	TIMS	3266 ± 33	3450	3450	3400	3400	3350	3350
NLS 7.2/08	3210	TIMS	3194 ± 44	3440	3440	3380	3380	3310	3310
NLS 8.1/08	3210	TIMS	3242 ± 32	3440	3440	3380	3380	3330	3330
NLS 5.3/08	3210	TIMS	3261 ± 21	3410	3410	3370	3370	3320	3320
NLS 5.1/08	3210	TIMS	3263 ± 68	3560	3560	3490	3490	3410	3410
NLS 2.2/08	3210	TIMS	3260 ± 21	3410	3410	3370	3370	3320	3320

^a Values from Jacobsen & Wasserburg (1980) and Goldstein et al. (1984) for Chondritic Uniform Reservoir - CHUR.

^b Model age for Earth evolution in a single and closed system.

Model age for Earth evolution in a double and closed system.

^d Evolution DM - $\epsilon\text{NdDM}(T) = 0.25T^2 - 3T + 8.5$, as proposed by DePaolo (1981).

General garnet compositions from EMS-1 at 2.5 GPa and 800°C. Structural formulae calculated for 12 oxygens.

wt.%	1	2 (core)	2 (rim)	3 (core)	3 (rim)	4 (core)	5 (core)	6 (core)	7	8	9	10 (rim)
SiO ₂	38.73	38.85	39.20	39.05	39.08	39.30	42.69	39.37	38.94	38.88	37.85	38.49
TiO ₂	1.27	1.43	1.90	2.10	1.33	1.17	0.87	0.97	1.59	1.07	1.83	0.96
Al ₂ O ₃	21.26	21.44	22.01	20.22	21.51	21.53	22.81	22.11	21.39	21.21	21.21	21.27
Cr ₂ O ₃	0.00	0.00	0.00	0.00	0.00	0.00	0.00	0.00	0.00	0.00	0.00	0.00
Fe ₂ O ₃	0.00	0.00	0.00	0.00	0.00	0.00	0.00	0.00	0.00	0.00	0.00	0.00
FeO	23.56	21.96	20.47	21.71	20.58	23.52	20.22	20.78	22.15	21.78	21.79	22.04
MnO	0.00	0.00	0.00	0.00	0.00	0.00	0.00	0.00	0.00	0.00	0.00	0.00
MgO	4.05	5.48	7.24	6.64	7.30	4.42	7.23	6.87	4.43	4.73	4.84	4.96
CaO	11.73	11.20	9.66	9.35	9.41	11.49	10.37	9.92	11.59	11.76	11.27	11.08
Na ₂ O	0.00	0.00	0.00	0.00	0.00	0.00	0.00	0.00	0.00	0.00	0.00	0.00
K ₂ O	0.00	0.00	0.00	0.00	0.00	0.00	0.00	0.00	0.00	0.00	0.00	0.00
Totals	100.60	100.36	100.48	99.07	99.21	101.43	104.19	100.02	100.09	99.43	98.79	98.80
Si	2.99	2.98	2.97	3.02	3.00	3.00	3.09	3.00	3.00	3.02	2.96	3.00
Ti	0.07	0.08	0.11	0.12	0.08	0.07	0.05	0.06	0.09	0.06	0.11	0.06
Al	1.94	1.94	1.97	1.84	1.95	1.94	1.95	1.99	1.94	1.94	1.96	1.96
Cr ³⁺	0.00	0.00	0.00	0.00	0.00	0.00	0.00	0.00	0.00	0.00	0.00	0.00
Fe ³⁺ ^a	0.00	0.00	0.00	0.00	0.00	0.00	0.00	0.00	0.00	0.00	0.00	0.00
Fe ²⁺	1.52	1.41	1.30	1.40	1.32	1.50	1.22	1.32	1.43	1.41	1.42	1.44
Mn	0.00	0.00	0.00	0.00	0.00	0.00	0.00	0.00	0.00	0.00	0.00	0.00
Mg	0.47	0.63	0.82	0.77	0.83	0.50	0.78	0.78	0.51	0.55	0.56	0.58
Ca	0.97	0.92	0.78	0.78	0.77	0.94	0.80	0.81	0.96	0.98	0.94	0.93
Na	0.00	0.00	0.00	0.00	0.00	0.00	0.00	0.00	0.00	0.00	0.00	0.00
K	0.00	0.00	0.00	0.00	0.00	0.00	0.00	0.00	0.00	0.00	0.00	0.00
Sum	7.96	7.96	7.94	7.93	7.95	7.96	7.89	7.95	7.93	7.95	7.96	7.96
Mg ^{#b}	23.45	30.78	38.66	35.28	38.73	25.09	38.92	37.07	26.28	27.90	28.36	28.62
gr ^c	0.33	0.31	0.27	0.26	0.26	0.32	0.29	0.28	0.33	0.33	0.32	0.31
al ^d	0.51	0.48	0.45	0.48	0.45	0.51	0.44	0.45	0.49	0.48	0.49	0.49
py ^e	0.16	0.21	0.28	0.26	0.28	0.17	0.28	0.27	0.18	0.19	0.19	0.20

a Fe³⁺ = 2*X*(1 - T/S), where X = oxygen in structural formulae; T = ideal number in structural formulae; S = cations per structural formulae calculated (Droop, 1987).

b Mg[#] = 100*Mg/(Mg+Fe²⁺+Fe³⁺).

c gr = Ca/(Ca+Fe+Mn+Mg).

d al = Fe/(Ca+Fe+Mn+Mg).

e py = Mg/(Ca+Fe+Mn+Mg).

General garnet compositions from EMS-1 at 2.5 GPa and 800°C. Structural formulae calculated for 12 oxygens.

wt.%	11 (inGt)	12	13	14	15	16	17	18	19	20	21	22
SiO ₂	39.07	38.78	39.24	37.81	36.83	38.04	37.31	38.12	36.13	37.26	37.05	37.72
TiO ₂	1.09	1.49	1.83	1.57	2.96	1.70	1.32	2.16	4.33	2.06	1.21	0.79
Al ₂ O ₃	21.55	21.84	22.05	20.71	20.71	21.10	21.81	20.55	20.10	20.38	20.35	21.07
Cr ₂ O ₃	0.00	0.00	0.00	0.00	0.00	0.00	0.00	0.00	0.00	0.00	0.00	0.00
Fe ₂ O ₃	0.00	0.00	0.00	0.00	0.00	0.00	0.00	0.00	0.00	0.00	0.00	0.00
FeO	22.88	21.97	21.73	23.24	22.59	23.33	22.56	22.21	21.97	22.90	23.30	21.62
MnO	0.00	0.00	0.00	0.00	0.00	0.00	0.00	0.00	0.00	0.00	0.00	0.00
MgO	4.84	4.86	5.57	4.56	4.90	5.40	4.89	5.85	4.62	4.38	4.18	7.25
CaO	11.11	11.27	10.82	11.34	10.57	10.59	11.39	10.74	11.10	11.49	11.60	9.09
Na ₂ O	0.00	0.00	0.00	0.00	0.00	0.00	0.00	0.00	0.00	0.00	0.00	0.00
K ₂ O	0.00	0.00	0.00	0.00	0.00	0.00	0.00	0.00	0.00	0.00	0.00	0.00
Totals	100.54	100.21	101.24	99.23	98.56	100.16	99.28	99.63	98.25	98.47	97.69	97.54
Si	3.00	2.98	2.97	2.97	2.90	2.95	2.92	2.96	2.86	2.95	2.96	2.97
Ti	0.06	0.09	0.10	0.09	0.18	0.10	0.08	0.13	0.26	0.12	0.07	0.05
Al	1.95	1.98	1.97	1.92	1.92	1.93	2.01	1.88	1.88	1.90	1.92	1.95
Cr	0.00	0.00	0.00	0.00	0.00	0.00	0.00	0.00	0.00	0.00	0.00	0.00
Fe ²⁺ ^a	0.00	0.00	0.00	0.00	0.00	0.00	0.00	0.00	0.00	0.00	0.00	0.00
Fe ³⁺	1.47	1.41	1.38	1.52	1.49	1.51	1.47	1.44	1.46	1.52	1.56	1.42
Mn	0.00	0.00	0.00	0.00	0.00	0.00	0.00	0.00	0.00	0.00	0.00	0.00
Mg	0.55	0.56	0.63	0.53	0.58	0.62	0.57	0.68	0.55	0.52	0.50	0.85
Ca	0.91	0.93	0.88	0.95	0.89	0.88	0.95	0.89	0.94	0.97	0.99	0.77
Na	0.00	0.00	0.00	0.00	0.00	0.00	0.00	0.00	0.00	0.00	0.00	0.00
K	0.00	0.00	0.00	0.00	0.00	0.00	0.00	0.00	0.00	0.00	0.00	0.00
Sum	7.96	7.94	7.94	7.98	7.96	7.99	8.00	7.98	7.94	7.98	8.00	8.01
Mgr ^b	27.38	28.27	31.36	25.91	27.88	29.20	27.86	31.94	27.26	25.42	24.22	37.40
gr ^c	0.31	0.32	0.30	0.32	0.30	0.29	0.32	0.30	0.32	0.32	0.33	0.25
al ^d	0.50	0.49	0.48	0.51	0.50	0.50	0.49	0.48	0.49	0.50	0.51	0.47
py ^e	0.19	0.19	0.22	0.18	0.19	0.21	0.19	0.22	0.19	0.17	0.16	0.28

a Fe³⁺ = 2*X*(1 - T/S); where X = oxygen in structural formulae; T = ideal number in structural formulae; S = cations per structural formulae calculated (Droop, 1987)

b Mgr^b = 100*Mg/(Mg+Fe²⁺+Fe³⁺).

c gr = Ca/(Ca+Fe+Mn+Mg).

d al = Fe/(Ca+Fe+Mn+Mg).

e py = Mg/(Ca+Fe+Mn+Mg).

General garnet compositions from EMS-1 at 2.5 GPa and 800°C. Structural formulae calculated for 12 oxygens.

wt %	23	24	25	26	27	28	29	30	31	32	33	34
SiO ₂	38.71	38.02	38.14	37.89	37.13	36.45	36.84	38.65	38.35	37.32	37.78	37.99
TiO ₂	1.59	1.11	1.03	1.48	1.98	1.68	2.52	1.27	1.11	1.55	1.34	1.44
Al ₂ O ₃	20.37	20.84	21.00	21.44	19.51	20.24	20.37	21.33	21.37	20.60	20.69	20.22
Cr ₂ O ₃	0.00	0.00	0.00	0.00	0.00	0.00	0.00	0.00	0.00	0.00	0.00	0.00
Fe ₂ O ₃	0.00	0.00	0.00	0.00	0.00	0.00	0.00	0.00	0.00	0.00	0.00	0.00
FeO	21.91	22.48	23.48	22.11	21.26	21.69	20.98	21.19	21.40	22.28	20.75	22.30
MnO	0.00	0.00	0.00	0.00	0.00	0.00	0.00	0.00	0.00	0.00	0.00	0.00
MgO	6.06	5.68	6.53	6.44	6.02	5.30	5.30	6.50	6.69	5.45	6.89	5.59
CaO	10.78	10.32	8.30	10.15	10.15	10.82	11.30	10.17	10.23	10.58	10.87	10.70
Na ₂ O	0.00	0.00	0.00	0.00	0.00	0.00	0.00	0.00	0.00	0.00	0.00	0.00
K ₂ O	0.00	0.00	0.00	0.00	0.00	0.00	0.00	0.00	0.00	0.00	0.00	0.00
Totals	99.42	98.45	98.48	99.51	96.05	96.18	97.31	99.11	99.15	97.78	98.32	98.24
Si	3.00	2.98	2.99	2.94	2.98	2.94	2.93	2.99	2.97	2.96	2.95	2.99
Ti	0.09	0.07	0.06	0.09	0.12	0.10	0.15	0.07	0.06	0.09	0.08	0.09
Al	1.86	1.93	1.94	1.96	1.85	1.92	1.91	1.94	1.95	1.92	1.91	1.88
Cr	0.00	0.00	0.00	0.00	0.00	0.00	0.00	0.00	0.00	0.00	0.00	0.00
Fe ³⁺ ^a	0.00	0.00	0.00	0.00	0.00	0.00	0.00	0.00	0.00	0.00	0.00	0.00
Fe ²⁺	1.42	1.48	1.54	1.43	1.43	1.46	1.39	1.37	1.39	1.48	1.36	1.47
Mn	0.00	0.00	0.00	0.00	0.00	0.00	0.00	0.00	0.00	0.00	0.00	0.00
Mg	0.70	0.66	0.76	0.74	0.72	0.64	0.63	0.75	0.77	0.64	0.80	0.66
Ca	0.90	0.87	0.70	0.84	0.87	0.93	0.96	0.84	0.85	0.90	0.91	0.90
Na	0.00	0.00	0.00	0.00	0.00	0.00	0.00	0.00	0.00	0.00	0.00	0.00
K	0.00	0.00	0.00	0.00	0.00	0.00	0.00	0.00	0.00	0.00	0.00	0.00
Sum	7.97	7.99	7.98	8.00	7.97	8.00	7.97	7.97	7.99	7.99	8.01	7.98
Mg# ^b	33.02	31.05	33.14	34.17	33.54	30.33	31.04	35.34	35.78	30.36	37.17	30.88
gr ^c	0.30	0.29	0.23	0.28	0.29	0.31	0.32	0.28	0.28	0.30	0.30	0.30
al ^d	0.47	0.49	0.51	0.47	0.47	0.48	0.47	0.46	0.46	0.49	0.44	0.49
py ^e	0.23	0.22	0.25	0.25	0.24	0.21	0.21	0.25	0.26	0.21	0.26	0.22

a Fe³⁺ = 2*X*(1 - T/S); where X = oxygen in structural formulae; T = ideal number in structural formulae; S = cations per structural formulae calculated (Droop, 1987).

b Mg# = 100*Mg/(Mg+Fe²⁺+Fe³⁺).

c gr = Ca/(Ca+Fe+Mn+Mg).

d al = Fe/(Ca+Fe+Mn+Mg).

e py = Mg/(Ca+Fe+Mn+Mg).

Pyroxene compositions from eclogitic starting material ESM-1 at 2.5 GPa and 800°C run products.

Structural formulae calculated for 6 oxygens

wt. %	1 (inGt)	2 (inGt)	3	4	5	6	7	8	9
SiO ₂	54.57	54.69	55.89	53.51	52.50	53.06	51.81	51.40	54.20
TiO ₂	0.65	0.71	1.07	0.95	1.55	0.53	0.50	0.62	0.77
Al ₂ O ₃	7.85	7.34	11.13	12.50	13.78	10.76	9.75	11.01	11.23
Cr ₂ O ₃	0.00	0.00	0.00	0.00	0.00	0.00	0.00	0.00	0.00
Fe ₂ O ₃	0.00	0.00	0.00	0.00	0.00	0.00	0.00	0.00	0.00
FeO	8.37	8.76	6.99	6.95	7.95	5.32	6.54	6.08	5.31
MnO	0.00	0.00	0.00	0.00	0.00	0.00	0.00	0.00	0.00
MgO	9.37	10.14	11.26	10.23	11.07	8.69	9.20	8.72	8.00
CaO	14.37	14.47	12.32	13.86	9.97	14.07	15.61	15.17	12.89
Na ₂ O	4.58	4.12	4.43	4.23	4.57	4.48	3.96	4.37	4.33
K ₂ O	0.00	0.00	1.78	1.07	2.76	0.27	0.00	0.00	0.51
Totals	99.76	100.23	104.87	103.30	104.15	97.18	97.37	97.37	97.24
Si	1.99	1.98	1.92	1.87	1.83	1.95	1.93	1.91	1.98
Ti	0.02	0.02	0.03	0.03	0.04	0.01	0.01	0.02	0.02
Al	0.34	0.31	0.45	0.52	0.57	0.47	0.43	0.48	0.48
Cr	0.00	0.00	0.00	0.00	0.00	0.00	0.00	0.00	0.00
Fe ³⁺ ^a	0.00	0.00	0.00	0.00	0.00	0.00	0.00	0.00	0.00
Fe ²⁺	0.25	0.27	0.20	0.20	0.23	0.16	0.20	0.19	0.16
Mn	0.00	0.00	0.00	0.00	0.00	0.00	0.00	0.00	0.00
Mg	0.51	0.55	0.58	0.53	0.58	0.48	0.51	0.48	0.44
Ca	0.56	0.56	0.45	0.52	0.37	0.56	0.62	0.60	0.50
Na	0.32	0.29	0.30	0.29	0.31	0.32	0.29	0.31	0.31
K	0.00	0.00	0.08	0.05	0.12	0.01	0.00	0.00	0.02
Sum	3.99	3.98	4.01	4.01	4.06	3.96	3.99	3.99	3.92
Mg# ^b	66.61	67.35	74.16	72.40	71.28	74.43	71.48	71.88	72.86
Class ^c	Omp	Omp	Omp	Omp	Omp	Omp	Omp	Omp	Omp

a $Fe^{3+} = 2 * X * (1 - T/S)$; where X = oxygen in structural formulae; T = ideal number in structural formulae; S = cations per structural formulae calculated (Droop, 1987).

b $Mg\# = 100 * Mg / (Mg + Fe^{2+} + Fe^{3+})$.

c Class= Classification: Omp—Omphacite.

Pyroxene compositions from eclogitic starting material ESM-1 at 2.5 GPa and 800°C run products. Structural formulae calculated for 6 oxygens

wt. %	10	11	12	13	14	15	16	17	18
SiO ₂	54.76	53.83	57.03	54.61	54.59	55.47	53.51	52.60	50.50
TiO ₂	1.00	0.41	0.37	0.88	1.15	1.76	0.66	0.68	0.72
Al ₂ O ₃	11.50	11.43	11.54	10.84	10.69	11.72	11.10	9.01	9.67
Cr ₂ O ₃	0.00	0.00	0.00	0.00	0.00	0.00	0.00	0.00	0.00
Fe ₂ O ₃	0.00	0.00	0.00	0.00	0.00	0.00	0.00	0.00	0.00
FeO	4.85	5.20	5.04	4.94	5.59	4.81	5.31	6.19	6.77
MnO	0.00	0.00	0.00	0.00	0.00	0.00	0.00	0.00	0.00
MgO	8.06	8.06	7.44	7.69	8.46	7.53	8.06	9.01	8.40
CaO	13.05	12.88	12.13	12.25	13.61	12.07	13.67	14.63	14.44
Na ₂ O	5.18	4.20	4.63	4.33	4.52	4.82	4.03	3.89	3.71
K ₂ O	0.37	0.44	0.88	0.68	0.42	0.61	0.45	0.28	0.22
Totals	98.77	96.45	99.06	96.22	99.03	98.79	96.79	96.29	94.43
Si	1.97	1.98	2.03	2.01	1.92	1.89	1.90	1.94	1.90
Ti	0.03	0.01	0.01	0.02	0.03	0.05	0.02	0.02	0.02
Al	0.49	0.50	0.48	0.47	0.44	0.47	0.46	0.39	0.43
Cr	0.00	0.00	0.00	0.00	0.00	0.00	0.00	0.00	0.00
Fe ³⁺ ^a	0.00	0.00	0.00	0.00	0.00	0.00	0.00	0.00	0.00
Fe ²⁺	0.15	0.16	0.15	0.15	0.25	0.25	0.21	0.21	0.25
Mn	0.00	0.00	0.00	0.00	0.00	0.00	0.00	0.00	0.00
Mg	0.43	0.44	0.40	0.42	0.49	0.51	0.60	0.56	0.62
Ca	0.50	0.51	0.46	0.48	0.54	0.53	0.47	0.55	0.40
Na	0.36	0.30	0.32	0.31	0.31	0.27	0.31	0.30	0.33
K	0.02	0.02	0.04	0.03	0.00	0.00	0.08	0.05	0.13
Sum	3.95	3.92	3.90	3.90	3.98	3.97	4.04	4.02	4.09
Mg# ^b	74.76	73.42	72.46	73.50	66.61	67.35	74.16	72.40	71.28
Class ^c	Omp	Omp	Omp	Omp	Omp	Omp	Omp	Omp	Omp

a $Fe^{3+} = 2 * X * (1 - T/S)$; where X = oxygen in structural formulae; T = ideal number in structural formulae; S = cations per structural formulae calculated (Droop, 1987).

b $Mg\# = 100 * Mg / (Mg + Fe^{2+} + Fe^{3+})$.

c Class = Classification: Omp—Omphacite.

Pyroxene compositions from eclogitic starting material ESM-1 at 2.5 GPa and 800°C run products. Structural formulae calculated for 6 oxygens

wt. %	19	20	21	22	23	24	25	26	27
SiO ₂	51.26	53.38	52.34	53.90	52.40	50.48	48.55	48.75	52.95
TiO ₂	1.58	1.00	1.66	1.05	1.41	0.53	6.94	0.53	0.71
Al ₂ O ₃	9.62	11.26	10.13	10.70	10.50	12.67	11.19	13.13	9.74
Cr ₂ O ₃	0.00	0.00	0.00	0.00	0.00	0.00	0.00	0.00	0.00
Fe ₂ O ₃	0.00	0.00	0.00	0.00	0.00	0.00	0.00	0.00	0.00
FeO	6.41	7.25	6.36	5.63	6.00	6.19	6.00	9.51	5.76
MnO	0.00	0.00	0.00	0.00	0.00	0.00	0.00	0.00	0.00
MgO	8.76	8.28	8.55	8.29	8.29	10.13	8.15	9.14	8.98
CaO	15.04	13.23	14.05	13.70	13.97	15.00	11.90	14.83	15.19
Na ₂ O	3.94	3.76	4.28	3.98	3.81	3.40	3.76	3.04	4.01
K ₂ O	0.20	0.63	0.40	0.62	0.54	0.57	1.00	0.00	0.28
Totals	96.81	98.79	97.77	97.87	96.92	98.97	97.49	98.93	97.62
Si	1.94	1.91	1.92	1.98	1.96	1.91	1.81	1.89	1.95
Ti	0.04	0.03	0.05	0.03	0.04	0.02	0.19	0.02	0.02
Al	0.43	0.47	0.44	0.46	0.46	0.56	0.49	0.60	0.42
Cr	0.00	0.00	0.00	0.00	0.00	0.00	0.00	0.00	0.00
Fe ³⁺ ^a	0.00	0.00	0.00	0.00	0.00	0.00	0.00	0.00	0.00
Fe ²⁺	0.17	0.20	0.19	0.16	0.15	0.16	0.16	0.16	0.18
Mn	0.00	0.00	0.00	0.00	0.00	0.00	0.00	0.00	0.00
Mg	0.49	0.49	0.48	0.44	0.45	0.45	0.41	0.44	0.49
Ca	0.57	0.60	0.60	0.51	0.52	0.52	0.49	0.51	0.60
Na	0.33	0.27	0.31	0.31	0.37	0.31	0.34	0.33	0.29
K	0.01	0.00	0.00	0.02	0.02	0.02	0.04	0.03	0.01
Sum	3.98	3.97	3.97	3.92	3.97	3.96	3.93	3.98	3.97
Mg# ^b	74.43	71.48	71.88	72.86	74.76	73.42	72.46	73.50	73.53
Class ^c	Omp	Omp	Omp	Omp	Omp	Omp	Omp	Omp	Omp

a $Fe^{3+} = 2 * X * (1 - T/S)$; where X = oxygen in structural formulae; T = ideal number in structural formulae; S = cations per structural formulae calculated (Droop, 1987).

b $Mg\# = 100 * Mg / (Mg + Fe^{2+} + Fe^{3+})$.

c Class = Classification: Omp—Omphacite.

Biotite compositions from eclogitic starting material ESM-1 at 2.5 GPa and 800°C run products. Structural formulae calculated for 22 oxygens

wt. %	1	2	3	4	5	6	7	8	9
SiO ₂	38.05	37.88	36.23	36.47	38.23	37.22	39.55	38.92	40.38
TiO ₂	2.70	2.47	4.02	5.02	3.08	3.22	3.68	4.71	3.82
Al ₂ O ₃	15.78	16.00	14.55	13.92	15.04	15.09	16.46	15.04	15.49
Cr ₂ O ₃	0.00	0.00	0.00	0.00	0.00	0.00	0.00	0.00	0.00
Fe ₂ O ₃	0.00	0.00	0.00	0.00	0.00	0.00	0.00	0.00	0.00
FeO	14.74	14.63	15.05	14.86	14.80	15.50	15.25	14.98	14.82
MnO	0.00	0.00	0.00	0.00	0.00	0.00	0.00	0.00	0.00
MgO	12.19	11.79	11.52	10.72	11.71	11.39	12.04	11.34	11.32
CaO	0.78	0.66	0.00	1.02	1.13	0.44	0.45	1.03	1.74
Na ₂ O	0.56	0.66	0.37	0.70	0.63	0.00	0.56	0.77	1.02
K ₂ O	8.02	8.14	8.47	7.69	7.94	8.15	8.33	7.94	7.56
Totals	92.83	92.23	90.21	90.40	92.56	91.00	96.32	94.72	96.15
Si	5.77	5.78	5.70	5.72	5.82	5.78	5.77	5.79	5.89
Ti	0.31	0.28	0.48	0.59	0.35	0.38	0.40	0.53	0.42
Al	2.82	2.88	2.70	2.57	2.70	2.76	2.83	2.64	2.66
Cr	0.00	0.00	0.00	0.00	0.00	0.00	0.00	0.00	0.00
Fe ³⁺ ^a	0.00	0.00	0.00	0.00	0.00	0.00	0.00	0.00	0.00
Fe ²⁺	1.87	1.87	1.98	1.95	1.89	2.01	1.86	1.86	1.81
Mn	0.00	0.00	0.00	0.00	0.00	0.00	0.00	0.00	0.00
Mg	2.76	2.68	2.70	2.51	2.66	2.64	2.62	2.52	2.46
Ca	0.13	0.11	0.00	0.17	0.18	0.07	0.07	0.16	0.27
Na	0.16	0.20	0.11	0.21	0.19	0.00	0.16	0.22	0.29
K	1.55	1.58	1.70	1.54	1.54	1.62	1.55	1.51	1.41
Sum	15.37	15.38	15.38	15.27	15.34	15.27	15.26	15.23	15.21
Mg# ^b	59.57	58.96	57.70	56.25	58.50	56.70	58.46	57.43	57.66

a $Fe^{3+} = 2 * X * (1 - T/S)$; where X = oxygen in structural formulae; T = ideal number in structural formulae; S = cations per structural formulae calculated (Droop, 1987).

b $Mg\# = 100 * Mg / (Mg + Fe^{2+} + Fe^{3+})$.

Biotite compositions from eclogitic starting material ESM-1 at 2.5 GPa and 800°C run products. Structural formulae calculated for 22 oxygens

wt.%	10	11	12	13	14	15	16	17	18
SiO ₂	40.10	40.55	37.23	40.13	38.09	37.50	40.91	36.64	40.16
TiO ₂	3.86	3.10	3.61	3.53	3.65	3.72	3.47	3.66	3.21
Al ₂ O ₃	16.57	17.25	15.64	16.29	15.15	15.39	16.37	15.15	16.23
Cr ₂ O ₃	0.00	0.00	0.00	0.00	0.00	0.00	0.00	0.00	0.00
Fe ₂ O ₃	0.00	0.00	0.00	0.00	0.00	0.00	0.00	0.00	0.00
FeO	15.31	14.87	15.36	15.61	14.48	15.56	15.19	15.36	14.07
MnO	0.00	0.00	0.00	0.00	0.00	0.00	0.00	0.00	0.00
MgO	12.42	12.85	11.93	12.29	11.15	11.57	11.99	11.44	11.72
CaO	0.80	0.41	0.00	1.04	1.02	0.56	0.63	0.00	0.88
Na ₂ O	0.68	0.63	0.52	0.78	0.69	0.42	0.73	0.48	0.70
K ₂ O	8.15	8.69	8.16	8.19	7.69	8.13	8.19	8.12	8.10
Totals	97.90	98.35	92.45	97.85	91.93	92.85	97.47	90.86	95.06
Si	5.75	5.78	5.69	5.78	5.82	5.72	5.88	5.71	5.90
Ti	0.42	0.33	0.42	0.38	0.42	0.43	0.37	0.43	0.35
Al	2.80	2.90	2.82	2.76	2.73	2.77	2.77	2.78	2.81
Cr	0.00	0.00	0.00	0.00	0.00	0.00	0.00	0.00	0.00
Fe ³⁺ ^a	0.00	0.00	0.00	0.00	0.00	0.00	0.00	0.00	0.00
Fe ²⁺	1.84	1.77	1.96	1.88	1.85	1.98	1.83	2.00	1.73
Mn	0.00	0.00	0.00	0.00	0.00	0.00	0.00	0.00	0.00
Mg	2.66	2.73	2.72	2.64	2.54	2.63	2.57	2.66	2.56
Ca	0.12	0.06	0.00	0.16	0.17	0.09	0.10	0.00	0.14
Na	0.19	0.17	0.15	0.22	0.21	0.12	0.20	0.15	0.20
K	1.49	1.58	1.59	1.50	1.50	1.58	1.50	1.61	1.52
Sum	15.27	15.32	15.36	15.32	15.24	15.32	15.22	15.35	15.20
Mg# ^b	59.11	60.63	58.05	58.40	57.86	56.98	58.43	57.03	59.74

a $Fe^{3+} = 2 * X * (1 - T/S)$; where X = oxygen in structural formulae; T = ideal number in structural formulae; S = cations per structural formulae calculated (Droop, 1987).

b $Mg\# = 100 * Mg / (Mg + Fe^{2+} + Fe^{3+})$.

Biotite compositions from eclogitic starting material ESM-1 at 2.5 GPa and 800°C run products. Structural formulae calculated for 22 oxygens

wt.%	19	20	21	22	23	24	25
SiO ₂	38.04	38.28	37.88	39.87	39.56	37.07	40.48
TiO ₂	3.35	3.13	4.96	3.15	3.28	3.26	2.93
Al ₂ O ₃	15.51	15.33	15.21	15.76	14.84	15.25	16.66
Cr ₂ O ₃	0.00	0.00	0.00	0.00	0.00	0.00	0.00
Fe ₂ O ₃	0.00	0.00	0.00	0.00	0.00	0.00	0.00
FeO	15.21	14.20	14.66	14.37	13.67	14.89	14.27
MnO	0.00	0.00	0.00	0.00	0.00	0.00	0.00
MgO	11.89	11.32	11.78	11.50	11.50	11.92	12.30
CaO	0.00	0.00	0.00	0.00	1.89	0.00	0.75
Na ₂ O	0.39	0.71	0.54	1.12	0.72	0.49	0.84
K ₂ O	8.58	8.15	8.31	8.32	7.47	8.37	8.22
Totals	92.97	91.12	93.33	94.09	92.92	91.23	96.44
Si	5.78	5.89	5.72	5.93	5.95	5.74	5.86
Ti	0.38	0.36	0.56	0.35	0.37	0.38	0.32
Al	2.78	2.78	2.71	2.76	2.63	2.78	2.84
Cr	0.00	0.00	0.00	0.00	0.00	0.00	0.00
Fe ³⁺ ^a	0.00	0.00	0.00	0.00	0.00	0.00	0.00
Fe ²⁺	1.93	1.83	1.85	1.79	1.72	1.93	1.73
Mn	0.00	0.00	0.00	0.00	0.00	0.00	0.00
Mg	2.69	2.59	2.65	2.55	2.58	2.75	2.65
Ca	0.00	0.00	0.00	0.00	0.30	0.00	0.12
Na	0.12	0.21	0.16	0.32	0.21	0.15	0.24
K	1.66	1.60	1.60	1.58	1.43	1.65	1.52
Sum	15.34	15.26	15.25	15.29	15.19	15.39	15.28
Mg# ^b	58.21	58.68	58.88	58.80	59.97	58.78	60.57

a $Fe^{3+} = 2 * X * (1 - T/S)$; where X = oxygen in structural formulae; T = ideal number in structural formulae; S = cations per structural formulae calculated (Droop, 1987).

b $Mg\# = 100 * Mg / (Mg + Fe^{2+} + Fe^{3+})$.

Melt compositions generated from eclogitic starting material ESM-1 at 2.5 Gpa and 800°C run products.

wt.%	1	2	3	4	5	6	7	8	9	10
SiO ₂	61.12	61.42	60.30	59.91	59.79	59.61	59.79	59.61	61.12	52.95
TiO ₂	0.00	0.00	0.00	0.00	0.00	0.00	0.00	0.00	0.00	0.00
Al ₂ O ₃	13.77	13.59	13.63	13.36	13.32	13.47	13.32	13.47	13.77	12.06
Cr ₂ O ₃	0.00	0.00	0.00	0.00	0.00	0.00	0.00	0.00	0.00	0.00
Fe ₂ O ₃	0.00	0.00	0.00	0.00	0.00	0.00	0.00	0.00	0.00	0.00
FeO	0.66	0.65	0.68	0.74	0.73	0.80	0.73	0.80	0.66	1.35
MnO	0.00	0.00	0.00	0.00	0.00	0.00	0.00	0.00	0.00	0.00
MgO	0.00	0.00	0.00	0.00	0.00	0.24	0.00	0.24	0.00	0.00
CaO	0.76	0.78	0.74	0.73	0.82	0.67	0.82	0.67	0.76	0.86
Na ₂ O	3.20	3.32	2.91	2.92	3.26	3.25	3.26	3.25	3.20	3.48
K ₂ O	3.53	3.41	3.46	3.35	3.50	3.28	3.50	3.28	3.53	2.81
Totals	83.04	83.18	81.72	81.01	81.41	81.32	81.42	81.32	83.04	73.51
AlS ^c	1.41	1.38	1.48	1.47	1.35	1.42	1.35	1.42	1.41	1.26

a $Fe_{3+} = 2 * X * (1 - T/S)$; where X = oxygen in structural formulae; T = ideal number in structural formulae; S = cations per structural formulae calculated (Droop, 1987).

b $Mg\# = 100 * Mg / (Mg + Fe_{2+} + Fe_{3+})$.

c AlS = Aluminium Saturation

Melt compositions generated from eclogitic starting material ESM-1 at 2.5 Gpa and 800°C run products.

wt.%	11	12	13	14	15	16	17	18	19	20
SiO ₂	61.42	60.30	59.91	56.84	63.53	61.55	60.07	61.39	59.63	61.05
TiO ₂	0.00	0.00	0.00	0.00	0.00	0.31	0.00	0.00	0.29	0.00
Al ₂ O ₃	13.59	13.63	13.36	13.21	14.18	13.84	13.69	14.07	13.52	13.80
Cr ₂ O ₃	0.00	0.00	0.00	0.00	0.00	0.00	0.00	0.00	0.00	0.00
Fe ₂ O ₃	0.00	0.00	0.00	0.00	0.00	0.00	0.00	0.00	0.00	0.00
FeO	0.65	0.68	0.74	0.82	1.35	1.22	1.57	1.46	1.89	1.18
MnO	0.00	0.00	0.00	0.00	0.00	0.00	0.00	0.00	0.00	0.00
MgO	0.00	0.00	0.00	0.30	0.44	0.44	0.34	0.33	0.49	0.26
CaO	0.78	0.74	0.73	0.71	1.81	1.17	1.02	1.08	0.77	0.88
Na ₂ O	3.32	2.91	2.92	4.80	4.60	5.03	4.91	4.97	4.82	5.02
K ₂ O	3.41	3.46	3.35	3.47	3.57	3.58	3.40	3.45	3.62	3.51
Totals	83.17	81.72	81.01	80.15	89.48	87.14	85.00	86.75	85.03	85.70
AlS ^c	1.38	1.48	1.47	1.07	1.08	1.05	1.08	1.09	1.08	1.07

a $Fe_{3+} = 2 * X * (1 - T/S)$; where X = oxygen in structural formulae; T = ideal number in structural formulae; S = cations per structural formulae calculated (Droop, 1987).

b $Mg\# = 100 * Mg / (Mg + Fe_{2+} + Fe_{3+})$.

c AlS = Aluminium Saturation

General garnet compositions from EMS-1 at 2.5 GPa and 850°C. Structural formulae calculated for 12 oxygens.

	1	2	3	4	5	6	7	8	9	10	11	12
wt.%												
SiO ₂	39.28	39.63	38.96	39.09	38.81	38.14	38.95	39.25	38.92	38.94	39.34	38.69
TiO ₂	1.59	0.91	1.96	1.03	1.33	4.00	1.31	1.53	1.15	1.89	1.28	2.49
Al ₂ O ₃	21.71	21.86	21.81	21.49	21.81	21.24	21.48	22.18	21.70	21.77	21.80	21.37
Cr ₂ O ₃	0.00	0.00	0.00	0.00	0.00	0.00	0.00	0.00	0.00	0.00	0.00	0.00
Fe ₂ O ₃	0.00	0.00	0.00	0.00	0.00	0.00	0.00	0.00	0.00	0.00	0.00	0.00
FeO	20.76	20.07	21.17	20.42	21.52	21.15	21.61	20.27	21.69	20.15	20.07	21.53
MnO	0.00	0.00	0.00	0.00	0.00	0.00	0.00	0.00	0.00	0.00	0.00	0.00
MgO	5.94	6.29	5.22	5.94	5.42	5.21	5.43	6.50	5.74	6.44	6.44	5.55
CaO	11.41	11.70	11.58	11.29	11.49	10.98	10.75	11.06	11.03	11.26	11.22	10.75
Na ₂ O	0.00	0.00	0.00	0.00	0.00	0.00	0.00	0.00	0.00	0.00	0.00	0.00
K ₂ O	0.00	0.00	0.00	0.00	0.00	0.00	0.00	0.00	0.00	0.00	0.00	0.07
Totals	100.69	100.46	100.70	99.26	100.38	100.72	99.53	100.79	100.23	100.45	100.15	100.45
Si	2.99	3.01	2.97	3.01	2.97	2.91	3.01	2.97	2.99	2.96	3.00	2.96
Ti	0.09	0.05	0.11	0.06	0.08	0.23	0.08	0.09	0.07	0.11	0.07	0.14
Al	1.95	1.96	1.96	1.95	1.97	1.91	1.95	1.98	1.96	1.95	1.96	1.93
Cr	0.00	0.00	0.00	0.00	0.00	0.00	0.00	0.00	0.00	0.00	0.00	0.00
Fe ^{3+/a}	0.00	0.00	0.00	0.00	0.00	0.00	0.00	0.00	0.00	0.00	0.00	0.00
Fe ^{2+/a}	1.32	1.27	1.35	1.32	1.38	1.35	1.39	1.28	1.39	1.28	1.28	1.38
Mn	0.00	0.00	0.00	0.00	0.00	0.00	0.00	0.00	0.00	0.00	0.00	0.00
Mg	0.67	0.71	0.59	0.68	0.62	0.59	0.62	0.73	0.66	0.73	0.73	0.63
Ca	0.93	0.95	0.95	0.93	0.94	0.90	0.89	0.90	0.91	0.92	0.92	0.88
Na	0.00	0.00	0.00	0.00	0.00	0.00	0.00	0.00	0.00	0.00	0.00	0.00
K	0.00	0.00	0.00	0.00	0.00	0.00	0.00	0.00	0.00	0.00	0.00	0.01
Sum	7.95	7.96	7.94	7.95	7.96	7.90	7.94	7.95	7.97	7.95	7.95	7.93
Mg# ^b	33.77	35.84	30.53	34.14	30.98	30.51	30.93	36.36	32.05	36.29	36.38	31.48
gr ^c	0.32	0.32	0.33	0.32	0.32	0.32	0.31	0.31	0.31	0.31	0.31	0.30
al ^d	0.45	0.43	0.47	0.45	0.47	0.48	0.48	0.44	0.47	0.44	0.44	0.48
py ^e	0.23	0.24	0.21	0.23	0.21	0.21	0.21	0.25	0.22	0.25	0.25	0.22

a $Fe^{3+} = 2 * X * (1 - T/S)$, where X = oxygen in structural formulae; T = ideal number in structural formulae; S = cations per structural formulae calculated (Droop, 1987).

b $Mg\# = 100 * Mg / (Mg + Fe^{2+} + Fe^{3+})$.

c $gr = Ca / (Ca + Fe + Mn + Mg)$.

d $al = Fe / (Ca + Fe + Mn + Mg)$.

e $py = Mg / (Ca + Fe + Mn + Mg)$.

General garnet compositions from EMS-1 at 2.5 GPa and 850°C. Structural formulae calculated for 12 oxygens.

wt.%	13	14	15	16	17	18	19	20	21	22	23	24	25
SiO ₂	38.14	38.95	39.25	38.92	38.94	39.34	38.69	38.51	39.29	38.95	38.97	38.96	39.05
TiO ₂	4.00	1.31	1.53	1.15	1.89	1.28	2.49	2.37	0.98	1.46	1.49	2.27	1.66
Al ₂ O ₃	21.24	21.48	22.18	21.70	21.77	21.80	21.37	21.12	21.93	21.88	21.99	21.69	21.20
Cr ₂ O ₃	0.00	0.00	0.00	0.00	0.00	0.00	0.00	0.00	0.00	0.00	0.00	0.00	0.00
Fe ₂ O ₃	0.00	0.00	0.00	0.00	0.00	0.00	0.00	0.00	0.00	0.00	0.00	0.00	0.00
FeO	21.15	21.61	20.27	21.69	20.15	20.07	21.53	22.16	21.64	21.08	21.62	20.40	24.69
MnO	0.00	0.00	0.00	0.00	0.00	0.00	0.00	0.00	0.00	0.00	0.00	0.00	0.00
MgO	5.21	5.43	6.50	5.74	6.44	6.44	5.55	4.92	6.09	6.62	5.76	6.42	4.54
CaO	10.98	10.75	11.06	11.03	11.26	11.22	10.75	10.96	10.05	9.64	11.23	10.35	10.15
Na ₂ O	0.00	0.00	0.00	0.00	0.00	0.00	0.00	0.00	0.00	0.00	0.23	0.00	0.18
K ₂ O	0.00	0.00	0.00	0.00	0.00	0.00	0.07	0.00	0.00	0.00	0.00	0.00	0.00
Totals	100.72	99.53	100.79	100.23	100.45	100.15	100.45	100.04	99.98	99.63	101.29	100.09	101.47
Si	2.91	3.01	2.97	2.99	2.96	3.00	2.96	2.97	3.01	2.98	2.96	2.97	2.99
Ti	0.23	0.08	0.09	0.07	0.11	0.07	0.14	0.14	0.06	0.08	0.09	0.13	0.10
Al	1.91	1.95	1.98	1.96	1.95	1.96	1.93	1.92	1.98	1.98	1.97	1.95	1.92
Cr	0.00	0.00	0.00	0.00	0.00	0.00	0.00	0.00	0.00	0.00	0.00	0.00	0.00
Fe ³⁺ ^a	0.00	0.00	0.00	0.00	0.00	0.00	0.00	0.00	0.00	0.00	0.00	0.00	0.00
Fe ²⁺	1.35	1.39	1.28	1.39	1.28	1.28	1.38	1.43	1.39	1.35	1.37	1.30	1.58
Mn	0.00	0.00	0.00	0.00	0.00	0.00	0.00	0.00	0.00	0.00	0.00	0.00	0.00
Mg	0.59	0.62	0.73	0.66	0.73	0.73	0.63	0.57	0.69	0.76	0.65	0.73	0.52
Ca	0.90	0.89	0.90	0.91	0.92	0.92	0.88	0.91	0.82	0.79	0.91	0.85	0.83
Na	0.00	0.00	0.00	0.00	0.00	0.00	0.00	0.00	0.00	0.00	0.03	0.00	0.03
K	0.00	0.00	0.00	0.00	0.00	0.00	0.01	0.00	0.00	0.00	0.00	0.00	0.00
Sum	7.90	7.94	7.95	7.97	7.95	7.95	7.93	7.93	7.95	7.94	7.99	7.93	7.97
Mg# ^b	30.51	30.93	36.36	32.05	36.29	36.38	31.48	28.35	33.40	35.88	32.19	35.93	24.68
gr ^c	0.32	0.31	0.31	0.31	0.31	0.31	0.30	0.31	0.28	0.27	0.31	0.29	0.28
al ^d	0.48	0.48	0.44	0.47	0.44	0.44	0.48	0.49	0.48	0.47	0.47	0.45	0.54
py ^e	0.21	0.21	0.25	0.22	0.25	0.25	0.22	0.19	0.24	0.26	0.22	0.25	0.18

^a Fe³⁺ = 2*X*(1 - T/S); where X = oxygen in structural formulae; T = ideal number in structural formulae; S = cations per structural formulae calculated (Droop, 1987).

^b Mg# = 100*Mg/(Mg+Fe²⁺+Fe³⁺).

^c gr = Ca/(Ca+Fe+Mn+Mg).

^d al = Fe/(Ca+Fe+Mn+Mg).

^e py = Mg/(Ca+Fe+Mn+Mg).

General garnet compositions from EMS-1 at 2.5 GPa and 850°C. Structural formulae calculated for 12 oxygens.

wt.%	26	27	28	29	30	31	32	33	34	35	36	37	38
SiO ₂	38.22	39.52	39.39	38.45	38.92	39.54	39.67	39.50	40.08	38.85	38.76	38.66	38.00
TiO ₂	2.83	1.05	1.29	0.99	0.82	0.75	0.91	0.92	0.73	0.94	2.38	3.22	2.31
Al ₂ O ₃	21.59	21.79	22.10	21.47	21.73	22.22	22.16	21.89	22.31	21.84	21.41	21.66	20.84
Cr ₂ O ₃	0.00	0.00	0.00	0.00	0.00	0.00	0.00	0.00	0.00	0.00	0.00	0.00	0.00
Fe ₂ O ₃	0.00	0.00	0.00	0.00	0.00	0.00	0.00	0.00	0.00	0.00	0.00	0.00	0.00
FeO	21.34	21.35	19.76	23.52	20.05	20.03	20.05	20.02	19.88	20.07	19.99	18.82	23.09
MnO	0.00	0.00	0.00	0.00	0.00	0.00	0.00	0.00	0.00	0.00	0.00	0.00	0.00
MgO	5.24	5.60	6.81	5.74	6.33	6.62	7.27	6.57	7.17	6.15	5.95	6.76	4.38
CaO	10.92	11.22	10.90	9.74	11.06	11.13	10.47	11.33	10.86	11.46	11.09	10.96	10.63
Na ₂ O	0.00	0.21	0.00	0.00	0.00	0.00	0.00	0.00	0.00	0.00	0.00	0.00	0.00
K ₂ O	0.00	0.00	0.00	0.00	0.00	0.00	0.00	0.00	0.00	0.00	0.00	0.00	0.00
Totals	100.14	100.74	100.25	99.91	98.91	100.29	100.53	100.23	101.03	99.31	99.58	100.08	99.25
Si	2.94	3.01	2.99	2.98	3.00	3.00	3.00	3.00	3.01	2.99	2.97	2.94	2.97
Ti	0.16	0.06	0.07	0.06	0.05	0.04	0.05	0.05	0.04	0.05	0.14	0.18	0.14
Al	1.96	1.96	1.98	1.96	1.98	1.99	1.98	1.96	1.98	1.98	1.94	1.94	1.92
Cr	0.00	0.00	0.00	0.00	0.00	0.00	0.00	0.00	0.00	0.00	0.00	0.00	0.00
Fe ^{3+a}	0.00	0.00	0.00	0.00	0.00	0.00	0.00	0.00	0.00	0.00	0.00	0.00	0.00
Fe ²⁺	1.37	1.36	1.25	1.52	1.29	1.27	1.27	1.27	1.25	1.29	1.28	1.20	1.51
Mn	0.00	0.00	0.00	0.00	0.00	0.00	0.00	0.00	0.00	0.00	0.00	0.00	0.00
Mg	0.60	0.64	0.77	0.66	0.73	0.75	0.82	0.74	0.80	0.71	0.68	0.77	0.51
Ca	0.90	0.92	0.89	0.81	0.91	0.91	0.85	0.92	0.87	0.94	0.91	0.89	0.89
Na	0.00	0.03	0.00	0.00	0.00	0.00	0.00	0.00	0.00	0.00	0.00	0.00	0.00
K	0.00	0.00	0.00	0.00	0.00	0.00	0.00	0.00	0.00	0.00	0.00	0.00	0.00
Sum	7.92	7.97	7.95	7.99	7.96	7.96	7.96	7.96	7.96	7.97	7.92	7.91	7.93
Mg# ^b	30.44	31.85	38.05	30.31	36.00	37.07	39.25	36.90	39.12	35.32	34.66	39.03	25.26
gr ^c	0.31	0.31	0.30	0.27	0.31	0.31	0.29	0.31	0.30	0.32	0.32	0.31	0.31
al ^d	0.48	0.47	0.43	0.51	0.44	0.43	0.43	0.43	0.43	0.44	0.45	0.42	0.52
py ^e	0.21	0.22	0.26	0.22	0.25	0.26	0.28	0.25	0.27	0.24	0.24	0.27	0.18

a $Fe^{3+} = 2 * X * (1 - T/S)$; where X = oxygen in structural formulae; T = ideal number in structural formulae; S = cations per structural formulae calculated (Droop, 1987).

b $Mg\# = 100 * Mg / (Mg + Fe^{2+} + Fe^{3+})$.

c $gr = Ca / (Ca + Fe + Mn + Mg)$.

d $al = Fe / (Ca + Fe + Mn + Mg)$.

e $py = Mg / (Ca + Fe + Mn + Mg)$.

General garnet compositions from EMS-1 at 2.5 GPa and 850°C. Structural formulae calculated for 12 oxygens.

wt.%	39	40	41	42	43	44	45	46	47	48	49
SiO ₂	38.41	38.47	38.54	38.47	37.51	39.33	39.59	39.54	39.23	38.84	39.53
TiO ₂	1.40	1.39	1.00	1.73	4.17	1.00	0.89	1.04	0.92	1.15	1.34
Al ₂ O ₃	21.47	21.25	21.61	21.41	20.92	21.95	21.89	22.02	21.95	21.51	22.03
Cr ₂ O ₃	0.00	0.00	0.00	0.00	0.00	0.00	0.00	0.00	0.00	0.00	0.00
Fe ₂ O ₃	0.00	0.00	0.00	0.00	0.00	0.00	0.00	0.00	0.00	0.00	0.00
FeO	22.87	24.12	22.88	21.30	21.07	21.88	22.25	21.11	19.91	21.44	20.25
MnO	0.00	0.00	0.00	0.00	0.00	0.00	0.00	0.00	0.00	0.00	0.00
MgO	4.74	4.45	5.61	5.42	5.01	6.17	6.92	6.25	6.65	5.50	5.99
CaO	10.61	10.40	9.85	10.99	10.82	10.12	9.27	10.80	10.98	11.19	11.57
Na ₂ O	0.00	0.18	0.00	0.00	0.00	0.00	0.00	0.00	0.00	0.00	0.00
K ₂ O	0.00	0.00	0.00	0.00	0.00	0.00	0.00	0.00	0.00	0.00	0.00
Totals	99.50	100.26	99.49	99.32	99.50	100.45	100.81	100.76	99.64	99.63	100.71
Si	2.98	2.98	2.99	2.98	2.90	3.00	3.01	3.00	3.00	3.00	3.00
Ti	0.08	0.08	0.06	0.10	0.24	0.06	0.05	0.06	0.05	0.07	0.08
Al	1.97	1.94	1.97	1.95	1.91	1.97	1.96	1.97	1.98	1.96	1.97
Cr	0.00	0.00	0.00	0.00	0.00	0.00	0.00	0.00	0.00	0.00	0.00
Fe ³⁺ ^a	0.00	0.00	0.00	0.00	0.00	0.00	0.00	0.00	0.00	0.00	0.00
Fe ²⁺	1.49	1.56	1.48	1.38	1.36	1.40	1.41	1.34	1.27	1.38	1.28
Mn	0.00	0.00	0.00	0.00	0.00	0.00	0.00	0.00	0.00	0.00	0.00
Mg	0.55	0.51	0.65	0.63	0.58	0.70	0.78	0.71	0.76	0.63	0.68
Ca	0.88	0.86	0.82	0.91	0.90	0.83	0.75	0.88	0.90	0.92	0.94
Na	0.00	0.03	0.00	0.00	0.00	0.00	0.00	0.00	0.00	0.00	0.00
K	0.00	0.00	0.00	0.00	0.00	0.00	0.00	0.00	0.00	0.00	0.00
Sum	7.95	7.98	7.97	7.95	7.90	7.96	7.96	7.95	7.96	7.96	7.94
Mg# ^b	26.97	24.74	30.41	31.20	29.76	33.44	35.66	34.54	37.31	31.37	34.52
gr ^c	0.30	0.29	0.28	0.31	0.32	0.28	0.26	0.30	0.31	0.31	0.32
al ^d	0.51	0.53	0.50	0.47	0.48	0.48	0.48	0.46	0.43	0.47	0.44
py ^e	0.19	0.17	0.22	0.21	0.20	0.24	0.27	0.24	0.26	0.22	0.23

^a Fe³⁺ = 2*X*(1 - T/S), where X = oxygen in structural formulae; T = ideal number in structural formulae; S = cations per structural formulae calculated (Droop, 1987).

^b Mg# = 100*Mg/(Mg+Fe²⁺+Fe³⁺).

^c gr = Ca/(Ca+Fe+Mn+Mg).

^d al = Fe/(Ca+Fe+Mn+Mg).

^e py = Mg/(Ca+Fe+Mn+Mg).

Iron-rich garnet core compositions from EMS-1 at 2.5 GPa and 850°C. Structural formulae calculated for 12 oxygens.

wt.%	1	2	3	4	5	6	7	8	9	10	11	12
SiO ₂	38.28	38.42	38.16	38.58	38.42	42.32	39.44	39.12	31.09	35.93	42.64	39.46
TiO ₂	1.14	0.89	0.60	0.76	0.37	0.87	0.84	0.33	0.90	2.02	0.27	1.12
Al ₂ O ₃	20.99	21.11	20.81	20.58	20.56	18.78	20.03	20.63	6.66	19.37	14.08	21.39
Cr ₂ O ₃	0.00	0.00	0.00	0.00	0.00	0.00	0.00	0.00	0.00	0.00	0.00	0.00
Fe ₂ O ₃	0.00	0.00	0.00	0.00	0.00	0.00	0.00	0.00	0.00	0.00	0.00	0.00
FeO	26.04	26.41	27.77	32.53	32.72	32.01	35.09	33.58	52.83	30.66	35.15	24.79
MnO	0.00	0.00	0.00	0.00	0.00	0.00	0.00	0.00	0.00	0.00	0.00	0.00
MgO	3.98	3.79	3.76	2.97	2.21	1.66	1.64	3.06	4.04	3.10	4.76	4.77
CaO	9.35	9.15	7.65	4.87	4.30	3.31	3.39	3.34	1.88	7.27	3.79	8.87
Na ₂ O	0.00	0.00	0.00	0.20	0.23	0.86	0.98	0.00	0.00	0.00	0.18	0.29
K ₂ O	0.00	0.00	0.00	0.08	0.11	0.41	0.12	0.00	0.00	0.00	0.00	0.09
Totals	99.80	99.76	98.75	100.58	98.93	100.21	101.52	100.08	97.40	98.34	100.87	100.76
Si	3.00	3.01	3.03	3.05	3.09	3.32	3.11	3.10	3.30	3.02	2.93	3.38
Ti	0.07	0.05	0.04	0.05	0.02	0.05	0.05	0.02	0.04	0.05	0.06	0.02
Al	1.94	1.95	1.95	1.92	1.95	1.74	1.86	1.93	1.78	1.95	0.74	1.32
Cr	0.00	0.00	0.00	0.00	0.00	0.00	0.00	0.00	0.00	0.00	0.00	0.00
Fe ³⁺ a	0.00	0.00	0.00	0.00	0.00	0.00	0.00	0.00	0.00	0.00	0.00	0.00
Fe ²⁺ a	1.71	1.73	1.84	2.15	2.20	2.10	2.32	2.23	1.92	2.17	4.16	2.33
Mn	0.00	0.00	0.00	0.00	0.00	0.00	0.00	0.00	0.00	0.00	0.00	0.00
Mg	0.47	0.44	0.45	0.35	0.27	0.19	0.19	0.36	0.33	0.40	0.57	0.56
Ca	0.79	0.77	0.65	0.41	0.37	0.28	0.29	0.28	0.31	0.36	0.19	0.32
Na	0.00	0.00	0.00	0.03	0.04	0.13	0.15	0.00	0.18	0.00	0.00	0.03
K	0.00	0.00	0.00	0.01	0.01	0.04	0.01	0.00	0.03	0.00	0.00	0.00
Sum	7.96	7.96	7.96	7.97	7.94	7.85	7.99	7.92	7.88	7.96	8.64	7.96
Mg# ^b	21.42	20.35	19.45	13.99	10.75	8.46	7.67	13.99	14.76	15.58	11.99	19.45
gr ^c	0.27	0.26	0.22	0.14	0.13	0.11	0.10	0.10	0.12	0.12	0.04	0.10
al ^d	0.58	0.59	0.63	0.74	0.78	0.82	0.83	0.78	0.75	0.74	0.85	0.72
py ^e	0.16	0.15	0.15	0.12	0.09	0.08	0.07	0.13	0.13	0.14	0.12	0.18

a Fe₃₊ = 2*X*(1 - T/S); where X = oxygen in structural formulae; T = ideal number in structural formulae; S = cations per structural formulae calculated (Droop, 1987).

b Mg# = 100*Mg/(Mg+Fe²⁺+Fe³⁺).

c gr = Ca/(Ca+Fe+Mn+Mg).

d al = Fe/(Ca+Fe+Mn+Mg).

e py = Mg/(Ca+Fe+Mn+Mg).

Pyroxene compositions from eclogitic starting material ESM-1 run products at 2.5 GPa and 850°C.
 Structural formulae calculated for 6 oxygens.

wt.%	1	2	3	4	5	6	7	8
SiO ₂	53.71	54.34	53.39	53.81	54.75	54.67	53.99	54.19
TiO ₂	1.01	0.41	0.00	0.38	0.27	0.44	0.55	0.55
Al ₂ O ₃	9.87	9.80	6.36	8.06	8.38	9.46	8.80	9.16
Cr ₂ O ₃	0.00	0.00	0.00	0.00	0.00	0.00	0.00	0.00
Fe ₂ O ₃	0.00	0.00	0.00	0.00	0.00	0.00	0.00	0.00
FeO	4.76	5.06	6.48	5.70	6.14	5.07	5.62	5.55
MnO	0.00	0.00	0.00	0.00	0.00	0.00	0.00	0.00
MgO	10.04	10.10	12.04	11.01	10.16	10.43	10.52	10.02
CaO	15.43	15.72	18.57	16.57	14.95	15.26	16.30	15.19
Na ₂ O	4.89	4.59	2.75	4.14	4.78	4.83	3.90	4.91
K ₂ O	0.00	0.00	0.00	0.00	0.00	0.00	0.00	0.00
Totals	99.70	100.03	99.58	99.68	99.44	100.14	99.69	99.57
Si	1.93	1.95	1.95	1.95	1.98	1.96	1.95	1.96
Ti	0.03	0.01	0.00	0.01	0.01	0.01	0.01	0.01
Al	0.42	0.41	0.27	0.34	0.36	0.40	0.38	0.39
Cr	0.00	0.00	0.00	0.00	0.00	0.00	0.00	0.00
Fe ³⁺ ^a	0.00	0.00	0.00	0.00	0.00	0.00	0.00	0.00
Fe ²⁺	0.14	0.15	0.20	0.17	0.19	0.15	0.17	0.17
Mn	0.00	0.00	0.00	0.00	0.00	0.00	0.00	0.00
Mg	0.54	0.54	0.66	0.60	0.55	0.56	0.57	0.54
Ca	0.60	0.60	0.73	0.64	0.58	0.59	0.63	0.59
Na	0.34	0.32	0.19	0.29	0.34	0.34	0.27	0.34
K	0.00	0.00	0.00	0.00	0.01	0.00	0.00	0.00
Sum	4.00	3.99	4.01	4.01	4.00	4.00	3.98	4.00
Mg# ^b	78.98	78.07	76.80	77.48	74.69	78.58	76.94	76.30
Class ^c	Omp	Omp	Omp	Omp	Omp	Omp	Omp	Omp

a $Fe^{3+} = 2 * X * (1 - T/S)$; where X = oxygen in structural formulae; T = ideal number in structural formulae; S = cations per structural formulae calculated (Droop, 1987).

b $Mg\# = 100 * Mg / (Mg + Fe^{2+} + Fe^{3+})$.

c Class= Classification: Omp—Omphacite.

Biotite compositions from eclogitic starting material ESM-1 at 2.5 GPa and 850°C run products. Structural formulae calculated for 22 oxygens.

wt.%	1	2	3	4	5	6	7	8	9	10
SiO ₂	39.53	40.55	39.86	40.68	41.27	41.15	40.42	41.10	40.77	41.96
TiO ₂	1.99	1.67	1.93	2.09	2.60	2.04	2.55	1.90	1.81	1.73
Al ₂ O ₃	15.27	15.72	16.81	14.08	13.77	12.93	12.96	15.54	16.73	16.23
Cr ₂ O ₃	0.00	0.00	0.00	0.00	0.00	0.00	0.00	0.00	0.00	0.00
Fe ₂ O ₃	0.00	0.00	0.00	0.00	0.00	0.00	0.00	0.00	0.00	0.00
FeO	13.43	13.00	12.20	13.01	14.14	14.20	14.61	12.93	12.63	12.68
MnO	0.00	0.00	0.00	0.00	0.00	0.00	0.00	0.00	0.00	0.00
MgO	14.66	14.21	14.11	15.38	14.81	14.53	13.97	15.56	14.45	12.54
CaO	0.00	0.00	0.00	0.00	0.00	0.00	0.00	0.00	0.00	1.57
Na ₂ O	0.34	0.46	0.37	0.41	0.39	0.53	0.00	0.00	0.51	0.48
K ₂ O	7.69	7.59	7.66	7.61	7.94	7.65	7.47	7.46	7.57	7.04
Totals	92.91	93.20	92.93	93.26	94.92	93.02	91.98	94.49	94.47	94.24
Si	5.90	6.00	5.89	6.03	6.05	6.15	6.12	5.98	5.93	6.11
Ti	0.22	0.19	0.21	0.23	0.29	0.23	0.29	0.21	0.20	0.19
Al	2.69	2.74	2.93	2.46	2.38	2.28	2.31	2.66	2.87	2.79
Cr	0.00	0.00	0.00	0.00	0.00	0.00	0.00	0.00	0.00	0.00
Fe ³⁺ a	0.00	0.00	0.00	0.00	0.00	0.00	0.00	0.00	0.00	0.00
Fe ²⁺	1.68	1.61	1.51	1.61	1.73	1.77	1.85	1.57	1.54	1.54
Mn	0.00	0.00	0.00	0.00	0.00	0.00	0.00	0.00	0.00	0.00
Mg	3.26	3.13	3.11	3.40	3.23	3.24	3.15	3.37	3.13	2.72
Ca	0.00	0.00	0.00	0.00	0.00	0.00	0.00	0.00	0.00	0.24
Na	0.10	0.13	0.11	0.12	0.11	0.15	0.00	0.00	0.14	0.14
K	1.46	1.43	1.44	1.44	1.48	1.46	1.44	1.38	1.40	1.31
Sum	15.31	15.23	15.20	15.29	15.27	15.28	15.16	15.18	15.21	15.03
Mg# ^b	66.05	66.07	67.34	67.81	65.12	64.59	63.02	68.21	67.09	63.79

a $Fe^{3+} = 2 * X * (1 - T/S)$; where X = oxygen in structural formulae; T = ideal number in structural formulae; S = cations per structural formulae calculated (Droop, 1987).

b $Mg\# = 100 * Mg / (Mg + Fe^{2+} + Fe^{3+})$.

Melt compositions generated from eclogitic starting material ESM-1 at 2.5GPa and 850°C - run products.

wt.%	1	2	3	4	5	6	7	8	9	10	11
SiO ₂	62.90	61.56	65.27	62.97	65.56	65.90	65.36	63.85	64.05	63.71	62.25
TiO ₂	0.00	0.00	0.26	0.00	0.00	0.00	0.00	0.00	0.00	0.00	0.00
Al ₂ O ₃	11.09	11.01	11.61	11.18	11.65	11.62	11.78	11.26	11.37	11.18	11.00
Cr ₂ O ₃	0.00	0.00	0.00	0.00	0.00	0.00	0.00	0.00	0.00	0.00	0.00
Fe ₂ O ₃	0.00	0.00	0.00	0.00	0.00	0.00	0.00	0.00	0.00	0.00	0.00
FeO	0.86	0.98	0.72	0.94	0.74	0.72	0.75	0.66	0.75	0.90	1.26
MnO	0.00	0.00	0.00	0.00	0.00	0.00	0.00	0.00	0.00	0.00	0.00
MgO	0.00	0.00	0.00	0.23	0.00	0.00	0.00	0.00	0.00	0.25	0.24
CaO	0.70	0.75	0.75	0.71	0.74	0.66	0.71	0.56	0.51	0.99	0.75
Na ₂ O	3.62	3.75	4.16	4.07	3.88	3.94	3.38	4.07	3.51	3.62	3.75
K ₂ O	2.20	2.24	2.45	2.27	2.24	2.57	2.43	2.34	2.23	2.20	2.18
Totals	81.37	80.29	85.22	82.37	84.81	85.41	84.41	82.74	82.42	82.85	81.43
Si	3.26	3.24	3.24	3.24	3.26	3.25	3.25	3.26	3.27	3.25	3.24
Ti	0.00	0.00	0.01	0.00	0.00	0.00	0.00	0.00	0.00	0.00	0.00
Al	0.68	0.68	0.68	0.68	0.68	0.68	0.69	0.68	0.68	0.67	0.68
Cr	0.00	0.00	0.00	0.00	0.00	0.00	0.00	0.00	0.00	0.00	0.00
Fe ³⁺ ^a	0.00	0.00	0.00	0.00	0.00	0.00	0.00	0.00	0.00	0.00	0.00
Fe ²⁺	0.00	0.00	0.00	0.00	0.00	0.00	0.00	0.00	0.00	0.00	0.00
Mn	0.04	0.04	0.03	0.04	0.03	0.03	0.03	0.03	0.03	0.04	0.06
Mg	0.00	0.00	0.00	0.00	0.00	0.00	0.00	0.00	0.00	0.00	0.00
Ca	0.00	0.00	0.00	0.01	0.00	0.00	0.00	0.00	0.00	0.01	0.01
Na	0.07	0.08	0.07	0.07	0.07	0.06	0.07	0.06	0.05	0.10	0.08
K	0.24	0.25	0.26	0.27	0.25	0.25	0.21	0.26	0.23	0.24	0.25
Sum	4.28	4.30	4.29	4.31	4.29	4.27	4.26	4.28	4.26	4.31	4.31
ALS ^c	1.24	1.19	1.14	1.14	1.23	1.18	1.33	1.16	1.31	1.21	1.19

^a $Fe^{3+} = 2 * X * (1 - T/S)$; where X = oxygen in structural formulae; T = ideal number in structural formulae; S = cations per structural formulae calculated (Droop, 1987).

^b $Mg\# = 100 * Mg / (Mg + Fe^{2+} + Fe^{3+})$.

^c ALS = Aluminium Saturation

General garnet compositions from EMS-1 at 2.5 GPa and 600°C. Structural formulae calculated for 12 oxygens.

wt.%	1	2	3	4	5	6	Ave
SiO ₂	39.97	35.53	36.85	37.22	37.72	37.49	37.36
TiO ₂	1.80	2.65	3.00	1.63	0.00	3.35	2.22
Al ₂ O ₃	13.18	14.55	16.82	19.34	17.54	12.94	15.68
Cr ₂ O ₃	0.00	0.00	0.00	0.00	0.00	0.00	0.00
Fe ₂ O ₃	0.00	0.00	0.00	0.00	0.00	0.00	0.00
FeO	30.73	36.19	31.46	28.45	34.15	31.61	31.54
MnO	0.00	0.00	0.00	0.00	0.00	0.00	0.00
MgO	5.49	4.27	3.19	3.23	2.96	4.93	3.75
CaO	7.04	7.43	6.97	9.94	6.75	7.33	7.19
Na ₂ O	0.00	0.00	0.00	0.00	0.00	0.00	0.00
K ₂ O	0.00	0.00	0.00	0.00	0.00	0.00	0.00
Totals	98.22	100.61	98.29	99.81	99.12	97.66	97.74
Si	3.25	2.93	3.02	2.97	3.09	3.11	
Ti	0.11	0.16	0.18	0.10	0.00	0.21	
Al	1.27	1.42	1.62	1.82	1.69	1.27	
Cr	0.00	0.00	0.00	0.00	0.00	0.00	
Fe ^{3+ a}	0.00	0.00	0.00	0.00	0.00	0.00	
Fe ²⁺	2.09	2.50	2.16	1.90	2.34	2.19	
Mn	0.00	0.00	0.00	0.00	0.00	0.00	
Mg	0.67	0.53	0.39	0.38	0.36	0.61	
Ca	0.61	0.66	0.61	0.85	0.59	0.65	
Na	0.00	0.00	0.00	0.00	0.00	0.00	
K	0.00	0.00	0.00	0.00	0.00	0.00	
Sum	8.00	8.19	7.98	8.02	8.07	8.04	
Mg# ^b	24.15	17.36	15.31	16.84	13.37	21.73	
gr ^c	0.18	0.18	0.19	0.27	0.18	0.19	
al ^d	0.62	0.68	0.68	0.61	0.71	0.63	
py ^e	0.20	0.14	0.12	0.12	0.11	0.18	

a $Fe^{3+} = 2 * X * (1 - T/S)$; where X = oxygen in structural formulae; T = ideal number in structural formulae; S = cations per structural formulae calculated (Droop, 1987).

b $Mg\# = 100 * Mg / (Mg + Fe^{2+} + Fe^{3+})$.

c $gr = Ca / (Ca + Fe + Mn + Mg)$.

d $al = Fe / (Ca + Fe + Mn + Mg)$.

e $py = Mg / (Ca + Fe + Mn + Mg)$.

General pyroxene compositions from EMS-1 at 2.5 GPa and 600°C. Structural formulae calculated for 6 oxygens.

wt. %	1	2	3	4	5	6	7	8	9	10
SiO ₂	49.82	47.88	48.88	47.31	42.69	43.16	44.09	46.06	45.83	47.37
TiO ₂	2.43	1.82	1.52	3.03	3.28	2.80	1.39	2.33	3.29	3.43
Al ₂ O ₃	15.93	15.29	17.10	16.02	16.27	15.25	19.13	15.38	15.10	16.52
Cr ₂ O ₃	0.00	0.00	0.00	0.00	0.00	0.00	0.00	0.00	0.00	0.00
Fe ₂ O ₃	0.00	0.00	0.00	0.00	0.00	0.00	0.00	0.00	0.00	0.00
FeO	8.80	11.29	8.87	11.18	12.92	14.47	8.13	11.71	12.66	11.68
MnO	0.00	0.00	0.00	0.00	0.00	0.00	0.00	0.00	0.00	0.00
MgO	7.16	7.40	6.20	7.95	7.81	8.19	8.14	8.06	7.58	8.93
CaO	10.16	10.85	10.01	9.20	9.32	8.59	13.61	8.71	8.36	10.23
Na ₂ O	3.48	2.80	4.46	3.33	2.83	2.87	2.27	2.99	2.87	3.12
K ₂ O	0.89	0.86	0.93	1.06	0.98	1.03	0.55	0.82	0.94	1.42
Totals	98.67	98.20	97.97	99.07	96.11	96.37	97.31	96.04	96.64	102.69
Si	1.82	1.79	1.80	1.75	1.65	1.68	1.65	1.76	1.75	1.70
Ti	0.07	0.05	0.04	0.08	0.10	0.08	0.04	0.07	0.09	0.09
Al	0.69	0.67	0.74	0.70	0.74	0.70	0.84	0.69	0.68	0.70
Cr	0.00	0.00	0.00	0.00	0.00	0.00	0.00	0.00	0.00	0.00
Fe ³⁺ ^a	0.00	0.00	0.00	0.00	0.00	0.00	0.00	0.00	0.00	0.00
Fe ²⁺	0.27	0.35	0.27	0.35	0.42	0.47	0.25	0.37	0.40	0.35
Mn	0.00	0.00	0.00	0.00	0.00	0.00	0.00	0.00	0.00	0.00
Mg	0.39	0.41	0.34	0.44	0.45	0.47	0.45	0.46	0.43	0.48
Ca	0.40	0.43	0.40	0.36	0.39	0.36	0.55	0.36	0.34	0.39
Na	0.25	0.20	0.32	0.24	0.21	0.22	0.17	0.22	0.21	0.22
K	0.04	0.04	0.04	0.05	0.05	0.05	0.03	0.04	0.05	0.07
Sum	3.92	3.95	3.96	3.96	4.01	4.03	3.98	3.96	3.95	4.00
Mg# ^b	59.21	53.88	55.45	55.90	51.87	50.23	64.07	55.08	51.62	57.68

a $Fe^{3+} = 2 * X * (1 - T/S)$; where X = oxygen in structural formulae; T = ideal number in structural formulae; S = cations per structural formulae calculated (Droop, 1987).

b $Mg\# = 100 * Mg / (Mg + Fe^{2+} + Fe^{3+})$.

General pyroxene compositions from EMS-1 at 2.5 GPa and 600°C. Structural formulae calculated for 6 oxygens.

wt. %	11	12	13	14	15	ave
SiO ₂	45.97	46.87	46.90	43.30	43.15	46.7
TiO ₂	2.44	2.87	0.55	1.38	1.94	2.7
Al ₂ O ₃	17.57	16.18	14.11	14.76	11.99	15.9
Cr ₂ O ₃	0.00	0.00	0.00	0.00	0.00	0.0
Fe ₂ O ₃	0.00	0.00	0.00	0.00	0.00	0.0
FeO	11.19	11.02	9.18	14.27	12.71	11.8
MnO	0.00	0.00	0.00	0.00	0.00	0.0
MgO	8.37	10.47	8.83	6.65	6.61	8.1
CaO	10.25	10.82	18.19	16.06	17.39	10.5
Na ₂ O	2.77	2.40	1.16	1.67	1.79	2.8
K ₂ O	1.34	1.12	0.37	0.67	0.42	0.9
Totals	99.89	101.74	99.28	98.77	96.01	99.5
Si	1.69	1.69	1.74	1.67	1.71	1.7
Ti	0.07	0.08	0.02	0.04	0.06	0.1
Al	0.76	0.69	0.62	0.67	0.56	0.7
Cr	0.00	0.00	0.00	0.00	0.00	0.0
Fe ^{3+a}	0.00	0.00	0.00	0.00	0.00	0.0
Fe ²⁺	0.34	0.33	0.29	0.46	0.42	0.3
Mn	0.00	0.00	0.00	0.00	0.00	0.0
Mg	0.46	0.56	0.49	0.38	0.39	0.5
Ca	0.40	0.42	0.73	0.66	0.74	0.7
Na	0.20	0.17	0.08	0.12	0.14	0.1
K	0.06	0.05	0.02	0.03	0.02	0.0
Sum	3.99	3.99	3.98	4.04	4.03	4.0
Mg# ^b	57.14	62.85	63.15	45.38	48.08	57.1

a $Fe^{3+} = 2 * X * (1 - T/S)$; where X = oxygen in structural formulae; T = ideal number in structural formulae; S = cations per structural formulae calculated (Droop, 1987).

b $Mg\# = 100 * Mg / (Mg + Fe^{2+} + Fe^{3+})$.

General garnet compositions from EMS-2 at 2.5 GPa and 820°C. Structural formulae calculated for 12 oxygens.

wt. %	Core1	Core2	Rim1	Core3	Rim2	Core4
SiO ₂	36.56	35.18	36.77	36.30	37.87	36.20
TiO ₂	1.09	1.49	0.58	1.05	0.46	0.89
Al ₂ O ₃	20.49	20.27	20.74	20.29	21.16	20.72
Cr ₂ O ₃	0.00	0.00	0.00	0.00	0.00	0.00
Fe ₂ O ₃	0.00	0.00	0.00	0.00	0.00	0.00
FeO	32.53	29.92	24.27	30.94	24.16	29.08
MnO	0.00	0.00	0.00	0.00	0.00	0.00
MgO	2.09	2.41	7.01	2.24	7.15	2.92
CaO	8.91	8.32	8.42	9.28	7.74	9.30
Na ₂ O	0.00	0.00	0.00	0.00	0.00	0.00
K ₂ O	0.00	0.00	0.00	0.00	0.00	0.00
Totals	101.67	97.60	97.79	100.10	98.54	99.11

General pyroxene compositions from EMS-2 at 2.5 GPa and 820°C. Structural formulae calculated for 6 oxygens.

wt. %	1	2	3	4	5
SiO ₂	53.94	55.30	55.08	54.46	54.8
TiO ₂	0.31	0.00	0.00	0.31	0.2
Al ₂ O ₃	10.90	10.67	10.27	11.35	10.8
Cr ₂ O ₃	0.00	0.00	0.00	0.00	0.0
Fe ₂ O ₃	0.00	0.00	0.00	0.00	0.0
FeO	4.71	4.98	4.58	4.87	4.8
MnO	0.00	0.00	0.00	0.00	0.0
MgO	9.00	10.10	9.80	9.93	9.9
CaO	13.75	14.93	15.04	15.75	15.0
Na ₂ O	5.43	4.97	5.12	4.72	5.0
K ₂ O	0.00	0.00	0.00	0.00	0.0
Totals	98.06	100.95	99.89	101.39	100.4

General melt compositions from EMS-2 at 2.5 GPa and 820°C.

wt. %	1	2	3	4
SiO ₂	51.18	50.04	47.77	50.04
TiO ₂	1.71	0.70	0.99	0.99
Al ₂ O ₃	20.47	20.76	19.89	20.47
Cr ₂ O ₃	0.00	0.00	0.00	0.00
Fe ₂ O ₃	0.00	0.00	0.00	0.00
FeO	3.71	2.72	3.46	3.46
MnO	0.00	0.00	0.00	0.00
MgO	5.37	5.38	4.58	5.37
CaO	3.54	3.87	3.34	3.54
Na ₂ O	1.33	1.23	1.22	1.23
K ₂ O	7.19	6.96	7.64	7.19
Totals	94.49	91.66	88.90	92.28

General garnet compositions from EMS-2 at 2.5 GPa and 790°C.

Structural formulae calculated for 12 oxygens.

wt. %	Core1	Rim 1	Rim2	Core2
SiO ₂	37.64	37.81	38.36	37.23
TiO ₂	1.12	1.01	0.70	0.88
Al ₂ O ₃	20.78	21.32	21.00	20.80
Cr ₂ O ₃	0.00	0.00	0.00	0.00
Fe ₂ O ₃	0.00	0.00	0.00	0.00
FeO	28.95	23.54	23.92	27.60
MnO	0.00	0.00	0.00	0.00
MgO	4.25	7.54	7.40	4.51
CaO	9.19	8.37	8.26	9.16
Na ₂ O	0.00	0.00	0.00	0.00
K ₂ O	0.00	0.00	0.00	0.00
Totals	101.93	99.58	99.64	100.17

General pyroxene compositions from EMS-2 at 2.5 GPa and 790°C.

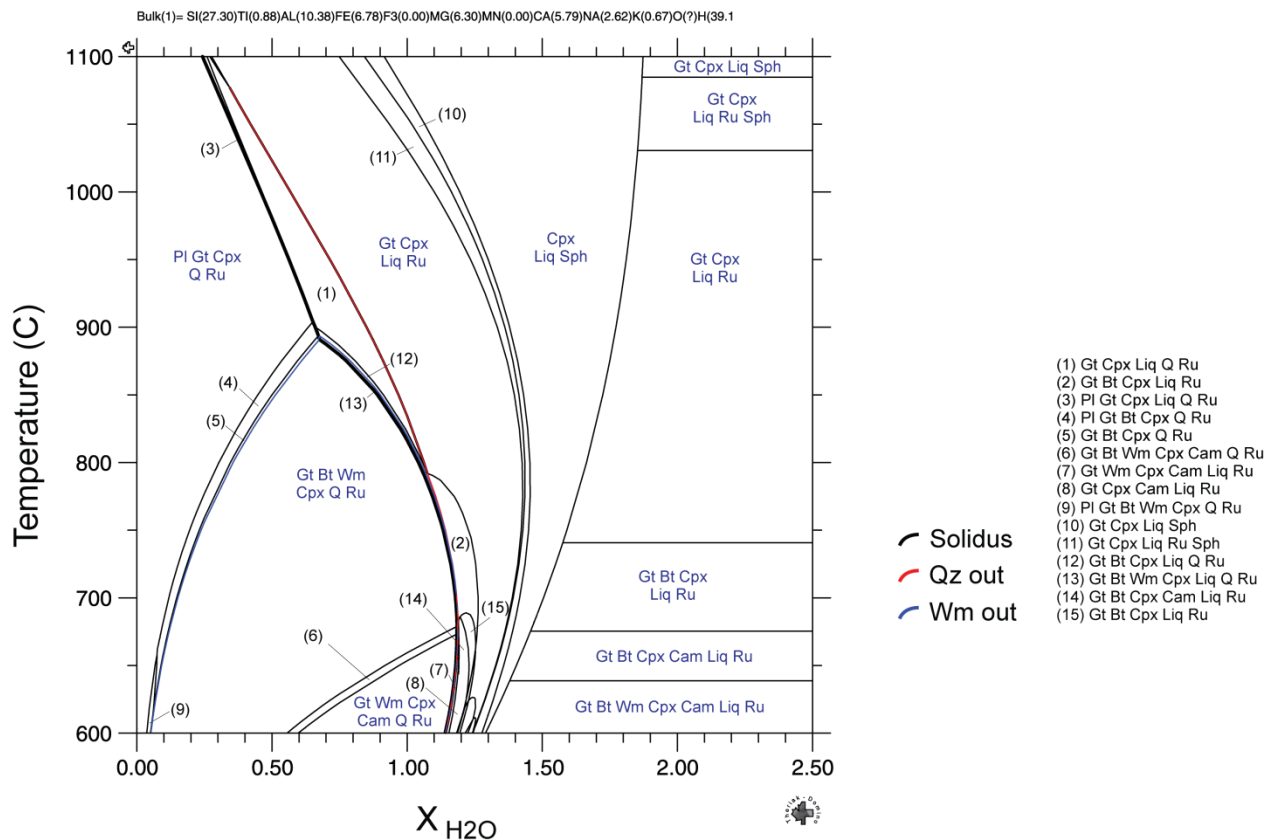
Structural formulae calculated for 6 oxygens.

wt. %	1	2	3	4	Ave
SiO ₂	53.56	54.87	54.74	54.65	54.7
TiO ₂	0.53	0.37	0.48	0.40	0.4
Al ₂ O ₃	10.86	11.02	10.16	10.80	10.8
Cr ₂ O ₃	0.00	0.00	0.00	0.00	0.0
Fe ₂ O ₃	0.00	0.00	0.00	0.00	0.0
FeO	5.26	4.93	5.94	4.98	5.1
MnO	0.00	0.00	0.00	0.00	0.0
MgO	9.73	10.03	9.32	9.50	9.6
CaO	15.55	15.07	14.69	15.11	15.1
Na ₂ O	4.38	4.49	4.38	4.37	4.4
K ₂ O	0.00	0.00	0.00	0.00	0.0
Totals	99.86	100.78	99.70	99.81	100.2

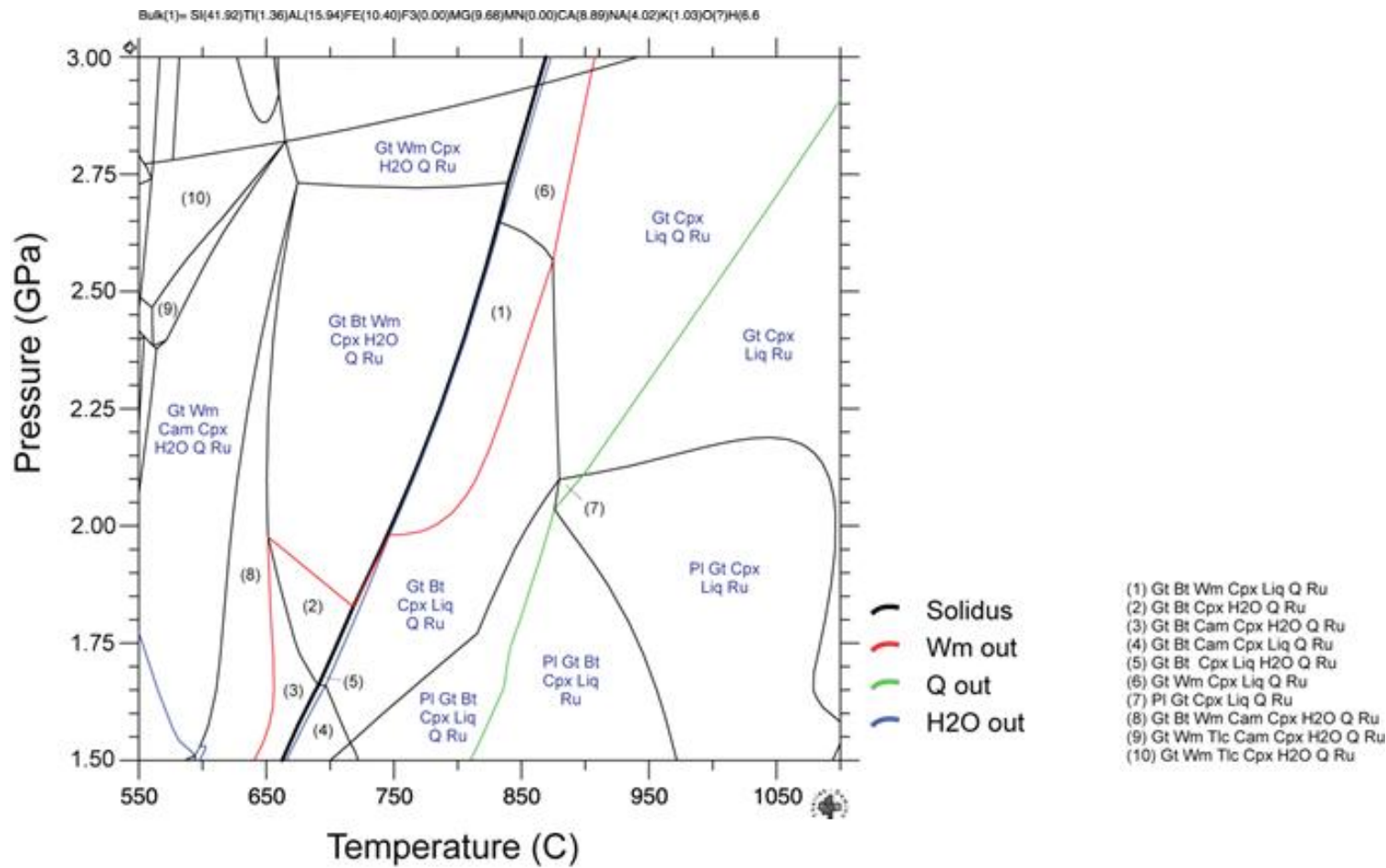
General melt compositions from EMS-2 at 2.5 GPa and 790°C.

wt. %	1	2	3	Ave
SiO ₂	49.14	48.45	49.37	49.14
TiO ₂	1.04	0.94	0.86	0.94
Al ₂ O ₃	20.19	19.12	20.26	20.19
Cr ₂ O ₃	0.00	0.00	0.00	0.00
Fe ₂ O ₃	0.00	0.00	0.00	0.00
FeO	3.93	3.45	3.62	3.62
MnO	0.00	0.00	0.00	0.00
MgO	5.36	5.19	5.07	5.19
CaO	6.01	4.59	5.34	5.34
Na ₂ O	1.45	1.54	1.55	1.54
K ₂ O	5.03	5.76	5.67	5.67
Totals	92.15	89.05	91.74	91.64

Pressure: 2.5 GPa

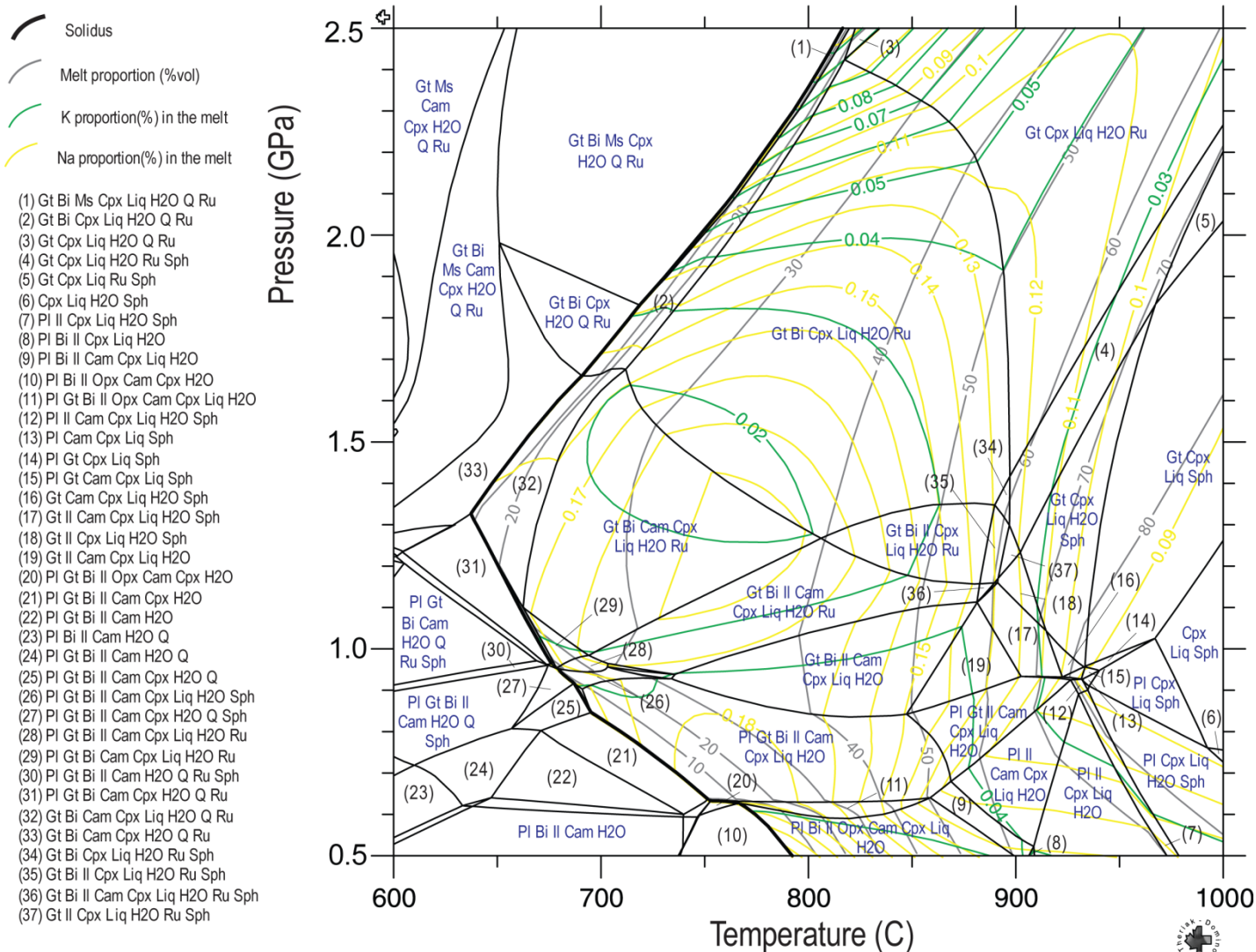


TX graphic of X_{H_2O} showing mineral assemblages in T(°C) vs $X_{(H_2O)}$ (water content) content).



Pseudosection showing mineral assemblages for EMS-2 composition (1.1 H₂O wt.%)

Bulk(1)= Si(27.30)Ti(0.88)Al(10.38)Fe(6.78)F3(0.00)MG(6.30)MN(0.00)CA(5.79)NA(2.62)K(0.67)O(?)H(39.1)



Pseudosection showing mineral assemblages for EMS-1 composition (10 H₂O wt.%), highlighting K, Na and melt proportions.

Gel ESM-1 calculation spreadsheet

Oxide	SiO2	Al2O3	MgO	CaO	Na2O	K2O	TiO2	FeO total	Total
Sample (wt%)	46.5000	15.0000	7.2000	9.2000	2.3000	0.9000	2.0000	13.8000	96.9000
Sample (100% wt)	47.9876	15.4799	7.4303	9.4943	2.3736	0.9288	2.0640	14.2415	100.0000
Sample (10 g)	4.7988	1.5480	0.7430	0.9494	0.2374	0.0929	0.2064	1.4241	

Oxide	Molar weight	Sample (10g)	Source	Molar weight	Grams required (for 10g gel)
SiO2	60.0800	4.7988	TEOS	208.3300	16.6399
Al2O3	101.9614	1.5480	Al	26.9800	0.8192
MgO	40.3044	0.7430	Mg	24.3050	0.4481
CaO	56.0774	0.9494	CaCO3	100.0869	1.6945
Na2O	61.9789	0.2374	Na2CO3	105.9886	0.4059
K2O	94.1960	0.0929	K2CO3	138.2057	0.1363
FeO	71.8440	1.4241	Fe	55.8500	0.3690
			Fe2O3	159.7000	1.0552
TiO2		0.2064	TiO2		0.2064

	Bulk Rock	Fayalite	Kaolinite	Gel
SiO2	47.9876	29.4900	46.7667	52.5171
Al2O3	15.4799	0.0000	39.4815	16.8139
MgO	7.4303	0.0000	0.0000	10.2230
CaO	9.4943	0.0000	0.0000	13.0627
Na2O	2.3736	0.0000	0.0000	3.2657
K2O	0.9288	0.0000	0.0000	1.2779
TiO2	2.0640	0.0000	0.0000	2.8397
FeO total	14.2415	70.5100	0.0000	0.0000
FeO	0.0000	0.0000	0.0000	0.0000
Fe2O3	0.0000	0.0000	0.0000	0.0000
H2O	0.0000	0.0000	13.7518	0.0000
Total	100.0000	100.0000	100.0000	100.0000

	X _{bullock}	X _{fayalite}	X _{kaolinite}	X _{gel}
1	0.19971	0.08162	0.71867	
10	1.9971	0.8162	7.1867	g
3	0.5991	0.2449	2.1560	g

	FINAL GEL
	7.1867(g)
SiO2	3.77423
Al2O3	1.20836
MgO	0.73469
CaO	0.93878
Na2O	0.23469
K2O	0.09184
TiO2	0.20408
FeO total	0.00000
FeO	0.00000
Fe2O3	0.00000
H2O	0.00000
Total	7.18667

	Final Gel	Already made	2nd Gel
TEOS	13.0873	10.0643	3.0230
Al	0.6395	0.4550	0.1845
MgO	0.7347	0.4126	0.3221
CaCO3	1.6755	0.9411	0.7345
Na2CO3	0.4013	0.2254	0.1759
K2CO3	0.1347	0.0757	0.0591
Fe	0.0000	0.0000	0.0000
Fe2O3	0.0000	0.0000	0.0000
TiO2	0.2041	0.0000	0.0000

To be added in the ongoing process